

# UC Riverside

## UC Riverside Electronic Theses and Dissertations

### Title

Emissions from Wild Land Fires, Diesel Engines and Other Combustion Sources

### Permalink

<https://escholarship.org/uc/item/03t0q649>

### Author

Dixit, Poornima

### Publication Date

2014

Peer reviewed|Thesis/dissertation

UNIVERSITY OF CALIFORNIA  
RIVERSIDE

Emissions from Wildland Fires, Diesel Engines and Other Combustion Sources

A Dissertation submitted in partial satisfaction  
of the requirements for the degree of

Doctor of Philosophy

in

Chemical and Environmental Engineering

by

Poornima C. Dixit

December 2014

Dissertation Committee:

Dr. David Cocker III, Chairperson

Dr. John Wayne Miller

Dr. Akua Asa Awuku

Copyright by  
Poornima C. Dixit  
2014

The Dissertation of Poornima C. Dixit is approved:

---

---

---

Committee Chairperson

University of California, Riverside

## **Acknowledgements**

I am grateful to many individuals who helped achieve my goal. I would have never accomplished any of my objectives if it weren't for them.

First and foremost I thank my father and mother who were my emotional support throughout this journey. My father has been my rock through all the moments when I doubted myself, and my mother has nurtured me until the day of the completion of my thesis.

Apart from family, my advisor Dr. David Cocker immensely inspired me to always keep trying and that solely enabled me to carry forward and not let go when times were rough. I cannot thank him enough for being an excellent mentor, who advised me with an ocean of patience and understanding. My co-advisor Dr. Wayne Miller has been my support system at CE-CERT, constantly pushing me to get better each day. He always motivated me to come out of my shell and become confident and try harder.

I would also thank Dr. Kent Johnson for showing me the power of hard work, systematic approach and perseverance in-order to complete any task at hand brilliantly. I learnt a great deal when it came to data interpretation and analysis just by watching him work and incorporating his approach. I thank Dr. Thomas Durbin for guiding me and ensuring I get my stipend till the very end. I thank Dr .George Karavalakis for providing me the opportunity to work on some challenging analysis which provided me with an insight on rare characterization methodologies. I thank my committee member Dr. Akua Asa Awuku for her precious advice on improving my work. I also thank Dr.Janet Arey for providing me with special guidance on a research problem involving characterization of

emissions. I thank Dr. Richard Kondrat and Dr. Ron New at the UCR Mass Spectrometry facility for helping me use their instrument and providing me with most needed assistance, analyzing samples.

I thank Ms. Kathy Cocker for helping me in my initial days at the research lab. I thank Mr. Eddie O'Neil, Mr. Don Pacocha and Mr. Kurt Bumiller for helping me greatly on the testing side during the AQMD in-use study. I thank Ms. Nicole Davis for being very supporting on the management side of many of my research projects.

I thank the funding support received from- SERDP, SCAQMD and ARB, UCR- Department of Chemical and Environmental Engineering and Esther F. Hays fellowship.

Last but not least I thank the graduate and undergraduate students who helped me constantly. My senior graduate students Dr. Ehsan Hosseini provided me an excellent opportunity to learn and coached me on several research problems during a collaborative project. Dr. Varalakshmi Jayram, Dr. Yusuf Khan, Dr. Shunsuke Nakao, Dr. Ping Tang and Dr. Maryam Hajbabaei taught me several new aspects of instrumentation and data analysis. Current graduate students Mr. Nicholas Gysel, Ms. Chia Li Chen, Mr. Derek Price and Ms. Diep Vu have supported me when I needed help to complete certain tasks of my research. I thank the undergraduate students Ms. Daisy Jiminez, Ms. Jinyu Xu, Ms. Stephanie Stasiuk, Mr. Henry Yang, Mr. Geoffery Tsai, Mr. James Pletcher, Mr. Allan De Leon, Mr. Christian Surdilla, Mr. Shrey Prajapati, and Mr. Jesus Sahagun for constantly working in the lab in-order to achieve the deadlines on several research projects. I am deeply grateful towards all your efforts.

## ABSTRACT OF THE DISSERTATION

Emissions from Wildland Fires, Diesel Engines and Other Combustion Sources.

by

Poornima C. Dixit

Doctor of Philosophy, Graduate Program in Chemical and Environmental Engineering  
University of California, Riverside, December 2014  
Dr. David R Cocker III, Chairperson

The overall goal of this research was an in depth investigation of emissions from a number of sources, with emphasis on two under-explored areas. One study delved into the characterization of emissions from wildland fires an increasingly important source due to climate change, and the other undertook a deeper examination of the in-use emissions from heavy duty trucks operating in the port regions of Southern California.

An in-depth characterization of emissions from lab scale wildland fires was carried out, including: polyaromatic hydrocarbons (PAHs), levoglucosan, anions and cations, elemental and organic carbon. The unique aspect of this research was the comparison of data from two independent measurement methods; one method used real-time analytical methods and the other collected a sample over time and was analyzed off-line with reference methods. A side-by-side comparison of the two approaches showed significant differences and inaccuracies for many of the analyses by the Aerosol Mass Spectrometer. Further analysis enabled transformation of real time analysis to useful data.

Usually marine ports have the highest emissions in a region as many of the sources have weak emission standards. In this research the emissions of criteria and toxic pollutants

were measured from the engines in heavy duty trucks representative of those operating in the port regions. An important finding was the emissions measured during real world drive cycles more accurately represented the emission characteristics for the vehicles than the certification cycle or values determined from in-use compliance testing. Further, emissions from NO<sub>x</sub> control technologies were important to understand as emissions were multiple times higher for near port activities as compared with regional activity. High emissions reduction benefits from the SCR were observed but largely depended on catalyst temperature. Another important analysis completed during this thesis was the emissions factors from yard tractors in the port region for a period of over ten years. Both case studies provide additional insight into the emissions from port sources.



## Table of Contents

List of Figures .....	xi
List of Tables .....	xv
1 Introduction .....	1
1.1 Introduction to dissertation.....	1
1.1.1 Importance of understanding NO <sub>x</sub> and PM emissions .....	1
2 Performance of High Resolution Time-of-flight Aerosol Mass Spectrometer during Characterization of Particle Emissions from Laboratory Burns of Chaparral and Related Plant Species. ....	8
2.1 Introduction .....	8
2.2 Experimental section .....	9
2.2.1 Laboratory set –up for Biomass burning .....	9
2.3 Online HR-ToF-AMS .....	10
2.4 Offline Analysis .....	12
2.4.1 Organic Carbon (OC) Analysis.....	12
2.4.2 Anion Analysis.....	12
2.4.3 Levoglucosan and PAH Analysis .....	13
2.5 Instrument Inter-comparison Results .....	15
2.5.1 HR-ToF-AMS versus ECOC Analyzer .....	15
2.5.2 HR-ToF-AMS versus GC-MS .....	16
2.5.3 HR-ToF-AMS versus Ion Chromatograph .....	21
2.6 Summary and Conclusion .....	25
3 Real World Cycles Better Gauge the Efficiency of Recent NO <sub>x</sub> Emissions for Heavy-duty, Diesel Trucks .....	31
3.1 Introduction .....	31
3.2 Experimental Section .....	33
3.2.1 Test Vehicles and Fuels .....	33
3.2.2 Emission Measurements .....	34
3.2.3 Test Cycles.....	34
3.3 Results and Discussion.....	36

3.3.1	Category 1: Model Year 2009 -2010; Cooled-EGR Technology .....	39
3.3.2	Category 2: Model Year $\geq$ 2010 without SCR.....	40
3.3.3	Category 3: Model Year $\geq$ 2010 with SCR.....	41
3.3.4	Analysis of Transient Data in for HDDTs in Category 3 .....	42
3.3.5	Analysis of Data for Category 3 for SCT Temperature $>250^{\circ}\text{C}$ .....	44
3.3.6	NTE (Not To Exceed) Analysis .....	45
3.3.7	Comparison of On-road and Chassis NO <sub>x</sub> Emission Data .....	49
3.4	Conclusions .....	52
4	Emissions from Natural Gas and Diesel Buses and Refuse Haulers in the South Coast Air Quality Region.....	55
4.1	Introduction: .....	55
4.2	Experimental Section .....	57
4.2.1	Test vehicles.....	57
4.2.2	Test Cycles.....	58
4.3	Emissions Testing Protocol.....	58
4.4	Results & Discussions.....	59
4.4.1	NO <sub>x</sub> Emissions .....	59
4.4.2	NO <sub>x</sub> emissions from SCR equipped diesel trucks:.....	61
4.4.3	PM Emissions .....	66
4.4.4	THC, NMHC, CH <sub>4</sub> and CO emissions.....	68
4.5	Conclusions .....	70
5	Technology Has Significantly Lowered Emissions from Yard Tractors over 10 years 78	
5.1	Introduction .....	78
5.2	Vehicle Matrix.....	79
5.3	Test Cycles and Emissions measurements .....	81
5.4	Discussions.....	82
5.4.1	Yard Tractor emissions from engine retrofits.....	82
5.4.2	Yard Tractor emissions from improved engine technology .....	84
5.4.3	Yard tractor emissions from engines fuelled with alternate fuels.....	86

5.5	Conclusions .....	88
6	Summary of the Dissertation .....	94
A.	APPENDIX.....	96
B.	APPENDIX.....	138
C.	APPENDIX.....	142
D.	APPENDIX.....	146

## List of Figures

Figure 1 Laboratory Setup for biomass burning .....	10
Figure 2 Block diagram showing the various online sampling as well as filter sampling systems located on the sampling platform (Hoesseini et al. 2010).....	10
Figure 3 Comparison of online (HR-ToF-AMS) to offline (filter NIOSH EC-OC) for the Organic Carbon mass during real-time biomass burning. ....	15
Figure 4 Comparison of online (HR-ToF-AMS) to offline (filter GCMS) for Levoglucosan mass during real-time biomass burning.....	17
Figure 5 Comparison of online (HR-ToF-AMS) to offline (filter GC-MS) for the sum of PAH's during real-time biomass burning for a) fluoranthene and pyrene; b) benzo(k)fluoranthene, benzo(a)pyrene and benzo(b)fluoranthene; c) indeno(1,2cd)perylene and benzo(ghi)perylene; and (d) dibenzo(a,h)anthracene.....	21
Figure 6 Comparison of online (HR-ToF-AMS) to offline (filter IC) for Cl- fresh biomass smoke plumes .....	23
Figure 7 Comparison of online (HR-ToF-AMS) to offline (filter IC) for SO <sub>4</sub> <sup>2-</sup> fresh biomass smoke plumes .....	24
Figure 8: Comparison of online (HR-ToF-AMS) to offline (filter IC) for NO <sub>3</sub> <sup>-</sup> in fresh biomass smoke plumes .....	24
Figure 9 PM <sub>2.5</sub> gravimetric in mg/bhp-h for the HDDT vehicles on all the port cycles...	37
Figure 10 PM <sub>2.5</sub> gravimetric in mg/bhp-h for the HDDT vehicles on UDSS cycle.....	37

Figure 11 NOx Emissions factors for the in-use emissions testing performed on the Heavy Duty Diesel Trucks. The nine vehicles from this study categorized according to their test cycle on the x-axis, while the NOx emissions in g/bhp-h are depicted on the y-axis.....	39
Figure 12 Speed (mph) , SCR inlet Temperature (deg C) and Accumulated NOx (g) versus accumulated Brake horsepower-hour for V12.8L on Regional Cycle .....	43
Figure 13 Speed (mph) , SCR inlet Temperature (deg C) and Accumulated NOx (g) versus accumulated Brake horsepower-hour for V12.8L on the Near Dock .....	44
Figure 14 Brake specific NOx emissions for SCR temperature > 250 <sup>0</sup> C and percent time of the cycle when the ATS was > 250 <sup>0</sup> C for the SCR equipped vehicles .....	45
Figure 15 NOx emissions in the Not to Exceed (NTE) zone for the 2011, 12.8L, Volvo equipped with SCR; the dotted line represents the emission standard for NOx in g/bhp-h .....	47
Figure 16 NOx emissions in the Not to Exceed (NTE) zone for the 2011, 11.9L, Cummins equipped with SCR; the dotted line represents the emission standard for NOx in g/bhp-h .....	48
Figure 17 NOx emissions in the Not to Exceed (NTE) zone for the 2008, 14L, Detroit Diesel equipped with a cooled EGR ; the dotted line represents the emission standard for NOx in g/bhp-h .....	49
Figure 18 SCR Temperature (deg C), Speed (mph) and Accumulated NOx (g) Emissions versus Time for Vehicle C11.9 during On-road testing with cold start.....	51

Figure 19 SCR Temperature (deg C), Speed (mph) and Accumulated NO <sub>x</sub> (g) Emissions versus Time for Vehicle C11.9 during On-road testing on highway condition.....	51
Figure 20 NO <sub>x</sub> emissions in g/mile for buses on the CBD cycle; * indicates NO <sub>x</sub> /10....	63
Figure 21 NO <sub>x</sub> emissions in g/mile from refuse trucks on hot and cold UDDS cycle.....	63
Figure 22 NO <sub>x</sub> emissions in g/mile from refuse trucks on RTC (Refuse Truck Cycles-William H. Martin and AQMD RTC).....	64
Figure 23 Cummins ISX 11.9 liter engine's cumulative NO <sub>x</sub> emissions in grams on the secondary y-axis; Exhaust temperature in °C and Speed in mph on the primary y-axis as a function of accumulated power (brake horse power hour) on x-axis .....	64
Figure 24 Brake specific NO <sub>x</sub> emissions for SCR temperature > 250 <sup>0</sup> C and percent time of the cycle when the ATS was > 250 <sup>0</sup> C for the SCR equipped vehicles .....	65
Figure 25 Cummins ISX 11.9 liter engine's NO <sub>x</sub> accumulated mass emissions for a cold and hot start UDDS cycle .....	65
Figure 26 PM <sub>2.5</sub> emissions in g/mile from the CBD cycle.....	67
Figure 27 PM <sub>2.5</sub> emissions in g/mile from refuse trucks on hot and cold UDDS cycles.	67
Figure 28 PM <sub>2.5</sub> emissions in g/mile refuse trucks on RTC (Refuse Truck Cycles-William H. Martin and AQMD RTC).....	68
Figure 29 NO <sub>x</sub> and Diesel PM Emission Distributions at California Ports .....	78
Figure 30 Test Modes, Torque and Weighting Factors for the ISO-8178-C1 Cycle.....	82
Figure 31 Emissions from baseline (CARB diesel) and retrofit technology (emulsified diesel) from Yard tractors; repeat tests were within 2% of uncertainty. ....	84

Figure 32 Yard Tractor emissions from different engine technologies, repeat tests were within 2% of uncertainty..... 86

Figure 33 Yard Tractor emission from using alternate fuels, repeat tests were within 2% of uncertainty. .... 88

Figure 34 Yard tractor emission trend over a decade. .... 90

## List of Tables

Table 1 Summary of the Polycyclic Aromatic Hydrocarbons quantified during this study .....	19
Table 2 Detailed information of the HDDT's tested .....	33
Table 3 Test cycles for measuring in use emissions measurements of HDDT's.....	34
Table 4 Heavy-Duty Engine Emission Conversion Factors for the UDDS cycle .....	38
Table 5 Percentage of emissions that exist in the NTE zones (After treatment system >2500C, 1 second and 30 second events) for all the real world cycles on the 2011, 12.8L, Volvo equipped with SCR .....	47
Table 6 Percentage of emissions that exist in the NTE zones (After treatment system >250 <sup>0</sup> C, 1 second and 30 second events) for all the real world cycles on the 2011, 11.9L, Cummins equipped with SCR.....	48
Table 7 Percentage of emissions that exist in the NTE zones (1 second and 30 second events) for all the real world cycles on both of the randomly selected 2008, 14L, Detroit Diesel vehicles equipped with cooled EGR.....	49
Table 8 Vehicle matrix describing the vehicle type, make and model, fuel used, after treatment technology, operating conditions and test cycle. ....	59
Table 9 Emission factors for the Buses and Refuse Trucks operated on CBD, WHM and AQMD-RT Cycle.....	72



Table 10 Diesel Engine Manufacturer for Yard Tractors <sup>1</sup> ..... 80

Table 11 Vehicle matrix showing the yard tractor manufacturer, manufacture year, fuels used and after treatment technology. .... 80

Table 12 Emissions and percent change in emissions for NO<sub>x</sub>, PM and THC emissions from Baseline (CARB diesel) and retrofit (Emulsified diesel Lubrizol); +indicates benefit and – indicates dis-benefit. .... 84

# 1 Introduction

## 1.1 Introduction to dissertation

“Clean air is considered to be a basic requirement of human health and well-being.

However, air pollution continues to pose a significant threat to health worldwide”<sup>1</sup>.

Air pollution has implications for a number of contemporary issues including human health, (e.g. respiratory, cancer, allergies.), ecosystems (e.g. crop yields, loss of biodiversity), national heritage (e.g. buildings), regional climate (aerosol and ozone exhibit a strong regionality in climate forcing)<sup>2</sup>. Air quality is determined by measuring the concentration of gaseous pollutants and size or number of particulate matter. The criteria pollutants designated by EPA as most detrimental to human health are NO<sub>2</sub>, PM<sub>2.5</sub> (particulate matter), CO, Ozone, lead and SO<sub>2</sub>. After years of efforts towards mitigating these pollutants NO<sub>x</sub> and PM<sub>2.5</sub> persist to have a significant impact on the air quality of the southern Californian region.

### 1.1.1 Importance of understanding NO<sub>x</sub> and PM emissions

Reactive nitrogen NO<sub>x</sub> which is essentially the sum of oxides of nitrogen (NO and NO<sub>2</sub>) promotes ground level ozone and smog formation in the troposphere<sup>3</sup>. NO<sub>x</sub> oxidation to nitric acid also promotes the formation of particulate matter in the atmosphere<sup>3</sup>. One of the factors greatly enhancing NO<sub>x</sub> levels in the troposphere are NO<sub>x</sub> emissions from combustion sources like burning of wood, burning of fuel (vehicles, ships etc...). PM with aerodynamic diameter < 2.5µm (PM<sub>2.5</sub>) is regulated by the U.S. EPA, mainly because of its health effects. Primary ultrafine particles are formed during gas-to-particle conversion

or during incomplete fuel combustion <sup>4</sup>. Due to their small size, high number concentration, and relatively large surface area per unit mass, ultrafine particulate matter have unique characteristics, including increased adsorption of organic molecules and enhanced ability to penetrate cellular targets in the lung and systemic circulation <sup>5,6,7,8</sup> and even cause premature deaths in case of vehicular PM <sup>9,10</sup>. Combustion processes represent the main source of PM in urban metropolitan areas <sup>11</sup>; these include primarily motor vehicles emissions <sup>12</sup> but also wood burning, food cooking, and other combustion activities <sup>13</sup>. Further the particulate phase emissions consist of elemental carbon (EC), organic carbon (OC), trace metals, and other inorganic compounds. The OC consists of semi volatile organic compounds (SVOC's) which partition into the particulate or gaseous phase depending on their vapor pressures. The SVOC's that are present in particulate phase are mainly compounds like polycyclic aromatic hydrocarbons (PAHs) which are a class of complex organic chemicals; include carbon and hydrogen with a fused ring structure containing at least 2 benzene rings. Reactions between PAHs and nitrogen oxides and/or nitric acid, all of which are commonly found in combustion effluents form Nitrated PAH's, which have garnered much attention over the years owing to their health affects <sup>14,15,16,17,18,19</sup>.

This dissertation is a diverse blend of investigating emissions and their characteristics from different sources. The following is a breakup of the contents dealt with each chapter in this dissertation.

Chapter 1 evaluates the performance of a HR-TOF AMS during lab scale biomass burns. This chapter assesses the chemical characterization performance of the high resolution Time-of-flight Aerosol Mass Spectrometer (HR-ToF-AMS) during flaming, mixed and smoldering phases of biomass burning. Correlations between HR-ToF-AMS and offline chemical characterizations following standardized methods are provided for levoglucosan, organic carbon, and particle bound PAHs, and inorganic ions, providing direct insight into the performance of the HR-ToF-AMS.

Chapter 2 describes emissions from port activities. Especially the critical question in this research was which emission factors of heavy-duty diesel trucks (HDDTs) should be used in developing inventories? Given that question the emissions were measured from a matrix of nine Class 8 HDDTs representing current manufacturers, diesel engines and control technologies on both certification and real-world cycles associated with goods movement. The analysis focused on the efficiency of the NO<sub>x</sub> control technologies, given a number of control technologies were employed during this regulatory transition period.

Chapter 3 presents a detailed evaluation of emission factors for ten different types of engines from different vocations and manufacture year. Among them four of the vehicles/engines used natural gas, one vehicle used propane and five vehicles used ultralow sulfur diesel. The control technologies for natural gas and propane were either a three way catalyst or an oxidation catalyst, while the diesel vehicles were equipped with a diesel particulate filter, either a cooled EGR or a SCR catalyst

Chapter 4 evaluates how over time as new technology was incorporated into the yard tractors, the emissions were significantly reduced. Some of the technology was introduced as emission limits were reduced by new regulations. This chapter will review the history of emissions over the last ten years and provide details on the technology changes that have led to this success story.

## References

1. WHO, 2005b. Air Quality Guidelines for Particulate Matter, Ozone, Nitrogen Dioxide and Sulfur Dioxide. World Health Organization, Geneva, Switzerland.
2. Atmospheric composition change – global and regional air quality. P.S.Monks et al. *Atmospheric Environment* 43 (2009) 5268–5350
3. Atmospheric Chemistry and Physics from Air pollution to Climate change. John H. Seinfeld and Spyros N. Pandis
4. HEI. 2002. Understanding the Health Effects of Components of the Particulate Matter Mix: Progress and Next Steps. Health Effects Institute Perspectives Series. Boston, MA: Health Effects Institute
5. Utell MJ, Frampton MW. 2000. Acute health effects of ambient air pollution: the ultrafine particle hypothesis. *J Aerosol Med* 13:355–359.
6. Oberdörster G. 1996. Significance of particle parameters in the evaluation of exposure-dose-response relationships of inhaled particles. *Inhal Toxicol* 8(suppl):73–89.
7. Nemmar A, Hoet PH, Vanquickenborne B, Dinsdale D, Thomeer M, Hoylaerts MF, et al. 2002. Passage of inhaled particles into the blood circulation in humans. *Circulation* 105:411–414.
8. Frampton MW. 2001. Systemic and cardiovascular effects of airway injury and inflammation: ultrafine particle exposure in humans. *Environ Health Perspect* 109(suppl 4):529–532.

9. Tsai, F. C.; Apte, M. G.; Daisey, J. M. An exploratory analysis of the relationship between mortality and the chemical composition of airborne particulate matter. *Inhalation Toxicol.* 2000,12, 121–135.
10. Hoek, G.; Brunekreef, B.; Goldbohm, S.; Fischer, P.; van den Brandt, P. A. Association between mortality and indicators of traffic-related air pollution in the Netherlands: a cohort study. *Lancet* 2002, 360 (9341), 1203–1209.
11. Sioutas, C.; Delfino, R. J.; Singh, M. Exposure assessment for atmospheric ultrafine particles (UFPs) and implications in epidemiologic research. *Environ. Health Perspect.* 2005, 113 (8), 947–955.
12. Westerdahl, D.; Fruin, S.; Sax, T.; Fine, P. M.; Sioutas, C. Mobile platform measurements of ultrafine particles and associated pollutant concentrations on freeways and residential streets in Los Angeles. *Atmos. Environ.* 2005, 39 (20), 3597–3610.
13. Kleeman, M. J.; Hughes, L. S.; Allen, J. O.; Cass, G. R. Source contributions to the size and composition distribution of atmospheric particles: Southern California in September 1996. *Environ. Sci. Technol.* 1999, 33 (23), 4331–4341.
14. Zielinska B, Arey J, Atkinson R, Winer AM (1989) *Atmos Environ* 23:223–229
15. Atkinson R, Winer AM, Pitts JN (1986) *Atmos Environ* 20:331–339
16. Li H, Westerholm R (1994) *J Chromatogr A* 664:177–182
17. Durant JL, Busby WF, Lafleur AL, Penman BW, Crespi CL (1996) *Mutation Res* 371:123–157

18. Talaska G, Underwood P, Maier A, Lewtas J, Rothman N, Jaeger M (1996)  
Environ Health Perspect 104:901–906
19. Schilhabel J, Levsen K (1989) Fresenius Z Anal Chem 333:800–805



## **2 Performance of High Resolution Time-of-flight Aerosol Mass Spectrometer during Characterization of Particle Emissions from Laboratory Burns of Chaparral and Related Plant Species.**

### **2.1 Introduction**

The impacts of aerosols on climatic changes and human health have triggered the development of instruments capable of making accurate and sensitive aerosol measurements. The measurement of aerosol chemical properties in realtime is difficult due to the inherent complexity of aerosols, their low mass concentrations (typically a few micrograms per cubic meter), and the large variability of their properties in space and time (Decarlo, et al. 2006). The Aerosol Mass Spectrometer (Aerodyne Research Incorporated, Billerica, MA) has been widely deployed for real-time measurements of aerosols (Jayne, et al. 2000; Jimenez, et al. 2003a). The High Resolution Time of flight Aerosol Mass Spectrometer (HR-ToF-AMS) measures size resolved chemical composition of non-refractory submicron aerosols with an integration time of the order of seconds/minute. A number of AMS instrumentation (Allan, et al. 2003a; Jimenez, et al. 2003; Middlebrook, et al. 2003) and intercomparison studies (Drewnick, et al. 2003 Schneider, et al. 2004 e.g. Zhang, et al.2005a, Takegawa, et al. 2005, Dzepina, et al.2007) have demonstrated the ability of AMS during different kinds of campaigns.

In this chapter we focus on the performance of the HR-ToF-AMS during the characterization of particulate matter emissions from laboratory scale biomass burning. The HR-ToF-AMS measurements are compared with results of offline analysis of integrated filter samples by an EC/OC analyzer, an ion chromatograph (IC), and a gas

chromatograph-mass spectrometer (GC-MS). Comparisons are made for nine and four plant species from the Southwest and Southeast U.S., respectively. Fuel description and details are summarized in Burling, et al. 2010 and Hosseini, et al. 2010.

## **2.2 Experimental section**

### **2.2.1 Laboratory set –up for Biomass burning**

All burns were conducted at the Missoula Fire Science Laboratory (FSL). A detailed facility description is found in (Yokelson, et al. 1996). Briefly, a 1.6 m stack is located in the center of a 12.5 m × 12.5 m × 22 m room, 2.1 m above the ground, and extends through the ceiling (Figure 1). Combustion exhaust is collected in a 3.6 m diameter hood attached to the 1.5 m stack. Sampling ports are located approximately 16.5 m above the floor. Real-time measurement instruments and filter sampling systems were located on the sampling platform (Figure 2). Smoke samples were withdrawn isokinetically from the center of the stack. The sample was diluted (13.5:1 for HR-ToF-AMS, 22.2:1 for filter sampling system) using a partial flow dilution system with a single venturi (Agrawal, et al. 2008). The fire lab was slightly pressurized with pre-conditioned outside air to precisely control temperature and relative humidity. The air velocity in the chimney was set to 1.5 m s<sup>-1</sup> or 3 m s<sup>-1</sup> by controlling the exhaust fan speed to maintain proper entrainment of combustion products.

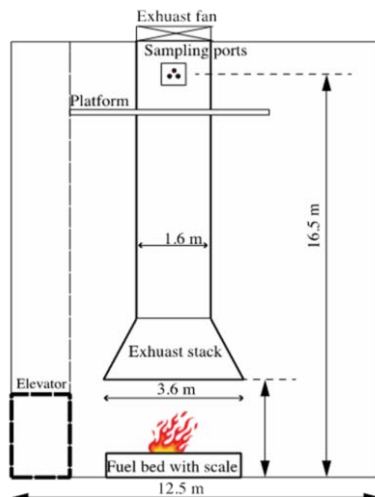


**Figure 1 Laboratory Setup for biomass burning**

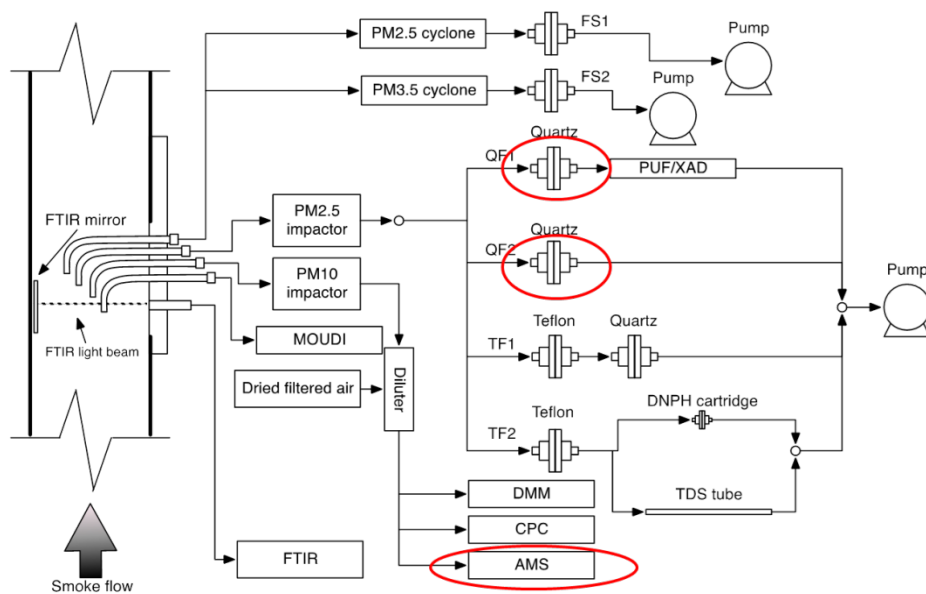


**Figure 2 Block diagram showing the various online sampling as well as filter sampling systems located on the sampling platform (Hoesseini et al. 2010)**

### 2.3 Online HR-ToF-AMS

The evolution of aerosol bulk chemical composition was tracked using an Aerodyne High Resolution Time-of-Flight Aerosol Mass Spectrometry (HR-ToF-AMS), which has been

described in detail previously (DeCarlo, et al. 2006). Dilute aerosol flow was passed through a PM10 impactor prior to entering the HR-ToF-AMS. HR-ToF-AMS was operated in both V-mode that offers higher sensitivity and lower resolving power, and W-mode that yields higher resolving power and lower mass sensitivity. The high-resolution W-mode allows for direct separation of each unit mass peak into a separate contribution for specific elemental compositions based on small differences in mass defect. Recently, a new elemental analysis (EA) technique was developed coupled with HR-ToF-AMS sampling data (Aiken, et al. 2007; 2008). Elemental ratios for the total organic mass, such as oxygen to carbon (O/C), hydrogen to carbon (H/C), and nitrogen to carbon (N/C), in addition to the organic mass to organic carbon ratio (OM/OC), can be determined. In this study, the C:O:H ratio of the total aerosol was determined using the high resolution capabilities of the HR-ToF-AMS following the Peak Integration by Key Analysis (PIKA) and Analytical Procedure for Elemental Separation (APES) templates (DeCarlo, et al. 2006, Aiken, et al. 2008). As a result of both the extensive fragmentation caused by electron impact ionization and the thermal decomposition of molecules by the vaporizer, most of the signal intensity occurred below mass to charge ratio ( $m/z$ ) 100; parent molecular peaks were weak or unobserved except for the PAH's. For the non-PAH species, a relative increase in the signal intensity at  $m/z$  44, (which is a common fragment of oxo- and dicarboxylic acids ( $\text{CO}_2^+$ )) and a relative decrease at  $m/z$  43, (which is a fragment of oxidized organic molecules containing carbonyl groups ( $\text{C}_2\text{H}_3\text{O}^+$ )).

## 2.4 Offline Analysis

### 2.4.1 Organic Carbon (OC) Analysis

OC was collected at 22.2 LPM onto precleaned (600 °C, 8 hours) 47mm diameter QAT Tissuquartz quartz fiber filters (Pall-Gelman, Ann Arbor, MI, USA). OC analysis was performed using an Thermal/Optical Carbon Aerosol Analyzer (Sunset Laboratory, Forest Grove, OR, USA) in the thermal-optical transmittance (TOT) mode following the National Institute for Occupational Safety and Health (NIOSH) Method 5040 protocol (Birch and Cary, 1996, NIOSH method 5040). Positive sampling artifacts induced by sorption of gaseous OC were corrected by subtracting OC measured on a separate quartz filter located behind a Teflon filter. OC was converted to OM assuming a correction factor of 1.5 confirmed by both AMS measured chemical composition and aerosol gravimetric mass balance of aerosol components more details in Turpin et al., 1994 and Hosseini, et al. 2013. The instrument uncertainty of measurement for EC was at 0.1 µg/filter and OC was at 0.09 µg/filter.

### 2.4.2 Anion Analysis

Anions were measured from a Teflon filter. Anions were wetted with isopropyl alcohol and ultrasonically extracted from 47mm Teflo™ (Pall-Gelman, Ann Arbor, MI, USA) substrates in 5 mL Mill-Q water for 20 min. The extracts were subsequently filtered with a 0.45 µm PTFE syringe filter (Pall Co. Ltd, USA) and analyzed by ion chromatography (ICS-1000, Dionex, USA; IonPac ASRS-4 suppressor; IonPac AS11-HC × 250 mm column, 2 mol L<sup>-1</sup> NaOH, 25 µL loop, following the ARB MLD142 method) for Cl<sup>-</sup>, NO<sub>3</sub><sup>-</sup>, and SO<sub>4</sub><sup>2-</sup>. The method detection limits of anions Cl<sup>-</sup>, NO<sub>3</sub><sup>-</sup> and SO<sub>4</sub><sup>2-</sup> were 0.74,

1.37 and 1.96 mg L<sup>-1</sup>, respectively. The uncertainty of the instrument for anion analysis was 1.98, 1.9 and 1.95 mgL<sup>-1</sup> for Cl<sup>-</sup>, NO<sub>3</sub><sup>-</sup> and SO<sub>4</sub><sup>2-</sup> respectively.

### **2.4.3 Levoglucosan and PAH Analysis**

47-mm quartz substrates were spiked with <sup>13</sup>C labeled levoglucosan (Cambridge Isotope Laboratories Inc., Andover, MA) and an internal recovery PAH standard (naphthalene-d8, acenaphthene-d10, phenanthrene-d10, chrysene-d12, perylene-d12, hexadecane-d34, and tetracosane-d50). Filters were subsequently extracted in dichloromethane and acetone (50:50) with a Dionex® Accelerated Solvent Extractor 200 (ASE; 21 minutes, 1500 psi and 100 °C). The extracted samples were split 50:50 for levoglucosan and PAH analysis.

#### **2.4.3.1 Polycyclic Aromatic Hydrocarbons (PAH)**

The PAH extract was rotary evaporated to 5 mL and then further concentrated to a volume of 1.5 mL under a gentle purified nitrogen stream. 25 µL were subsequently injected through an Agilent Programmable Temperature Vaporizer (PTV) inlet into an Agilent 6890N GC (0.32mm internal diameter; 60mDB-5ms select PAH column) equipped with a 5973N MS detector operating in electrical ionization mode. Quantification was performed using a five-point calibration and target ion extraction. The analysis is a modified version of EPA Method TO-13A.

#### **2.4.3.2 Levoglucosan**

The Levoglucosan extract was rotary evaporated to 5 mL was and further reduced to a 250µL aliquot with a gentle nitrogen stream. 50 µL of the aliquot was transferred into an amber vial and evaporated to dryness using a nitrogen stream. Levoglucosan was then derivatized by adding 50µL of N, O-bis (trimethylsilyl) trifluoroacetamide and 25µL of

pyridine (Sigma-Aldrich Chemle GmbH, Switzerland) followed by heating at 70°C for 2 hours. The derivatized sample was diluted with acetone and analyzed by GC-MS at the same operating conditions used during PAH analysis. Fragments m/z 217 and m/z 333 was used for quantification. The uncertainty for GC measurements was 6.6% while the HR-TOF-AMS were 8.4%.

#### **2.4.3.3 Possible Offline Artifacts**

This section briefly discusses the possible offline artifacts that could cause a bias between the real-time (HR-ToF-AMS) and offline reference methods. The particle size cut point of HR-ToF-AMS is between 50-100nm. Hosseini, et al. 2012 describe the particle size distribution for these biomass burns which show that all the particles resulting from the burns were in the range of total capture of the HR-ToF-AMS. The temperature of the transfer line is important to be considered to avoid thermophoretic losses. Positive filter artifact if present will lower filter GC-MS PAH measurements and increase the PAHs measured by HR-ToF-AMS. If the length of the transfer line is long, then the HR-ToF-AMS measurements biased higher. The filter vaporization losses were negligible as no trend was seen between the slope and vaporization or molecular weight of PAHs. Errors on behalf of GC-MS could also be seen since the methods used were traditional methods and they could be subject to artifacts caused by percentage of recoveries. Finally, biases could also be observed due to gas-particle partitioning differences.

## 2.5 Instrument Inter-comparison Results

### 2.5.1 HR-ToF-AMS versus ECOC Analyzer

Filter-based organic mass derived from ECOC analysis compared directly to integrated organic mass HR-ToF-AMS measurements for all laboratory burns (Figure 3). A 50% particle collection efficiency (CE) for organic particles collected by the HR-ToF-AMS (Docherty, et al. 2013) yields a 1:1 correlation with the ECOC analyzer, similar to that obtained by (Takegawa, et al. 2005) and (Allan, et al. 2004). An excellent regression of 0.92 ( $r^2$ ) is observed between the instruments.

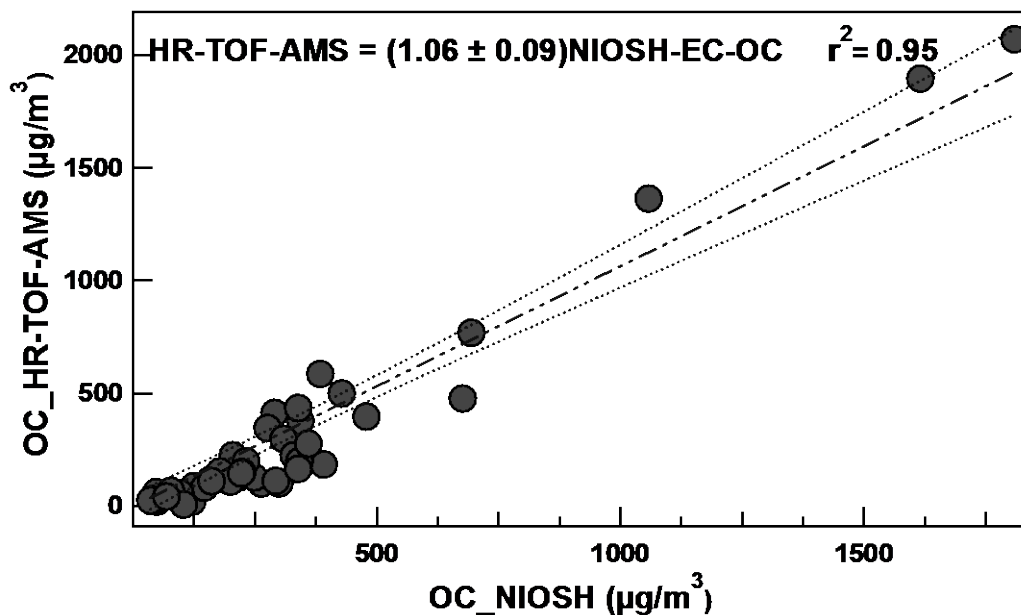


**Figure 3 Comparison of online (HR-ToF-AMS) to offline (filter NIOSH EC-OC) for the Organic Carbon mass during real-time biomass burning.**



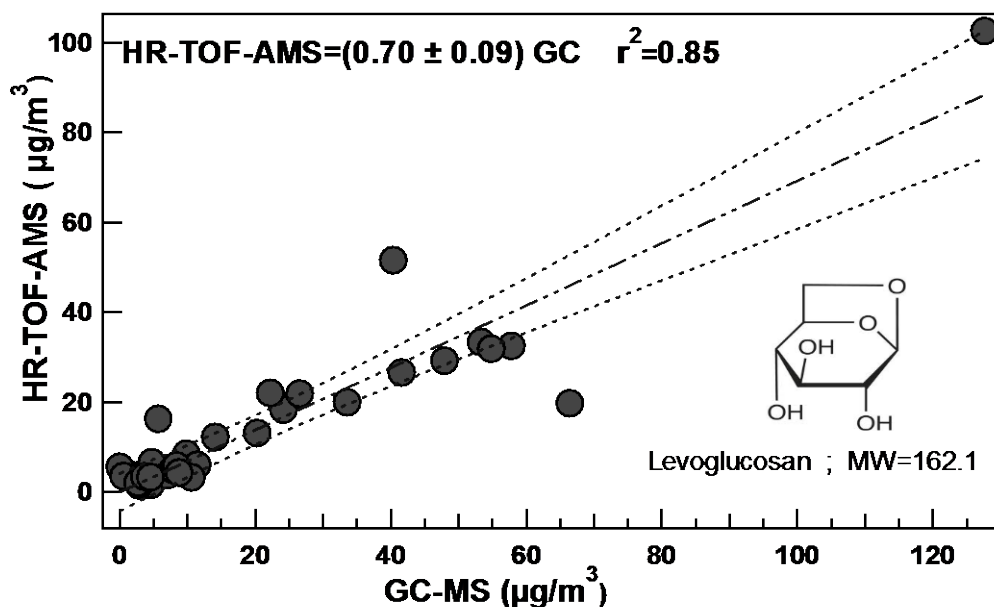
## 2.5.2 HR-ToF-AMS versus GC-MS

### 2.5.2.1 Levoglucosan

Levoglucosan (1,6-anhydro- $\beta$ -D-glucopyranose), a byproduct of cellulosic partial oxidation, is widely used as a biomass burning marker (e.g., Shauer, et al. 2001, Simoneit, et al. 2002, Frasier and Lakshmanan, et al. 2000, Zhang, et al. 2008) although there is some concern about its atmospheric stability (e.g., Robinson, et al. 2010). The gas chromatography (GC) method for quantifying levoglucosan is tedious and requires long sample preparation and derivitization times. The HR-ToF-AMS provides an attractive, alternative, realtime measure for levoglucosan.

Cleavage of levoglucosan by EI ionization yields the major fragmented ions of  $C_2H_4O_2^+$  at  $m/z$  60.021 and  $C_3H_5O_2^+$  at  $m/z$  73.029 (Alfarra, et al. 2007, Mohr, et al. 2009, Schneider, et al. 2006). The  $m/z$  73 is observed to contain two fragmented ions: a levoglucosan fragment  $C_3H_5O_2^+$  ( $m/z$  73.0301) and an interfering  $C_3H_7NO^+$  ( $m/z$  73.0378) for most fuel types in this study. However, the UMR 60 fragment contains only one high resolution peak ( $m/z$  60.021) for all fuels types within this study. Therefore,  $m/z$  60 is recommended as being the best UMR for levoglucosan similar to the study by Alfarra, et al. 2007. The UMR at  $m/z$  60 was normalized by the expected fractional fragmentation of the parent molecule to  $m/z$  60 from the NIST EI mass spectral database (NIST mass spec data center). The AMS levoglucosan values correlate well (slope=0.7,  $r^2=0.85$ ) with filter based offline GC-MS measurements (Figure 5) although the HR-ToF-AMS is found to consistently underestimate levoglucosan by ~30% for these burns. The removal of the largest OC ( $>100 \mu\text{g}/\text{m}^3$ ) changed the slope, intercept and regression to 0.538, 2.9 and 0.725. This contrasts the observations from (Lee, et al. 2010) who

observed a positive AMS bias of 1.5 when they co-related their AMS  $C_2H_4O^+$  signal with filter based levoglucosan, and a positive bias of 8.5 when they co-related the same AMS signal with filter based levoglucosan+mannosan+galactosan.

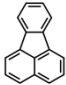
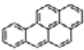
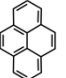
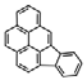
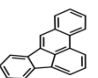
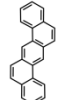
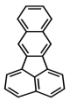
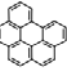


**Figure 4 Comparison of online (HR-ToF-AMS) to offline (filter GCMS) for Levoglucosan mass during real-time biomass burning.**

#### 2.5.2.2 Polycyclic Aromatic Hydrocarbons

There are very few studies comparing online AMS PAH measurements with traditional offline methods. Dzepina, et al. 2007 is one such study comparing UMR Q-AMS to offline filter GC-MS measurements of ambient particle phase PAH's. They observed that the ambient particle phase PAH measurements by Q-AMS exceeded (in the range of 0.3 to  $0.8 \text{ ngm}^{-3}$ ) their GC-MS filter measurements for some PAH's. Whereas Poulain, et al. 2011 observed a strong correlation ( $\text{AMS} = (0.77 \pm 0.05) \text{PM CPP-GC-MS}$ ;  $r^2 = 0.97$ ) between their AMS PAH concentrations and the sum of 18 identified filter based CPP-GC-MS PAH measurements.

PAHs evaluated as part of this study and their major fragmentation ion is provided in Table 1. Sixteen PAH's were quantified on the filter using offline GC-MS techniques (section 2.3.2.1); however, only PAHs expected to be predominantly in the particle-phase were considered for comparison to HR-ToF-AMS. PAH's from offline analysis with identical major  $m/z$  fragment ions were totaled and correlated against the UMR signal from the HR-ToF-AMS (Figure 5, Figure 6, Figure 7, Figure 8) AMS particle phase PAH measurements are found to greatly exceed GC-MS measurements. Interferences on the HR-ToF-AMS from other organics were investigated on a UMR basis using the subtraction procedure outlined by (Dzepina, et al. 2007); using this method interference by other organics was estimated to be very low. Further, the high resolution spectrum indicates that the only fragment at the given UMR was consistent with the targeted PAH. Additionally, lab prepared PAH solutions were analyzed on the HR-ToF-AMS and the resulting concentration on the HR-ToF-AMS greatly exceeded the initial concentration. The HR-ToF-AMS bias may be attributable to surface ionization (Murphy, et al. 2006), although additional work must be conducted to verify this explanation.

Molecular Structure, Chemical name & Molecular weight of the PAH's determined by HR-TOF-AMS in this study			
	Fluoranthene C <sub>16</sub> H <sub>10</sub> 202.25		Benzo(a)pyrene C <sub>20</sub> H <sub>12</sub> 252.30
	Pyrene C <sub>16</sub> H <sub>10</sub> 202.07		Indeno(1,2,3-cd)pyrene C <sub>22</sub> H <sub>12</sub> 276.33
	Benzo(b)fluoranthene C <sub>20</sub> H <sub>12</sub> 252.30		Dibenz(a,h)anthracene C <sub>22</sub> H <sub>14</sub> 278.10
	Benzo(k)fluoranthene C <sub>20</sub> H <sub>12</sub> 252.30		Benzo(ghi)perylene C <sub>22</sub> H <sub>12</sub> 276.33

**Table 1 Summary of the Polycyclic Aromatic Hydrocarbons quantified during this study**

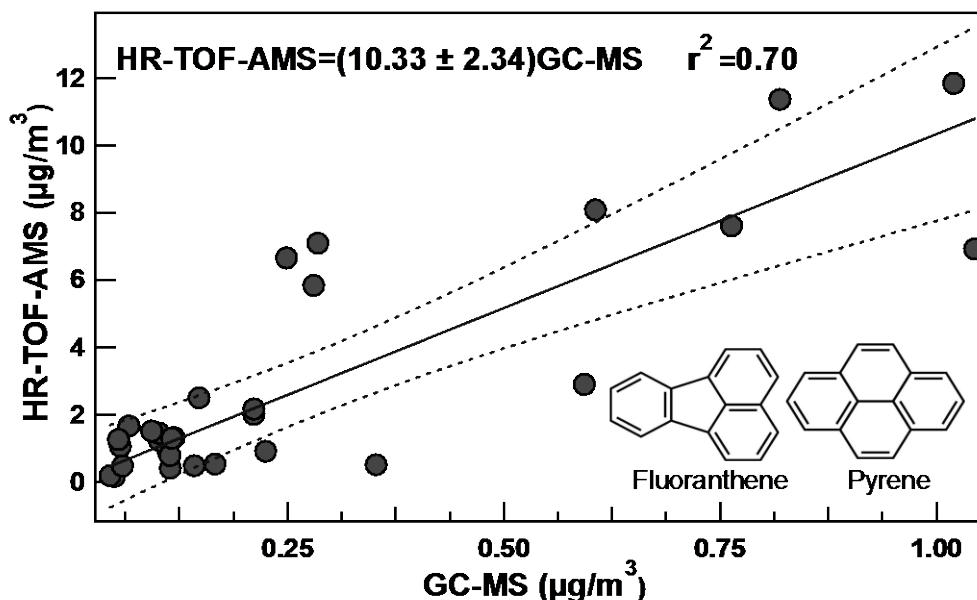


**Figure 5 Comparison of online (HR-ToF-AMS) to offline (filter GC-MS) for the sum of PAH's during real-time biomass burning for fluoranthene and pyrene;**

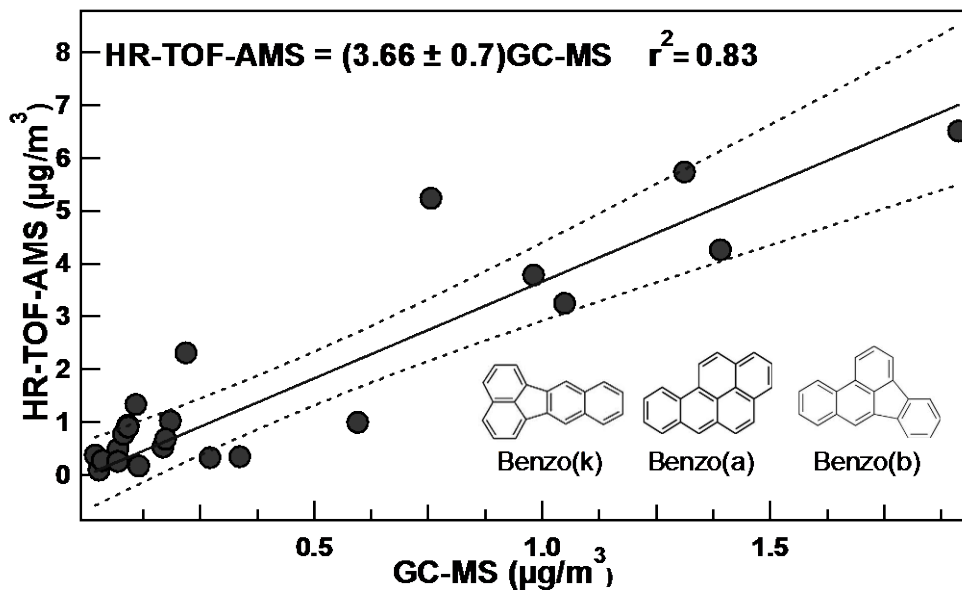


Figure 6 Comparison of online (HR-ToF-AMS) to offline (filter GC-MS) for the sum of PAH's during real-time biomass burning for benzo(k)fluoranthene, benzo(a)pyrene and benzo(b)fluoranthene;

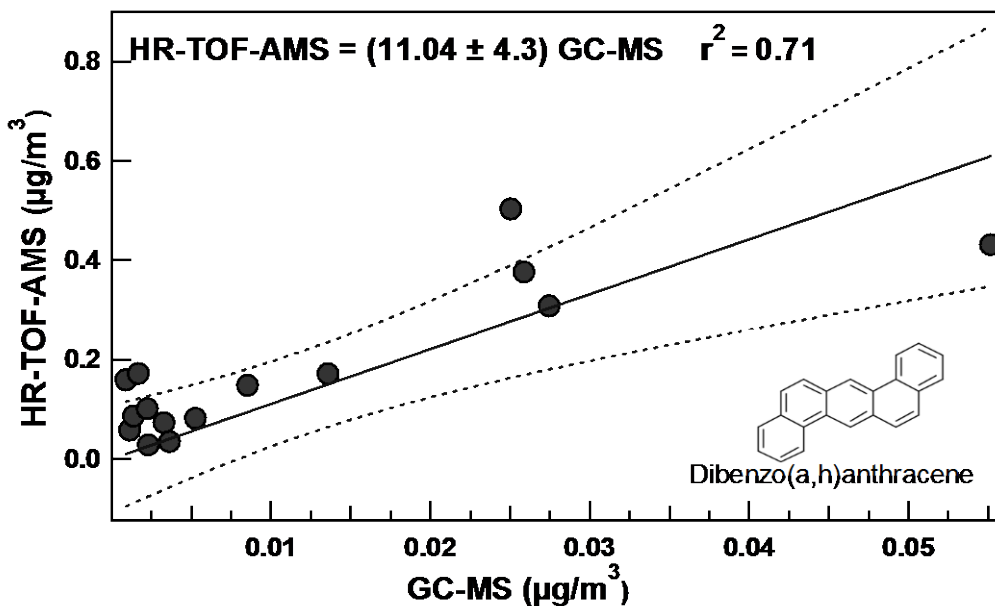
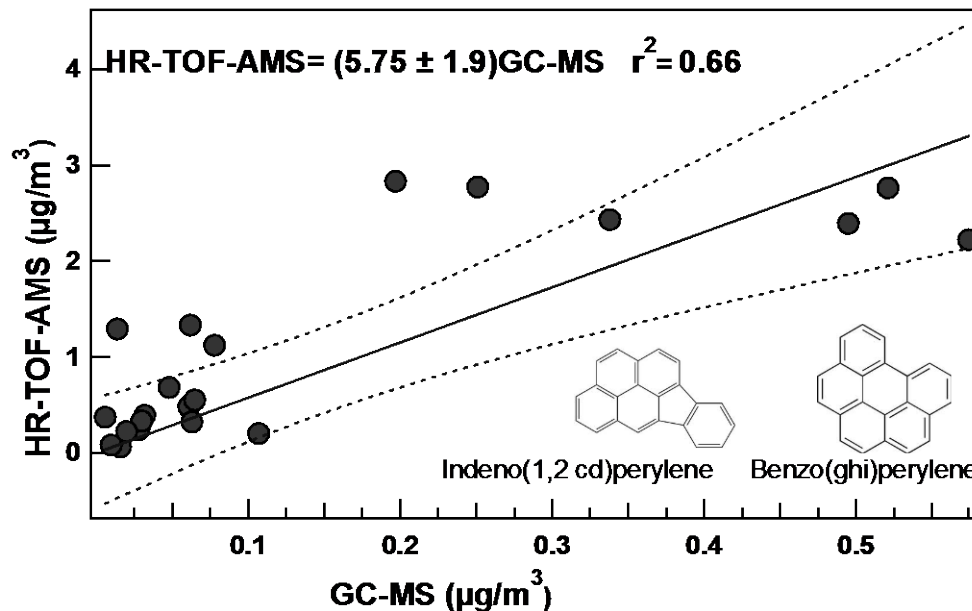


Figure 7 Comparison of online (HR-ToF-AMS) to offline (filter GC-MS) for the sum of PAH's during real-time biomass burning for dibenzo(a,h)anthracene



**Figure 8 Comparison of online (HR-ToF-AMS) to offline (filter GC-MS) for the sum of PAH's during real-time biomass burning for indeno(1,2cd)perylene and benzo(ghi)perylene;**

### 2.5.3 HR-ToF-AMS versus Ion Chromatograph

Filter based ions ( $\text{Cl}^-$ ,  $\text{NO}_3^-$ ,  $\text{SO}_4^{2-}$ ) are correlated against integrated HR-ToF-AMS measurements assuming an AMS ion collection efficiency of 1.0 (Figure 9, Figure 10, Figure 11). The standard mass fragments  $m/z$  30 ( $\text{NO}$ ) and  $m/z$  46 ( $\text{NO}_2$ ) for  $\text{NO}_3^-$ ,  $m/z$  48 ( $\text{SO}$ ) and  $m/z$  64 ( $\text{SO}_2$ ) for  $\text{SO}_4^{2-}$ , and  $m/z$  35 for  $\text{Cl}^-$  are used to quantify each of the anions in the HR-ToF-AMS. The HR-ToF-AMS response is observed to be low for  $\text{Cl}^-$  ( $0.11 \pm 0.02$ ,  $R^2=0.52$ ) and  $\text{SO}_4^{2-}$  ( $0.35 \pm 0.04$ ,  $R^2=0.78$ ) and high for  $\text{NO}_3^-$  ( $1.25 \pm 0.30$ ,  $R^2=0.44$ ); weaker  $R^2$  values and lower AMS responses than typically observed for ambient AMS-anions instrument comparisons (Takegawa, et al. 2005, Drewnick, et al. 2003) are observed for woodsmoke emissions.

XRF filter analysis (Hosseini, et al. 2013) reveals that elements  $K^+$ ,  $Cl^-$ ,  $Na^+$  and  $S^{2-}$  comprise >90% of the in-organic elemental mass (elements listed in order of decreasing filter loadings). For each filter loading, it is expected that  $Cl^-$  will preferentially form KCl salts (Levin, et al. 2010). Freney, et al. 2009 further reports in a separate study that the majority of salts formed in their biomass burns were KCl. As KCl is a refractory salt (thermal decomposition temperature of  $770^{\circ}C$ ), it is not expected to volatilize on the AMS vaporizer, consistent with the low  $Cl^-$  measurements on HR-ToF-AMS. The refractory nature of HR-ToF-AMS was confirmed by analyzing laboratory generated fried KCl particles. Therefore, the low AMS Cl readings observed are readily explained; use of a correction factor based on the slope of the regression is not recommended. Use of higher vaporizer temperatures ( $>\sim 770^{\circ}C$ ) should improve the  $Cl^-$  signal in biomass plumes.

$K^+$  not bound by  $Cl^-$  is expected to apportion to  $NO_3^-$  next followed by  $SO_4^{2-}$  to form  $KNO_3$  and  $K_2SO_4$  salts, respectively.  $KNO_3$  and  $K_2SO_4$ , similar to KCl, are refractory salts (thermal decomposition temperature of  $400^{\circ}C$  and  $1069^{\circ}C$ , respectively) were not observed (confirmed with lab generated KCl and  $K_2SO_4$ ) by the HR-ToF-AMS. However, insufficient  $K^+$  remains to bind all available sulfates into  $K_2SO_4$  salts. The slope from regression of HR-ToF-AMS  $SO_4^{2-}$  vs IC  $SO_4^{2-}$  is 0.35 and so the greater fraction detected by IC is  $1-0.35= 0.65$ . The remainder of the sulfate is available as sulfuric acid leading to the detection of 35% of the available sulfur and the improved correlation ( $r^2=0.78$ ) between the HR-ToF-AMS and filter based offline measurements. This likely leaves the remainder of the sulfate available as sulfuric acid leading to the

detection of a greater fraction (0.35) of the available sulfur and the improved correlation ( $r^2=0.78$ ) between HR-ToF-AMS and filter based offline measurements. It is important to recognize that biomass burning has high K compared to typical ambient conditions leading to these less robust ion relationships between ions and HR-ToF-AMS.

HR-ToF-AMS based nitrates concentrations were found to correlate closest to IC measurements, with a slight positive bias observed for the nitrate ion.  $\text{KNO}_3$ , unlike other potassium salts, thermally decomposes at typical AMS vaporizer temperatures and is readily detected by the HR-ToF-AMS. Some positive bias is attributed to additional NO and  $\text{NO}_2$  fragments from nitrogen bound organics (Farmer, et al. PNAS 2010).

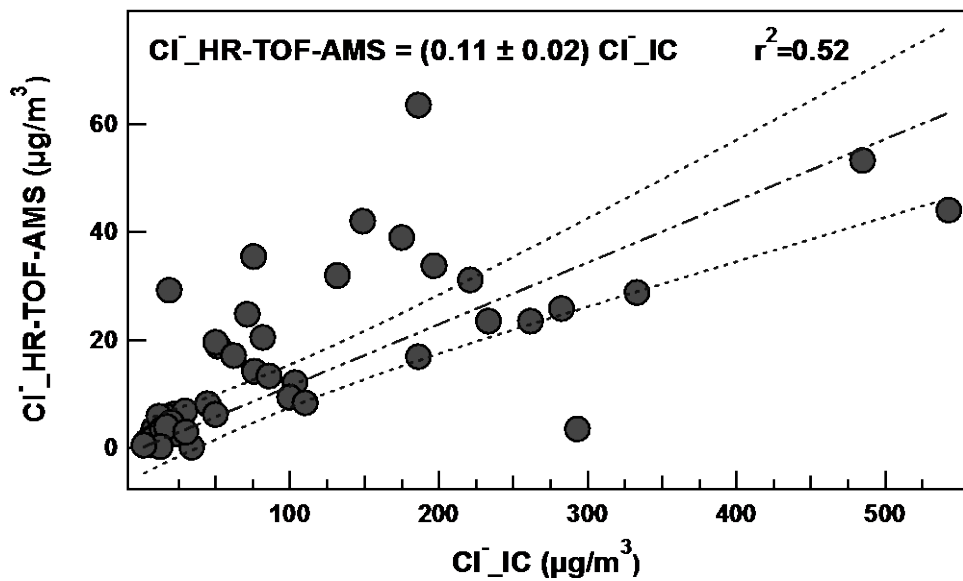


Figure 9 Comparison of online (HR-ToF-AMS) to offline (filter IC) for  $\text{Cl}^-$  fresh biomass smoke plumes



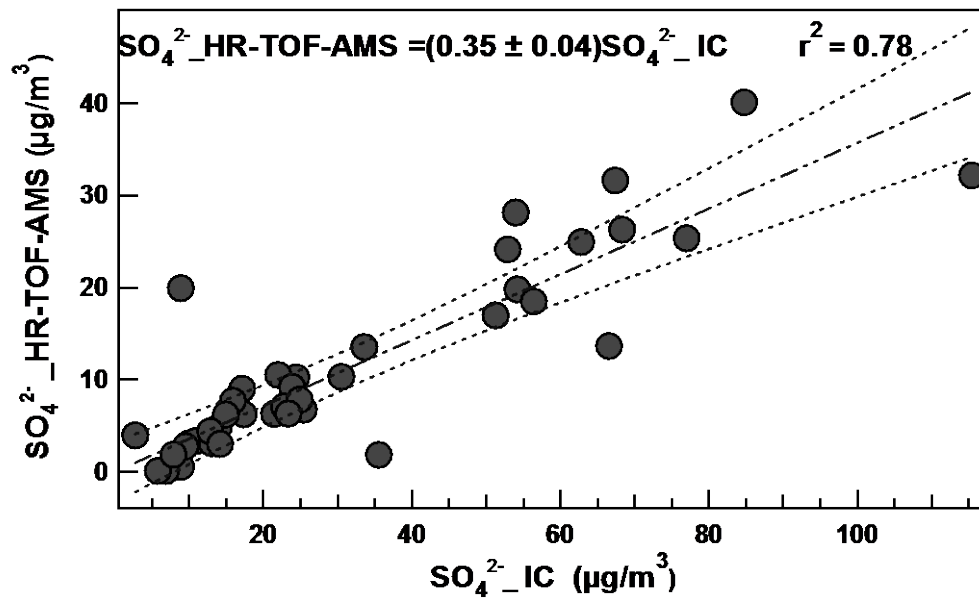


Figure 10 Comparison of online (HR-ToF-AMS) to offline (filter IC) for  $SO_4^{2-}$  fresh biomass smoke plumes

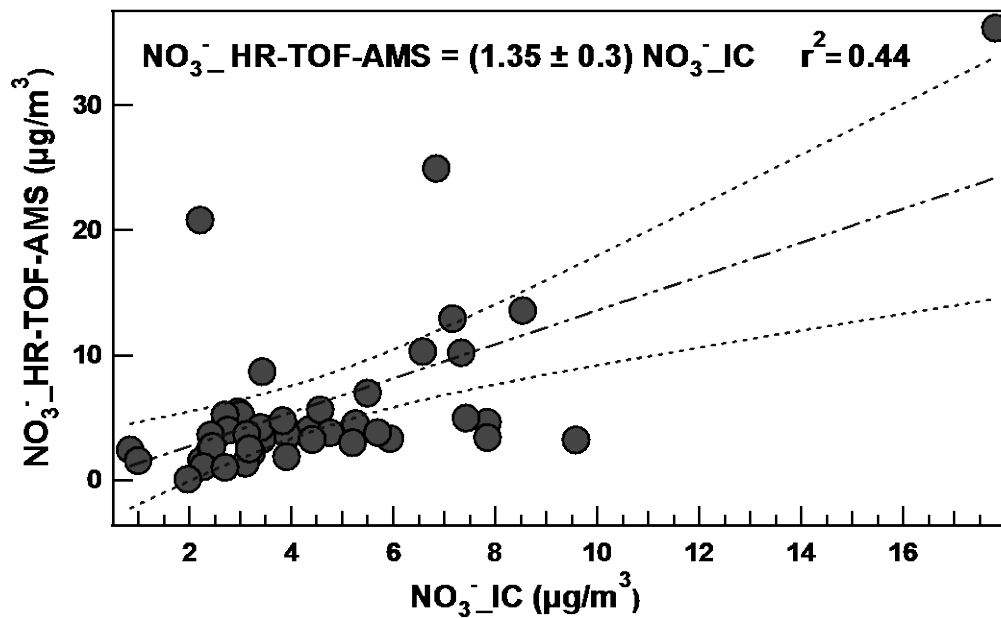


Figure 11: Comparison of online (HR-ToF-AMS) to offline (filter IC) for  $NO_3^-$  in fresh biomass smoke plumes

## 2.6 Summary and Conclusion

The summary of the inter comparison between different instruments is tabulated below.

<b>Instrument Inter-comparison Results</b>				
<b>Species</b>	<b>Fit Parameters<sup>a</sup></b>		<b>Instruments</b>	
	<b>Slope</b>	<b>r<sup>2</sup></b>		
Organic Carbon	1.06±0.09	0.95	AMS vs EC/OC	
Nitrates	1.35±0.3	0.44		
Sulphates	0.35±0.04	0.78	AMS vs IC	
Chlorides	0.11±0.02	0.52		
Levoglucosan	0.7±0.09	0.85	AMS vs GC-MS	
Fluoranthene+Pyrene	10.33±2.34	0.70		
(Benzo(b) + Benzo(k))Fluoranthene + Benzo(a)Pyrene	3.66±0.97	0.83	AMS vs GC-MS	
Indeno(1,2,3-cd)Perylene+Benzo(ghi) Perylene	5.75±1.99	0.66		
Dibenz(a,h)anthracene	11.04±4.3	0.71		

<sup>a</sup> Fit Co-efficient Confidence Intervals at 99% Confidence Interval; Linear Fit

Overall, OC measurement by HR-ToF-AMS correlated well with offline measurements, whereas the chlorides and sulfates were under estimated due to formation of refractory salts of potassium during wildland fires. Levoglucosan estimates from HR-ToF-AMS using UMR of 60 correlated well with offline GC-MS characterization; however a 30% underestimation in the online technique is observed. PAHs were not estimated well using selected HR-ToF-AMS m/z (UMR) fragments; further investigations are necessary to understand why the PAH measurements from the HR-ToF-AMS greatly exceeded particle phase PAH's measured by GC-MS from PAHs collected on the filter. These comparisons support use of HR-ToF-AMS estimates of OC, nitrates and levoglucosan for fresh biomass burning, while caution should be used in estimating sulfates, chlorides, and PAHs.

## References:

1. DeCarlo, P.F., Kimmel, J.R., Trimborn, A., Northway, M.J., Jayne, J.T., Aiken, A.C., Gonin, M., Fuhrer, K., Horvath, T., Docherty, K., Worsnop, D.R., and Jimenez, J.L.: Field-Deployable, High-Resolution, Time-of-Flight Aerosol Mass Spectrometer, *Anal. Chem.* 78, 8281-8289, 2006.
2. Jayne, J.T., D.C. Leard, X. Zhang, P. Davidovits, K.A. Smith, C.E. Kolb, and D.R. Worsnop, Development of an Aerosol Mass Spectrometer for Size and Composition. *Analysis of Submicron Particles, Aerosol Science and Technology*, 33, 49-70, 2000
3. Jimenez, J.L., J.T. Jayne, Q. Shi, C.E. Kolb, D.R. Worsnop, I. Yourshaw, J.H. Seinfeld, R.C. Flagan, X. Zhang, K.A. Smith, J. Morris, and P. Davidovits, Ambient Aerosol Sampling with an Aerosol Mass Spectrometer. *Journal of Geophysical Research - Atmospheres*, 108(D7), 8425, doi:10.1029/2001JD001213, 2003.
4. Allan, J.D., J.L. Jimenez, H. Coe, K.N. Bower, P.I. Williams, and D.R. Worsnop, Quantitative Sampling Using an Aerodyne Aerosol Mass Spectrometer. Part 1: Techniques of Data Interpretation and Error Analysis, *Journal of Geophysical Research – Atmospheres*, Vol. 108, No. D3, 4090, doi:10.1029/2002JD002358, 2003.
5. Drewnick, F., S.S. Hings, P.F. DeCarlo, J.T. Jayne, M. Gonin, K. Fuhrer, S. Weimer, J.L. Jimenez, K.L. Demerjian, S. Borrmann, D.R. Worsnop. A new

- Time-of-Flight Aerosol Mass Spectrometer (ToF-AMS) – Instrument Description and First Field Deployment, *Aerosol Science and Technology*, 39:637–658, 2005.
6. Middlebrook, A., D.M. Murphy, S.H. Lee, D.S. Thomson, K.A. Prather, R.J. Wenzel, D.Y. Liu, D.J. Phares, K.P. Rhoads, A.S. Wexler, M.V. Johnston, J.L. Jimenez, J.T. Jayne, D.R. Worsnop, I. Yourshaw, J.H. Seinfeld, and R.C. Flagan, An Comparison of Particle Mass Spectrometers During the 1999 Atlanta Supersite Project, *Journal of Geophysical Research-Atmospheres*, 108(D7), 8424, doi:10.1029/2001JD000660, 2003
  7. Hogrefe, O., J.J. Schwab, F. Drewnick, G.G. Lala, S. Peters, K.L. Demerjian, K. Rhoads, H.D. Felton, O.V. Rattigan, L. Husain, and V.A. Dutkiewicz, Semicontinuous PM<sub>2.5</sub> Sulfate and Nitrate Measurements at an Urban and a Rural Location in New York: PMTACS-NY Summer 2001 and 2002 Campaigns. *Journal of Air and Waste Management Association*, 54:1040–1060.
  8. Boudries, H., M.R. Canagaratna, J.T. Jayne, R. Alfarra, J. Allan, H. Coe, S.C. Pryor, J.L. Jimenez, J.R. Brook, S. Li, and D.R. Worsnop, Chemical and Physical Processes Controlling the Distribution of Aerosols in the Lower Fraser Valley, Canada, During the PACIFIC 2001 Field Campaign, *Atmospheric Environment*, 38: 5759–5774, 2004
  9. Takegawa, N., Y. Miyazaki, Y. Kondo, Y. Komazaki, T. Miyakawa, J.L. Jimenez, J.T. Jayne, D.R. Worsnop, J. Allan, and R. J. Weber (2005), Characterization of an Aerodyne Aerosol Mass Spectrometer (AMS): Intercomparison with other Aerosol Instruments, *Aerosol Science and Technology*, 39, 760-770, 2005

10. Topping, D., H. Coe, G. McFiggans, R. Burgess, J. Allan, M. R. Alfarra, K. Bower, T. W. Choularton, S. Decesari, and M. C. Facchini, Aerosol Chemical Characteristics from Sampling Conducted on the Island of Jeju, Korea During ACE-Asia. *Atmospheric Environment*, 38 (14) 2111-2123, doi:10.1016/j.atmosenv.2004.01.022, 2004.
11. Schneider, J., S. Borrmann, A. G. Wollny, M. Bläsner, N. Mihalopoulos, K. Oikonomou, J. Sciare, A. Teller, Z. Levin, and D. R. Worsnop, Online Mass Spectrometric Aerosol Measurements During the MINOS Campaign (Crete, August 2001), *Atmospheric Chemistry and Physics*, 4(1), 65-80, 2004.
12. Zhang, Q., C. O. Stanier, M. C. Canagaratna, J. T. Jayne, D. R. Worsnop, S. Pandis, and J. L. Jimenez, Insights into the Chemistry of New Particle Formation and Growth Events in Pittsburgh Based on Aerosol Mass Spectrometry, *Environmental Science & Technology*, 38: 4797-4809, 2004.
13. Burling, I. R., Yokelson, R. J., Griffith, D. W. T., Johnson, T. J., Veres, P., Roberts, J. M., Warneke, C., Urbanski, S. P., Reardon, J., Weise, D. R., Hao, W. M., and de Gouw, J. Laboratory measurements of trace gas emissions from biomass burning of fuel types from the southeastern and southwestern United States, *Atmos. Chem. Phys.*, 10, 11115–11130, doi:10.5194/acp-10-11115-2010, 2010
14. Yokelson, R. J., D. W. T. Griffith, and D. E. Ward, Open-path Fourier transform infrared studies of large-scale laboratory biomass fires, *J. Geophys. Res.*, 101, 21067-21080, 1996.

15. H.Agrawal, Q.G.J.Malloy, W.Welch, J.Miller, D.Cocker, "In-use gaseous and particulate matter emissions from a modern ocean going container vessel," *Atmospheric Environment*, 42, 21, 5504-5510, 2008.
16. DeCarlo, P.F., J.R. Kimmel, A. Trimborn, M.J. Northway, J.T. Jayne, A.C. Aiken, M. Gonin, K. Fuhrer, T. Horvath, K. Docherty, D.R. Worsnop, and J.L. Jimenez, Field-Deployable, High-Resolution, Time-of-Flight Aerosol Mass Spectrometer, *Analytical Chemistry*, 78: 8281-8289, 2006.
17. A.C. Aiken, P.F. DeCarlo, and J.L. Jimenez. Elemental Analysis of Organic Species with Electron Ionization High-Resolution Mass Spectrometry. *Analytical Chemistry*, 79, 8350-8358, doi:10.1021/ac071150w, 2007
18. Aiken, A.C., P.F. DeCarlo, J.H. Kroll, D.R. Worsnop, J.A. Huffman, K. Docherty, I.M. Ulbrich, C. Mohr, J.R. Kimmel, D. Sueper, Q. Zhang, Y. Sun, A. Trimborn, M. Northway, P.J. Ziemann, M.R. Canagaratna, T.B. Onasch, R. Alfarra, A.S.H. Prevot, J. Dommen, J. Duplissy, A. Metzger, U. Baltensperger, and J.L. Jimenez. O/C and OM/OC Ratios of Primary, Secondary, and Ambient Organic Aerosols with High Resolution Time-of-Flight Aerosol Mass Spectrometry *Environmental Science & Technology*, 42, 4478–4485, doi: 10.1021/es703009q, 2008
19. Simoneit, B. R. T.: Biomass burning – A review of organic tracers for smoke from incomplete combustion, *Appl. Chem.* 17, 129-162, 2002.
20. Rebecca J. Sheesley , J. Schauer Zohir Chowdhury , Glen R. Cass, Bernd R. T. Simoneit Characterization of organic aerosols emitted from the combustion of

biomass indigenous to South Asia, *Journal of Geophysical Research*, vol. 108, NO. D9, 4285, doi:10.1029/2002JD002981, 2003

21. Fraser, M. P., and Lakshmanan, K.: Using levoglucosan as a molecular marker for the long-range transport of biomass combustion aerosols, *Environ. Sci. Technol.* 34 (21), 4560-4564, 2000.
22. Robinson, A. L., Subramanian, R., Donahue, N. M., Bernardo-Bricker, A., and Rogge, W. F.: Source apportionment of molecular markers and organic aerosol. 2. Biomass smoke, *Environ. Sci. Technol.* 40(24), 7811-7819, doi:10.1021/es060782h, 2006.
23. Alfarra, M. R., Prévôt, A. S. H., Szidat, S., Sandradewi, J., Weimer, S., Lanz, V., Schreiber, D., Mohr, M. and Baltensperger, U.: Identification of the mass spectral signature of organic aerosols from wood burning emissions, *Environ. Sci. Technol.* 41, 5770-5777, doi:10.1021/es062289b, 2007
24. Dzepina, K., J. Arey, L.C. Marr, D.R. Worsnop, D. Salcedo, Q. Zhang, L.T. Molina, M.J. Molina, and J.L. Jimenez, Detection of Particle-Phase Polycyclic Aromatic Hydrocarbons in Mexico City using an Aerosol Mass Spectrometer, *International Journal of Mass Spectrometry*, 263(2-3), 152-170, 2007
25. Turpin, B.J., Huntzicker, J.J., Hering, S.V., 1994. Investigation of organic aerosol sampling artifacts in the Los Angeles Basin. *Atmospheric Environment* 28, 3061–3071.

### **3 Real World Cycles Better Gauge the Efficiency of Recent NOx Emissions for Heavy-duty, Diesel Trucks**

#### **3.1 Introduction**

Emissions from port activities are associated with five sources: ships, harbor craft, cargo handling equipment, locomotives and trucks. While regulations have reduced emissions from all five sources, these sources remain a concern as their percent contribution to the local inventory of criteria and toxic pollutants continues to grow. This is especially true for an area with considerable port activity and one where the air fails to meet air quality standards, like Los Angeles. Substandard air quality represents a major health concern for residents of port communities (San Pedro Bay Ports CAAP 2006). Regional

One area of concern was emissions from heavy-duty truck engines associated with the goods movement, mainly because of the number of trucks involved in a city with a large port. For example, in Los Angeles about 40% of all containerized trade enters the United States, and there are about 10,000 number of heavy-duty, diesel trucks (HDDT) working the ports. These trucks remain a significant source of oxides of nitrogen (NOx) <sup>1</sup>. In order to reduce emissions of NOx and particulate matter (PM), a series of Federal regulations for HDDT's were implemented starting in 1990 requiring NOx emissions to be reduced from 10.7 g/bhp-hr to 0.2 g/bhp-hr<sup>7</sup> when the engine is tested on an engine dyno while following the federal test procedure. The new standards included in-use measurements and a defined "Not to Exceed" (NTE) zone within the engine map where emissions must meet certification standards. See appendix about meaning of NTE.



Meeting tough PM and NOx emissions standards required advanced fuels and engine technology with exhaust treatment systems. For example, for natural gas fuelled engines, particular matter (PM) is low and NOx control requires a three-way catalyst system<sup>8</sup>. For diesel fuelled engines, PM is controlled with a Diesel Particulate Filter (DPF) and NOx is controlled with a cooled exhaust gas recirculation (EGR) and a selective catalytic reduction (SCR) unit. SCR's operating with urea added to the exhaust is reported to be greater than 75% efficient in reducing NOx<sup>2</sup>. However, the exhaust temperature is critical for when urea is introduced and for catalyst conversion efficiency<sup>3</sup> in reducing NOx emissions. Optimum operation of the SCR systems depends on a number of factors including catalyst composition, exhaust flow and exhaust temperature. Outside the design region, the catalyst efficiency for NOx conversion is low and NH<sub>3</sub> emissions are higher than desired<sup>4</sup>.

In this research nine HDDTs were tested on a chassis dynamometer following driving cycles that simulated both the certification cycle and a number of real-world operations representing goods movement from the ports or distribution centers. The HDDTs represented different manufacturers and control technologies. A critical question in this research was whether the emissions factors from certification runs should be used in development of inventories or whether the emission values from real-world/off-certification cycles more accurately represented the emissions values. A similar question was asked about the year 2000 model engines when it was found that off-certification cycles more accurately represented values needed for developing inventories associated with HDDTs<sup>9</sup>.

## 3.2 Experimental Section

### 3.2.1 Test Vehicles and Fuels

Nomenclature	Odometer	Model	MY	Disp. L	rated HP	Control	Cert. (g/bhp-h)
C8.3	14,269	CumminsM2	2010	8.3	300 @ 2100	DPF+SCR	0.2
C11.9	4,769	Cummins ISX	2011	11.9	425 @ 1800	DPF+SCR	0.12
V12.8	36,982	Volvo Mack MP8445C	2011	12.8	445 @ 1500	DPF+SCR	0.2
N12.4c	80,651	Navistar MAXXFORCE13	2011	12.4	475 @ 1700	DPF+Adv EGR	0.5
N12.4b	67,373	Navistar 12WZJB	2011	12.4	430 @ 1700	DPF+Adv EGR	0.46
N12.4a	80,412	Navistar MAXXFORCE13	2009	12.4	430 @ 1700	DPF+Adv EGR	1.2
D14a	1,29,815	DDC/60	2008	14	425 @ 1800	DOC/DPF	1.07
D14b	1,21,766	DDC/60	2008	14	425 @ 1800	DOC/DPF	1.07
DDC RT		DDC/60	1998	12.7	426 @ 1800	Retro SCRT	4

**Table 2 Detailed information of the HDDT's tested**

Selected properties of the engines and controls used in the nine HDDT's tested in this research are in Table 2. The table provides the information on the vehicle make, model year, displacement, rated horse power, the after treatment system, certification value for NO<sub>x</sub> and the test cycles. Vehicles represented a mix of manufacturers and control technologies that were being used in commercial service. The 1998 Detroit diesel engine had a retrofit SCR and an ammonia slip catalyst. Before testing, vehicle maintenance records for engine repairs, brakes, steering, fluids, and tires were reviewed to ensure safe operation. The inspection included a download of the Electronic Control Module (ECM) both before and after the test to ensure there were no active fault codes.

As this research was intended to measure emissions at near in-use/real-world conditions, the engines were fueled with #2 street diesel fuel meeting CARB standards rather than the certification fuels. While CARB street and certification fuels are quite similar, the street fuel is likely to have an aromatic content closer to 20 volume% than the 10 volume% in the certification fuel.

### 3.2.2 Emission Measurements

The heavy duty diesel port trucks were tested on CE-CERT's Heavy-Duty Chassis Dynamometer and emissions measured with UCR's MEL (Mobile Emissions Laboratory) following the Code OF federal Regulations Part 1065/1066. The MEL is a full dilution tunnel emissions sampling system meeting the Code of Federal Regulations requirements<sup>5</sup>. Each test cycle was repeated three times and the emission rates and factors for the regulated and non-regulated pollutants were the average of three tests. For all tests, emissions of THC, NMHC, CH<sub>4</sub>, CO, NO<sub>x</sub>, CO<sub>2</sub>, and PM mass were measured. Measurements of NH<sub>3</sub> were obtained on a real time basis using a tunable diode laser (TDL) <sup>6</sup>. The greenhouse gas, N<sub>2</sub>O, and some non-regulated toxics, such as the carbonyl compounds and C<sub>4</sub>–C<sub>12</sub> hydrocarbons, were measured off-line for all tests. In addition to PM mass, the elemental and organic carbon was determined as was the real-time particle size distribution and number concentration. All of the non-regulated emissions are shown in appendix. In this chapter NO<sub>x</sub> and PM results are discussed.

### 3.2.3 Test Cycles

Veh. Nomenclature	IN-USE TEST CYCLE
<b>C8.3</b> <b>C11.9</b> <b>V12.8</b> <b>N12.4c</b> <b>N12.4b</b> <b>N12.4a</b> <b>D14a</b> <b>D14b</b>	<b>URBAN DYNAMOMETER DRIVING SCHEDULE (cold &amp; hot cycles); PORT CYCLES - (near dock, local &amp; regional cycles)</b>
<b>DDC RT</b>	<b>CRUISE CYCLE ONLY</b>

**Table 3 Test cycles for measuring in use emissions measurements of HDDT's**

Nine trucks with OEM equipment were tested on the EPA Urban Dynamometer Driving Schedule (UDDS) and the drayage port truck cycles shown in Table 2 and one truck retrofitted with a SCR was tested on the cruise cycle. The UDDS cycle was used in the development of the transient Federal Test Procedure (FTP) on an engine dynamometer cycle so values from the UDDS are often compared with values from a FTP “certification test.” Comparison of the two test cycles is in the Supporting Information. The emission value from the UDDS was one of the screening parameters used to confirm that the selected engine was representative of the targeted technology. The test program also included a cold-start UDDS as that is similar to the cold start FTP used in the certification testing. Given the importance of trucking used to move goods to/from the harbors and distribution centers, the testing included three driving schedules developed by TIAX<sup>10</sup>. These cycles were based on the analysis of activity data for over 1,000 Class 8 drayage trucks with a focus on five characteristic operating parameters: average speed, maximum speed, energy per mile, distance, and number of stops. The final port drayage cycles, are represented by three distinct driving cycles, each composed of three phases. Some information is provided in Table 3 and detailed traces i.e. velocity versus time in the Appendix.

Testing for the vehicle retrofit with the SCR was limited to driving at 50mph for 757 seconds so results are described in detail in the Supporting Information. Results of the retrofit truck are included in the discussion section of the Regional Port Cycle as the transient conditions are similar and present a perspective on retrofit technology.

### 3.3 Results and Discussion

The criteria pollutant emissions of primary interest were nitrogen oxides (NO<sub>x</sub>) and particulate matter (PM). Hydrocarbons, carbon monoxide, some greenhouse gases and air toxics were all low and most of those emissions were below ambient levels. The low levels of the non-regulated emissions and their uncertainties are shown in the Appendix. Additionally, results for the UDDS cycle are provided in the Supporting Information so the focus of this section are the driving cycles that differ from near-certification schedules and that are more representative of real-world driving schedules.

Looking first at the PM mass emissions, data are summarized in Figure 9 and Figure 10. Since all trucks were equipped with diesel particulate filters as the control technology, the level of PM mass emissions was very low (less than or equal to 0.001g/bhp-h), even lower than the EPA standard. Attempts to measure the particle size distribution with a fast-SMPS were not fruitful as the level of PM emissions was so low.

Thus the heart of the results and discussion section is about the NO<sub>x</sub> emissions. One area of wide spread interest is analysis of emissions data to provide emission factors both on a brake-specific and per mile basis. EPA and ARB have used 2.9 bhp-hr per mile as the conversion factor for 1996+ heavy-duty trucks <sup>11, 9</sup>. In this chapter, it can be seen that testing on a chassis dynamometer allowed the direct determination of the conversion factor and are listed in Table 4 . Values in that table indicate an average value closer to 4.4 bhp-h/mile would be more appropriate with current technology.

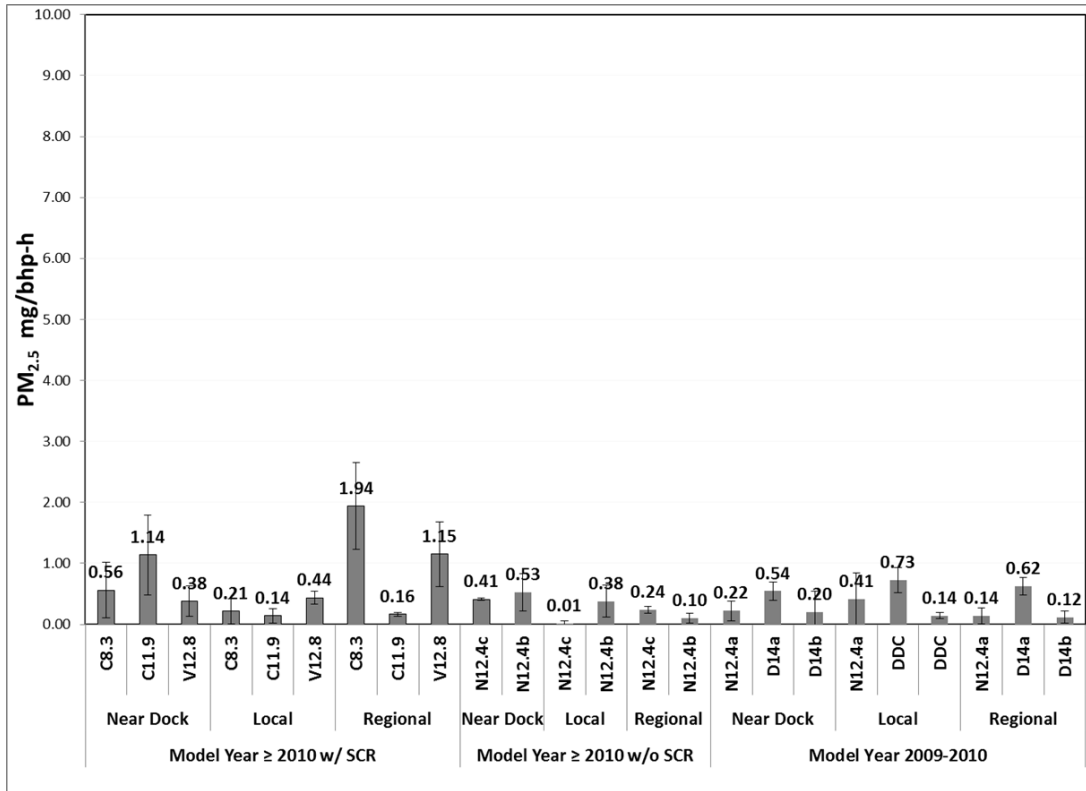


Figure 12 PM<sub>2.5</sub> gravimetric in mg/bhp-h for the HDDT vehicles on all the port cycles

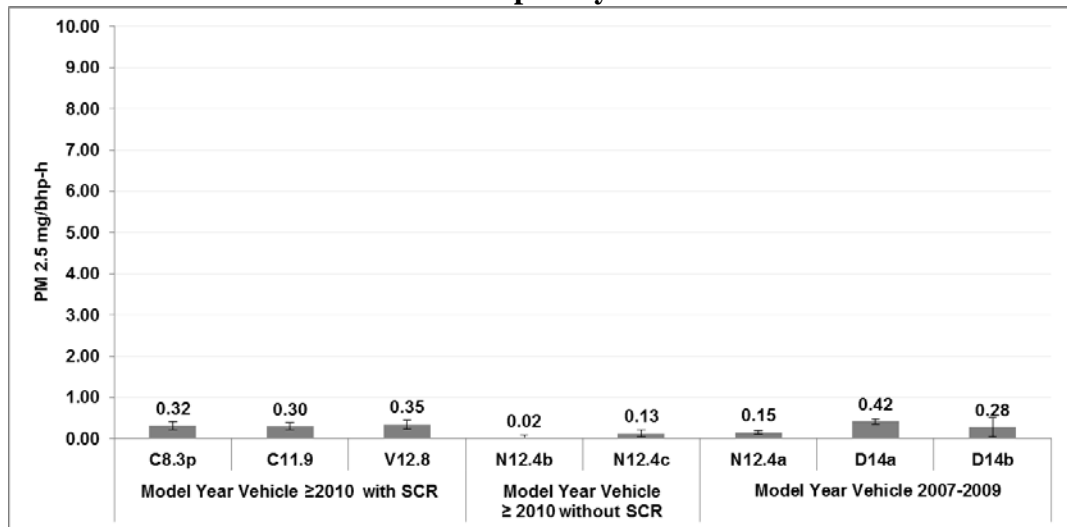
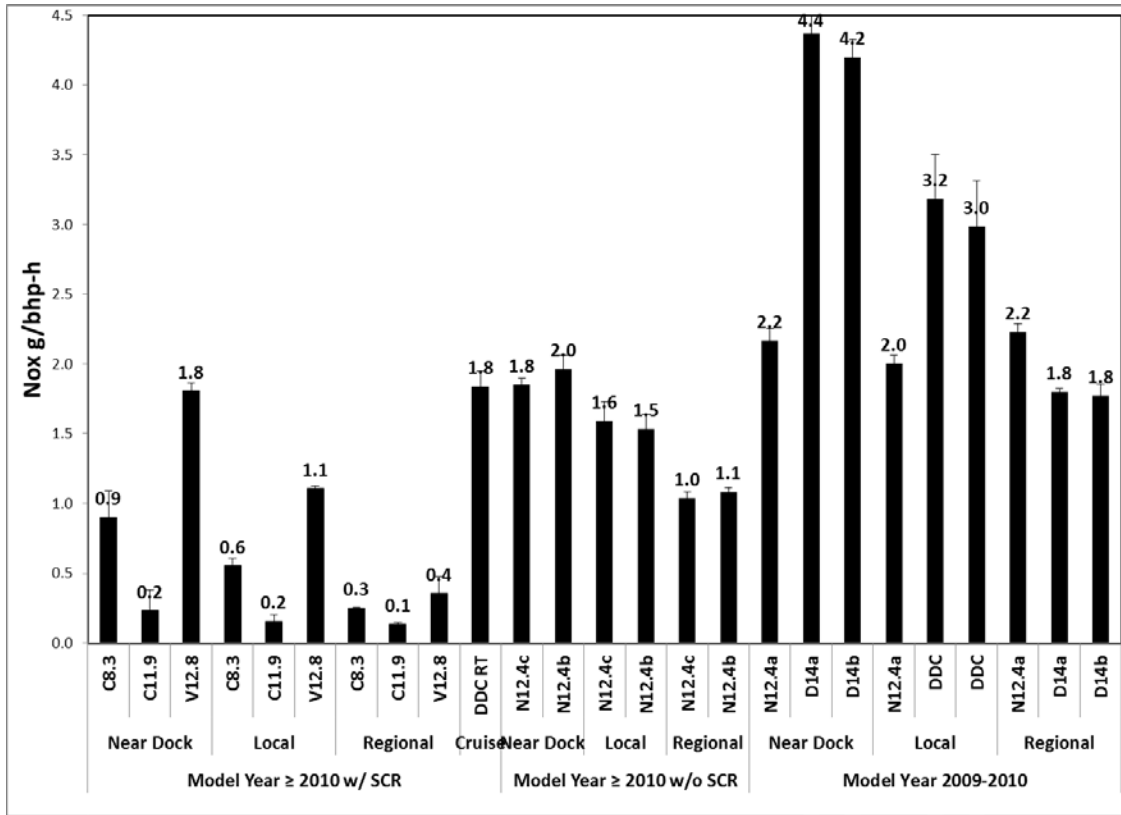


Figure 13 PM<sub>2.5</sub> gravimetric in mg/bhp-h for the HDDT vehicles on UDSS cycle

<b>Units</b>	<b>C 8.3</b>	<b>C 11.9</b>	<b>V 12.8</b>	<b>N 12.4b</b>	<b>N 12.4c</b>	<b>N 12.4a</b>	<b>D 14a</b>	<b>D 14b</b>
<b>g/mi</b>	1.07	0.25	1.27	3.91	5.35	8.04	10.95	9.54
<b>g/bhp-h</b>	0.25	0.06	0.27	0.93	1.15	1.56	2.66	2.3
<b>ratio</b>	4.3	4.2	4.7	4.2	4.7	5.2	4.1	4.1

**Table 4 Heavy-Duty Engine Emission Conversion Factors for the UDDS cycle**

Figure 1 is a plot of the NO<sub>x</sub> emission factors for the various trucks and operating cycles. Measured NO<sub>x</sub> emission factors varied over a wide range, from 0.1 to 4.4 g/bhp-h. The wide range occurred as the NO<sub>x</sub> regulation was transitioning to the final standard so the manufacturer had several interim standards and options to meet those standards. Cooled exhaust gas recirculation (EGR) and selective catalytic reduction (SCR) yielded the greatest control efficiencies and lowest NO<sub>x</sub> emission factors.



**Figure 14 NO<sub>x</sub> Emissions factors for the in-use emissions testing performed on the Heavy Duty Diesel Trucks. The nine vehicles from this study categorized according to their test cycle on the x-axis, while the NO<sub>x</sub> emissions in g/bhp-h are depicted on the y-axis.**

### 3.3.1 Category 1: Model Year 2009 -2010; Cooled-EGR Technology

The three trucks in this category only had cooled EGR, and as a consequence the range of emissions was narrow, from 1.8 to 4.4 g/bhp-hr. and strongly depended on the driving schedule and manufacturer. The data showed several interesting findings. For example, two of the trucks, D14a and D14b, were from the same manufacturer and randomly selected from the Los Angeles area. Comparison of the emission values at each driving schedule shows values within 6% and gives an indication of the fleet reproducibility.



Another interesting finding with these trucks was the emissions from the Regional cycle were 1.8 g/bhp-hr while emissions for the Near Dock averaged 4.3 g/bhp-hr, an increase of 239%. This finding differs from other reports that emissions are the same without an SCR and demonstrate the importance of measuring emission factors at in-use conditions. Rationale for the cause of the significant difference came from diesel engine engineers who indicated the diesel engine is mostly operating in the NTE zone during the Regional cycle; however, for the Near Dock cycle, there are long periods of operation outside the NTE zone. Accordingly emissions generated outside the NTE zone are not exempt from the calculation of the certified emissions factor. By way of comparison the emissions factor for the UDDS is 2.48 g/bhp-h midway between the Regional and Near Port cycles. Looking at the truck from the other engine manufacturer in this category indicates the emissions did not vary for the different cycles and were close to the UDDS value. Presumably the control technology design for this truck was less sensitive to the NTE zone. Findings from this category of trucks indicate the importance of the relationship between the measurement of in-use emissions and the NTE zone, even for trucks that do not have SCRs.

### **3.3.2 Category 2: Model Year $\geq$ 2010 without SCR**

Two trucks were tested in this category and were from the same manufacturer as all other HDDT manufacturers had opted for SCR technology. This manufacturer stuck with the cooled EGR approach and added prescribed shift points for the driver. Reproducibility for randomly selected trucks provided excellent agreement, as emission values were within 5%. However, as compared with a truck from the same manufacturer in Category

1, these trucks showed a dependence on the truck cycle as emissions ranged from 1 g/bhp-hr for the Regional cycle to 1.9 g/bhp-hr for the Near Port cycle, an increase of 190%. Again trucks without SCR can and do have a significant dependence on the in-use cycle. Rationale for the increase is the same offered in Category 1; namely, the Regional cycle has considerable operation in the NTE zone as compared with the Near Dock cycle. Further complicating the data in this category is the manufacturer had received a higher emission limits from the EPA but even these were not met so the technology was abandoned and controls on new trucks for this manufacturer included cooled EGR plus SCR.

### **3.3.3 Category 3: Model Year $\geq$ 2010 with SCR**

For this category, three trucks were factory (OEM) equipped with SCRs and tested on all three port cycles. Another truck manufactured before 2010 was retrofitted with a SCR and tested on one mode of the Regional cycle. For Category 3, there were no results that could be directly compared. Looking first at all the trucks retrofitted with an SCR, the emissions on the cruise cycle were 1.8 g/bhp-hr as compared with an average of about 0.3 g/bhp-hr for the OEM trucks. This comparison gives a perspective of the magnitude of the control efficiency possible with retrofitted SCR. For this case the emission reduction was quite small as compared with other technologies.

Category 3 tests over all three port cycles included a single engine platform from one engine manufacturer and two engine platforms from another manufacturer. Looking first at truck V12.8, the emission factor varied over the range from 0.4 g/bhp-hr for the Regional cycle to 1.8 g/bhp-hr for the Near Port cycle, an increase of 450%. Similar

trends are observed for the two trucks from the other manufacturer. For C8.3, the increase is 300% and for C11.9, the increase is 200% when comparing the Regional to the Near Port cycle. Again, the data point out the importance of collecting emission data following cycles that most closely represent real world activity rather than simply accepting certification data.

### **3.3.4 Analysis of Transient Data in for HDDTs in Category 3**

In the earlier section we reported that the emissions factor for trucks in Categories 1 and 2 and following the Regional cycle was less than half of that for the port cycle where the engine operated out of the NTE zone. However, the fundamental cause for the higher emissions with Near Port cycle is more complicated for trucks in Category 3 and a path to understanding is gained by analyzing the transient data and efficiency of the SCR control system. As mentioned in the introduction, during the design phase of the emissions control system, the composition and size of the SCR catalyst are selected for the expected exhaust flow and temperature. Once in operation then temperature is the primary parameter that determines the efficiency of the SCR control system. It is important to point out that the emission factor depends on definition. In this report, emission factor is calculated as the ratio of grams of NO<sub>x</sub> produced divided by the work (bhp-hr) over the entire drive time. However, for the EPA in-use regulation, the only grams of NO<sub>x</sub> that count are when the engine operates within the NTE zone and when the temperature of the after treatment system is  $\geq 250^{\circ}\text{C}$ . Practically speaking, the values for the emission factors will be similar as the catalyst efficiency is low below  $250^{\circ}\text{C}$  and often the urea is not introduced until the temperature is  $>250^{\circ}\text{C}$ .

Figure 2a and 2b shows continuous plots of exhaust temperature, NO<sub>x</sub> accumulation and speed versus accumulated work in bhp-hr with a line at 250°C for truck V12.8 following the Regional and Near Dock cycles. Recall the NO<sub>x</sub> emissions for the Regional Cycle was 0.4g/bhp-hr and for the Near Port Cycle was 1.8g/bhp-hr. Note for the Regional Cycle that 250°C is reached when 20 of the 32 grams of NO<sub>x</sub> and about 15 bhp-h of work are accumulated leading to an emission factor of 1.34 g/bhp-hr. For the next segment, the temperature quickly rises to about 350°C and 75 bhp-hr of work is done for an emissions factor of 0.028 g/bhp-hr. In comparison, for the Near Dock Cycle, 250°C is reached when 30 of the 50 grams of NO<sub>x</sub> are accumulated and 12 bhp-hr of work are completed for an emissions factor of 2.5 g/bhp-hr.

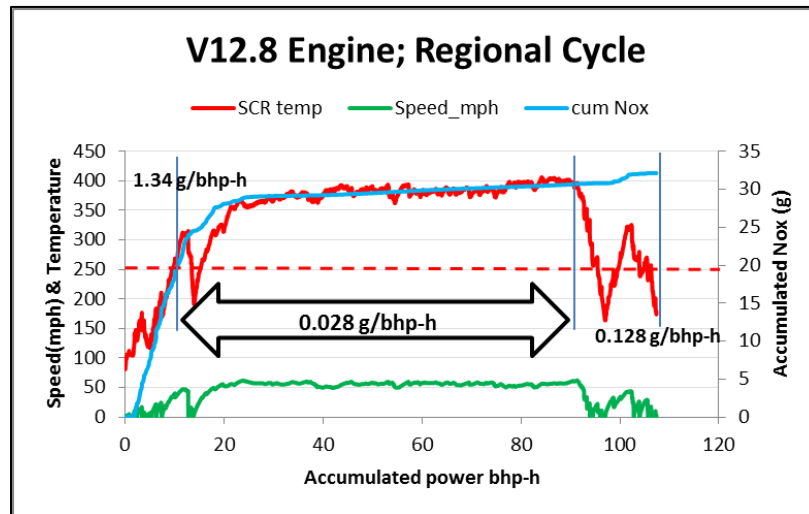


**Figure 15 Speed (mph) , SCR inlet Temperature (deg C) and Accumulated NO<sub>x</sub> (g) versus accumulated Brake horsepower-hour for V12.8L on Regional Cycle**

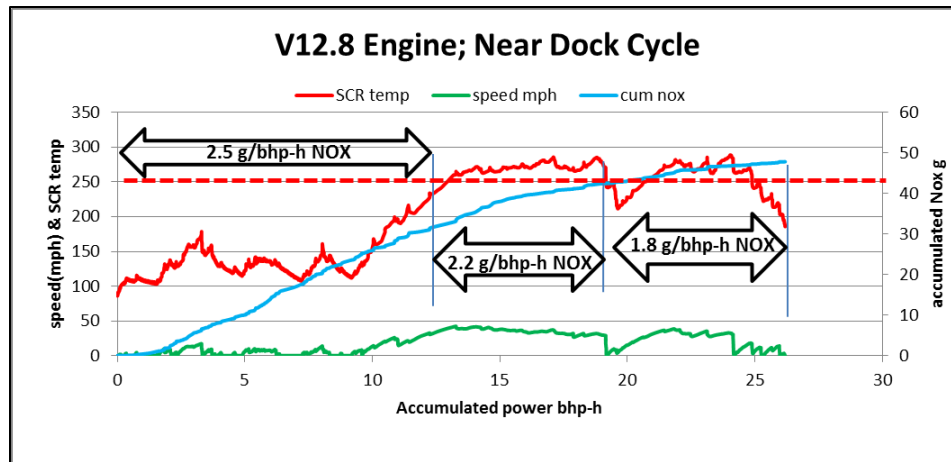


**Figure 16 Speed (mph) , SCR inlet Temperature (deg C) and Accumulated NOx (g) versus accumulated Brake horsepower-hour for V12.8L on the Near Dock**

### 3.3.5 Analysis of Data for Category 3 for SCT Temperature >250°C

As >250°C is the temperature when urea solution is likely to be added and also above which in-use emissions factors can be measured, an additional data analysis was carried out for this segment. Data shown in Figure 4 show the percentage of time that the SCR operates >250°C and the emissions factor for the three port cycles. Interestingly the V12.8 tractor shows emission factors ranging for 0.15 g/bhp-hr for the regional cycle to 0.77 g/bhp-hr for the port cycle; values from below the certification limit to values over three times the certification limit. At the same time, the two HDDTs with different engines made by another manufacturer show less sensitivity to real world driving cycle and the emissions factor always is <0.2 g/bhp-hr, regardless of cycle. To be clear the emission factors in this analysis are for temperature >250°C; however, there are likely other NTE criteria that would exclude the calculation of an emission factor for this

period. For example, much of the time the engine was operating outside the NTE zone. Still there are clearly implications in an inventory if the emissions factor was 300% greater for one cycle.

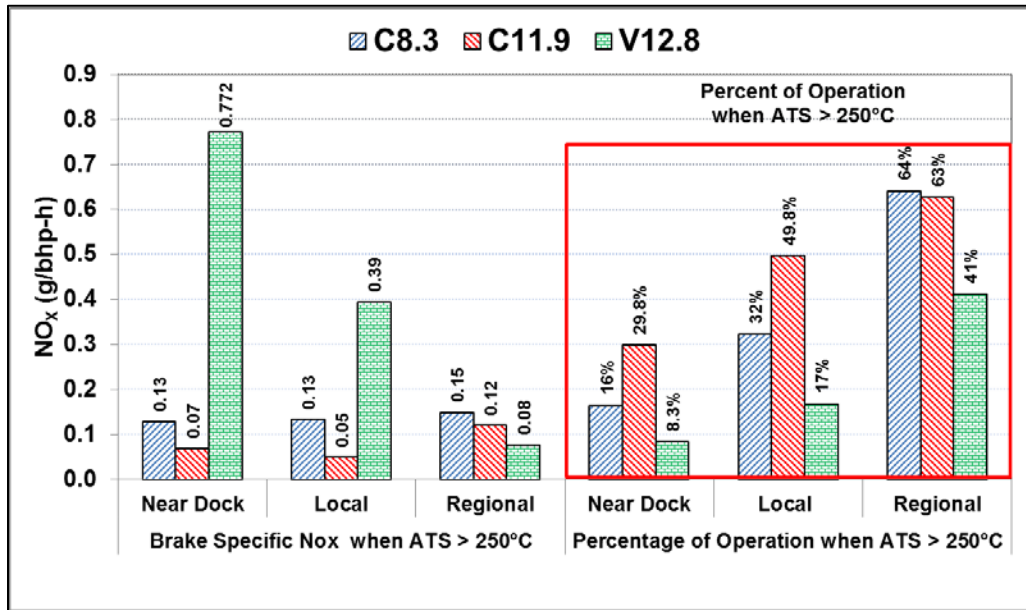


**Figure 17 Brake specific NOx emissions for SCR temperature > 250 °C and percent time of the cycle when the ATS was > 250° C for the SCR equipped vehicles**

### 3.3.6 NTE (Not To Exceed) Analysis

This section describes the NTE analysis performed on the port vehicles. Information on the NTE exclusions is listed in the Appendix. The vehicles are in-use compliant when real-world emissions are within the NTE region. All the other emissions outside of this NTE region are not considered when testing the vehicle for in-use compliance. The emissions that fall outside of the NTE realm do contribute to the overall air-quality though in the view of compliance they do not matter. Figure 15 and Table 5 summarize the NTE analysis on the 2011 Volvo engine equipped with an SCR. Of all the cycles some emissions from the regional cycle and very few

emissions from the UDDS cycle exist in the NTE zone. The dotted line indicates the NOx emission standard and the vehicle was compliant as the NTE emissions were within the standard. Table 5 shows the NTE events (1 second and 30 second) and also the percentage of emissions when the after treatment system was operating at a temperature greater than 250°C. Figure 16 and Table 6 summarize the NTE analysis for another SCR equipped vehicle the 2011 Cummins engine, where in only 4% of the emissions existed in the NTE zone and all the other real world emissions were outside the NTE zone for 30 second event time. In case of 1 second NTE events a slightly larger part of the emissions existed in the NTE region. Similar type of analysis was performed on the two randomly selected 2008 Detroit Diesel engines. The emissions from the two vehicles surprisingly showed statistically significance even on the NTE analysis. These two vehicles were equipped with a cooled EGR as an emission control strategy and best represent vehicles which are not equipped with SCR. Similar to the vehicles in the SCR category most of the real-world emissions existed outside of the NTE regions. On all of the vehicles none of the emissions on the near-dock cycle existed in the NTE region. The near dock cycle showed highest NOx emissions for all categories of vehicles. It can be seen in Figure 11 that NOx emissions from the near dock cycle surpass the emissions standard and yet the vehicles pass the in-use compliance owing to the fact that those real-world emissions were not considered at all. These high emissions from near dock cycle contribute to the air quality problem and are a concern for people settled around the port area. Perhaps, a solution in the direction of lowering the emissions standard itself can cause a greater part of the real-world emissions to fall within the NTE region, thus meeting the compliance

criteria and also broadening the boundary conditions so that more number of emissions may exist within the NTE region.

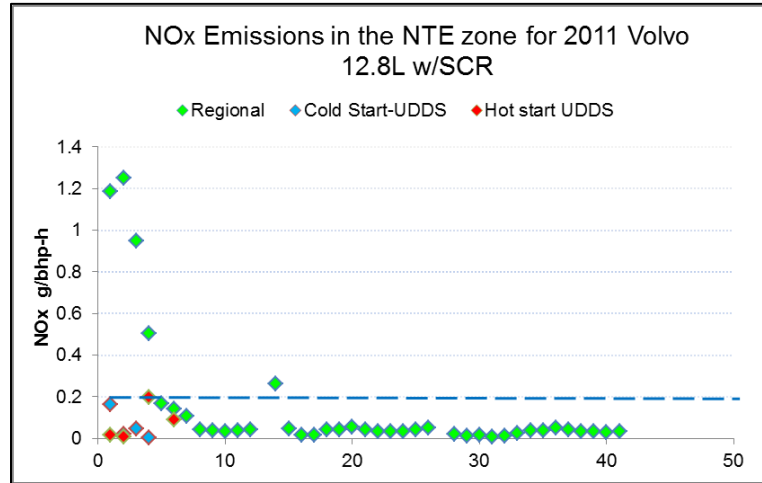


**Figure 18 NOx emissions in the Not to Exceed (NTE) zone for the 2011, 12.8L, Volvo equipped with SCR; the dotted line represents the emission standard for NOx in g/bhp-h**

NTE data for 2011 Volvo Mack 12.9L			
Cycle	ATS 250	NTE 1sec	NTE 30sec
UDDS		24%	2%
Near Dock	8%	3%	0%
Local	17%	8%	0%
Regional	41%	32%	14%

**Table 5 Percentage of emissions that exist in the NTE zones (After treatment system >2500C, 1 second and 30 second events) for all the real world cycles on the 2011, 12.8L, Volvo equipped with SCR**



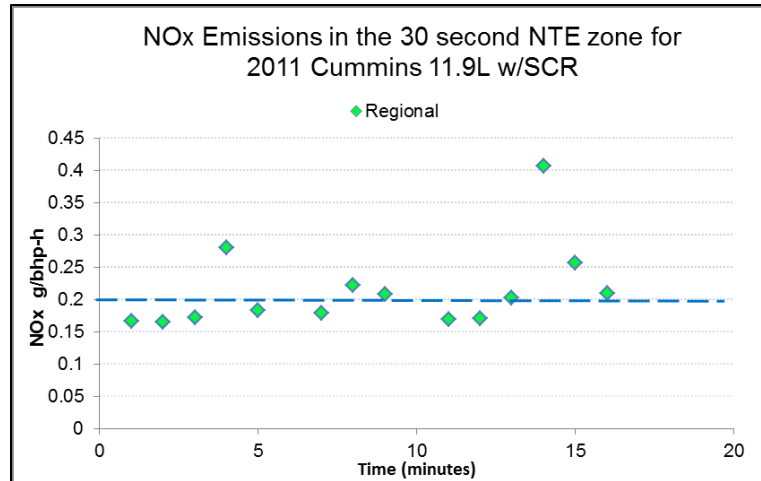


**Figure 19 NOx emissions in the Not to Exceed (NTE) zone for the 2011, 11.9L, Cummins equipped with SCR; the dotted line represents the emission standard for NOx in g/bhp-h**

NTE data for 2011 Cummins ISX 11.9L			
Cycle	ATS 250	NTE 1sec	NTE 30sec
UDDS	50%	27%	0%
Near Dock	30%	4%	0%
Local	50%	11%	0%
Regional	63%	25%	4%

**Table 6 Percentage of emissions that exist in the NTE zones (After treatment system >250<sup>0</sup>C, 1 second and 30 second events) for all the real world cycles on the 2011, 11.9L, Cummins equipped with SCR**

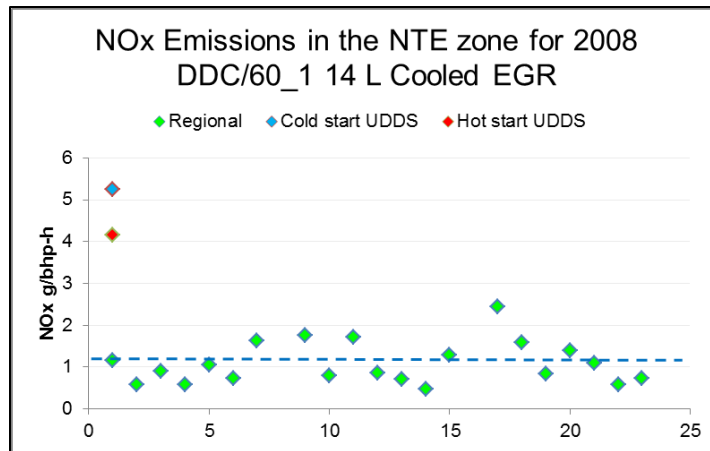


**Figure 20 NOx emissions in the Not to Exceed (NTE) zone for the 2008, 14L, Detroit Diesel equipped with a cooled EGR ; the dotted line represents the emission standard for NOx in g/bhp-h**

NTE data for 2008 DDC/60 14L (a)		
Cycle	NTE 1sec	NTE 30sec
UDDS	24%	1%
Near Dock	4%	0%
Local	8%	0%
Regional	27%	7%

NTE data for 2008 DDC/60 14L (b)		
Cycle	NTE 1sec	NTE 30sec
UDDS	26%	5%
Near Dock	4%	0%
Local	7%	0%
Regional	28%	11%

**Table 7 Percentage of emissions that exist in the NTE zones (1 second and 30 second events) for all the real world cycles on both of the randomly selected 2008, 14L, Detroit Diesel vehicles equipped with cooled EGR.**

### 3.3.7 Comparison of On-road and Chassis NOx Emission Data

Emissions were measured for Vehicle C11.9 both on the chassis dynamometer and on-road as part of the quality assurance/verification element of the project. Each drive was about 2,500-3,000 seconds long and consisted of mostly highway driving but included startup and low speed operation. Data are shown in Figures 4a and 4b and details about the route and data are in the Supplementary Information. In the figure, double headed arrows identify a drive segment, above which drive activity is described and the average brake specific NOx emissions calculated. For example, the cold start emissions were

when the truck was turned on and driven for a few miles before reaching the highway. During this period conditions are highly transient as load, speed and temperature of the SCR increase. Consequently the emission factor is 0.71 g/bhp-hr, a level above the 0.2 certification value. However, emissions accumulated during this segment would be excluded from determination of the in-use NO<sub>x</sub> emission factor due to NTE provisions. After the truck starts cruising on the highway, the temperature of the SCR is ~375°C and steady so NO<sub>x</sub> removal efficiency is high and the emission factor is 0.06 g/bhp-hr and considerably less than the standard. NO<sub>x</sub> control efficiency for the SCR catalyst is clearly exhaust temperature dependent. In Figure 6b, during the latter part of the drive, a similar observation was made when the SCR inlet temperature <250<sup>0</sup>C and accumulation of NO<sub>x</sub> emissions were higher. Subsequent low speed arterial and industrial driving conditions lowered temperature and increased accumulation of NO<sub>x</sub> emissions. Basically the on-road data for Vehicle C11.9 mirror results found on the chassis dynamometer adding confidence to the findings.

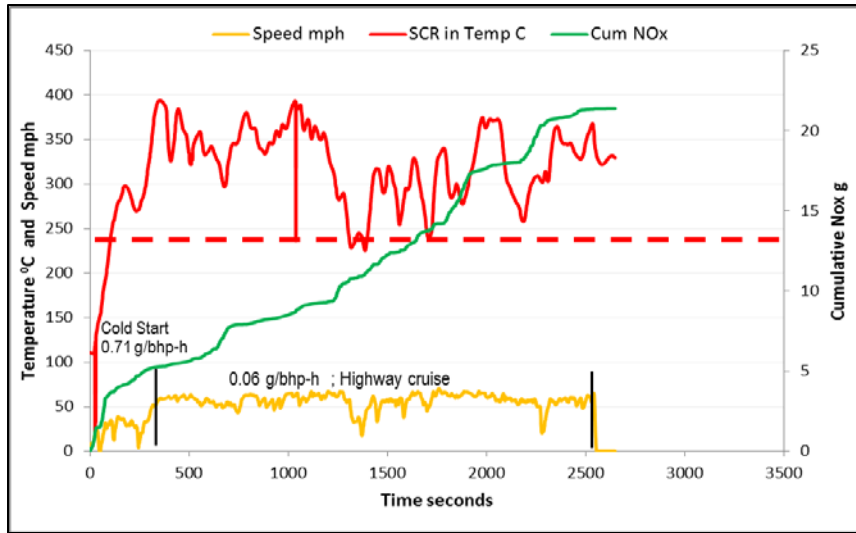


**Figure 21 SCR Temperature (deg C), Speed (mph) and Accumulated NOx (g) Emissions versus Time for Vehicle C11.9 during On-road testing with cold start**

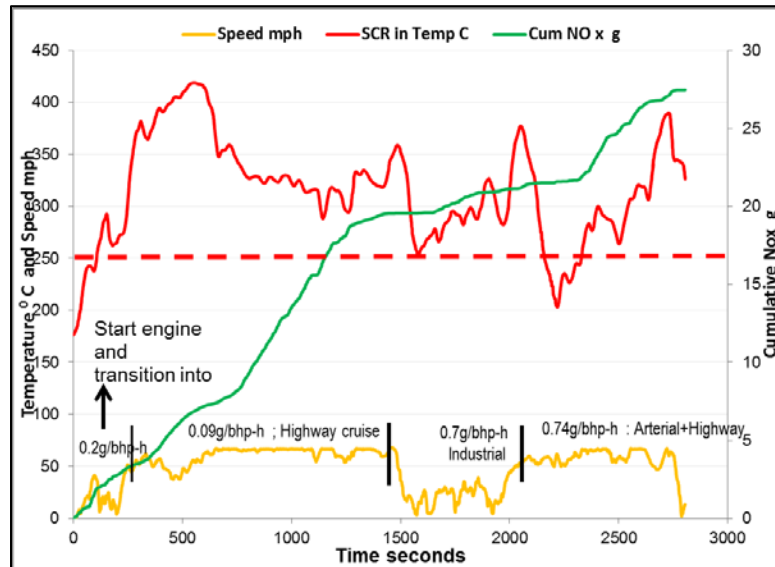


**Figure 22 SCR Temperature (deg C), Speed (mph) and Accumulated NOx(g) Emissions versus Time for Vehicle C11.9 during On-road testing on highway condition**

### **3.4 Conclusions**

The goal of the project was to investigate whether real-world driving or certification values better represented the emissions from current HDDTs. Results from this study of nine HDDTs demonstrate the vehicles easily met the PM standards for all driving conditions; however, the findings were different for NO<sub>x</sub> emissions. Looking at the vehicles using only cooled EGR technology for NO<sub>x</sub> control, the results show the emissions for goods movement in port activities were 239% greater than for HDDTs operating in a regional cycle. One manufacturer's HDDTs did not show an effect of driving cycle. Looking at data for trucks equipped with SCR, the same phenomena occur, namely the HDDTs operating near the port had up to 600% greater emissions rate than those in regional drayage. Even only analyzing the data for SCR temperature >250<sup>0</sup> C showed a divergence. For one manufacturer NO<sub>x</sub> emissions increased 600% for near port activities while emissions from another manufacturer did not increase. To put results in perspective, while all vehicles used certified engines in good working order, the difference between the definition of accumulated emissions for a certification cycle and in-use cycles can be significantly different due to the engine operation and NTE provisions. The only way to discover this difference is to measure emissions using real world driving conditions. These differences would be significant given the importance of NO<sub>x</sub> in the SIP inventories for some metropolitan areas.

## References:

1. Sawyer, R. F.; Harley, R. A.; Cadle, S. H.; Norbeck, J. M.; Slott, R.; Bravo, H. A. Mobile sources critical review. *Atmos. Environ.* 2000, 34, 2161–2181
2. Herner, D. J.; Hu, S.; Robertson, H. W.; Huai, T.; Collins, F. J.; Dwyer, H.; Ayala, A. Effect of advanced after treatment for PM and NO<sub>x</sub> control on heavy-duty diesel truck emissions. *Environ. Sci. Technol.* 2009, 43, 5928–5933
3. Yanguang Zhao.; Jing Hu.; Lun Hua.; Shijin Shuai.; Jianxin Wang. Ammonia Storage and Slip in a Urea Selective Catalytic Reduction Catalyst under Steady and Transient Conditions. *IE&C* 2011, 50, 11863–11871
4. Strots, O. V.; Santhanam, S.; Adelman, J. B.; Griffin, A. G.; Derybowski, M. E. Deposit formation in urea-SCR systems. *SAE* 2009, 2009-, 01–2780.
5. Cocker DR, Shah S, Johnson K, Miller JW, Norbeck J. Development and application of a mobile laboratory for measuring emissions from diesel engines. I regulated gaseous emissions. *Environmental Science and Technology* 2004; 38: 2182e9
6. Huai T, Durbin TD, Miller JW, Pisano JT, Sauer CG, Rhee SH, et al. Investigation of the formation of NH<sub>3</sub> emissions as a function of vehicle load and operating condition. *Environmental Science and Technology* 2003; 37:4841e7
7. Delphi. Worldwide Emissions Standards Heavy Duty and Off-Highway Vehicles; Delphi-Heavy- Duty-Emissions-Brochure-2012-2013.pdf (accessed Feb. 2013)

8. Yoon S, Collins J, Thiruvengadam A, Gautam M, Herner J, Ayala A. Criteria pollutant and greenhouse gas emissions from CNG transit buses equipped with three-way catalysts compared to lean-burn engines and oxidation catalyst technologies. *J Air Waste Manag Assoc* 2013;63(8):926e33
9. Analysis of BSFCs and Calculation of Heavy-Duty Engine Emission Conversion Factors, US EPA, EPA420-R-02-005 January 2002 M6.HDE.004
10. Development of a Drayage Truck Chassis Dynamometer Test Cycle, TIAX report, Port of Long Beach/ Contract HD-7188 Port of Los Angeles/ Tetra Tech, September 2011.
11. Emissions Calculations Tables for Discussion at November, 2007 Carl Moyer Program Workshop. Air Resources Board.
12. Nigel N. Clark, Justin M. Kern, Christopher M. Atkinson, Ralph D. Nine. Factors affecting heavy-duty diesel vehicle emissions. *J Air Waste Manag Assoc* 2002.

## **4 Emissions from Natural Gas and Diesel Buses and Refuse Haulers in the South Coast Air Quality Region**

### **4.1 Introduction:**

Emissions from heavy-duty trucks and buses accounted for about one-third of NO<sub>x</sub> emissions and one-quarter of PM emissions from mobile sources when stringent emission standards were introduced by the EPA on December 21, 2000 and by CARB in October 2001. The new standards (PM<sub>0.01</sub> 0.01 g/bhp-hr, NO<sub>x</sub> 0.20 g/bhp-hr, NMHC 0.14 g/bhp-hr), required emissions reductions of PM by 90% and NO<sub>x</sub> by 95%. Despite the implementation of emissions standards, the southern Californian region is still a non-attainment area for PM and Ozone. In order to achieve better air-quality different strategies have been implemented. The Most widely implemented strategies are: use of diesel particulate filters for PM mitigation, SCR technology and three way catalysts in LPG and LNG vehicles, both as after treatment for NO<sub>x</sub> reduction. Using LPG and LNG fuels as an alternate to diesel or gasoline has increasingly become common as they have their advantages. LPG mainly comprises of propane and butane, which combust more completely in engines than gasoline or diesel. Therefore, LPG is thought to be a cleaner fuel than gasoline <sup>1</sup>. Studies have shown that LPG-powered vehicles can considerably lower the emissions of greenhouse gases <sup>1</sup>, ozone formation precursors <sup>2</sup>, and particulate matter <sup>3</sup>, metal elements <sup>4</sup>, and polycyclic aromatic hydrocarbons (PAHs) <sup>5</sup>. Similar advantages are seen with the use of natural gas as an alternative fuel to the use of diesel <sup>6</sup>. Natural gas mainly consists of CH<sub>4</sub> (methane) with smaller percentages of other gas including heavier hydrocarbons, such as C<sub>2</sub>H<sub>6</sub> (ethane), C<sub>3</sub>H<sub>8</sub> (propane), and C<sub>4</sub>H<sub>10</sub> (butane), and inert diluents such as molecular N<sub>2</sub> (nitrogen) and CO<sub>2</sub> (carbon dioxide).



There is also a presence trace levels of sulfur compounds and other hydrocarbon species. Natural gas vehicles, generally, produce lower levels of NO<sub>x</sub>, CO (carbon monoxide), and NMHC (non-methane hydrocarbon) emissions <sup>[7, 8, 9]</sup>. In comparison to diesel vehicles, natural gas vehicles emit virtually no visible PM (particulate matter) or black soot at the tailpipe <sup>10</sup>. Although particle number emissions from diesel and CNG buses, and concluded that CNG exhaust produced 10 to 100 times lower particle number emissions than diesel exhaust <sup>11</sup>. Moving on to the diesel vehicles, urea based selective Catalytic reduction (SCR) exhaust after-treatment system has emerged as feasible strategies to meet the 2010 USEPA NO<sub>x</sub> regulation <sup>12</sup>. A NO<sub>x</sub> reduction efficiency of greater than 75% over various transient and steady-state operating regimes of the engine with use of SCR after-treatment was reported by Herner et al. <sup>13</sup>. However, the optimum efficiency of the SCR systems depends on critical exhaust temperature thresholds. Below these thresholds, incomplete decomposition of urea within the after treatment system could produce secondary emissions which in turn can act as precursors for ultrafine PM formation <sup>14</sup>.

This chapter has the following objectives:

1. To understand if cycle variations can change the emissions from various natural gas and propane gas fuelled vehicles from different manufacture years. The vehicles selected in this study were buses (transit and school) and refuse trucks.
2. To understand the effectiveness of SCR and its ability to convert NO<sub>x</sub> to N<sub>2</sub>, in the case of the diesel trucks post MY 2010. The two SCR equipped vehicles in this study were refuse haulers and were tested on a refuse cycle which is based on

the real-time operation of a refuse truck during its refuse hauling activity. The SCR catalyst temperatures are not simply either less/greater than 250°C. Instead the exhaust temperature is highly dynamic and follows the dynamic nature of the actual driving schedule.

3. To contribute to the emissions inventory from such an elaborate study incorporating various vehicles from different manufacture years and different real-time operating conditions.

## **4.2 Experimental Section**

### **4.2.1 Test vehicles**

Table 8 describes the different vehicles tested in this study. The vehicles used were from different areas of application including yard tractors to school buses and refuse haulers. The refuse haulers were operated on diesel, several buses used NG or propane gas as their main fuel. The after treatment system for natural gas was either an oxidation catalyst or a three way catalyst. The Cummins C Gas Plus, lean burn, SI (spark ignited) engine operating on lean burn. The Cummins I Gas plus being a newer version was used post 2007 used a spark stoichiometric burn engine along with a three way catalyst. The LPG school bus was a GM engine using a three way catalyst, while the only diesel school bus in the study was a Cummins engine which was equipped with a diesel particulate filter and a fuel borne catalyst (FBC). The refuse haulers used were all diesel fuelled, with two of them equipped with a diesel particulate filter (DPF) and cooled engine gas

recirculation (EGR) and the other two with a DPF and SCR catalyst described in the vehicle matrix.

#### **4.2.2 Test Cycles**

The buses were tested on a Central Business District (CBD) cycle and the refuse trucks were tested on William H. Martin refuse truck cycle and the Air Quality Management District Refuse Truck cycle (AQMD –RT). The cycle trace and details are mentioned in the Appendix.

#### **4.3 Emissions Testing Protocol**

Emissions testing were performed at UCR CE-CERT's Dynamometer facility. Emissions measurements were obtained using the CE-CERT MEL (Mobile Emissions Laboratory). The MEL being a full dilution tunnel emissions sampling system designed to meet Code of Federal Regulations requirements <sup>27</sup>. Emissions measurements were made to measure THC, NMHC, CH<sub>4</sub>, CO, NO<sub>x</sub>, CO<sub>2</sub>, and PM <sub>2.5</sub>. Measurements of NH<sub>3</sub> (ammonia) were also obtained on a real time basis using a TDL (tunable diode laser) near infrared absorption Spectrometer <sup>28</sup>. The non-regulated emissions for diesel vehicles were very low and so are very briefly discussed in this chapter.

Type	Mfg/Model	L	MY	Fuel	Air/Fuel	ATS	CYCLE
Bus	JD/NG	8.1	2004	CNG	Spark ignited lean burn	OC	CBDX2
Bus	JD/6081H	8.1	2009	CNG (5&6)	Spark ignited lean burn	OC	CBDX2
Bus	CUM/ISLG-280	8.9	2009	LNG	Spark ignited stoichiometric burn	TWC	CBDX2
Bus	GM/LPI	8.1	2008	LPG	-	TWC	CBDX2
Bus	CUM/ISB-220	6.7	2007	DIESEL	-	DPF	CBDX2
RT	CUM/CG	8.3	2001	CNG	Spark Ignited lean burn	OC	WHM
RT	NAV/GDT260	7.6	2008	ULSD	-	DPF+EGR	UDDS, AQMD RTC
RT	NAV/A260	7.6	2011	ULSD	-	DPF+EGR	UDDS, AQMD RTC
RT	CUM/ISL3970	8.9	2011	ULSD	-	DPF+SCR	UDDS, AQMD RTC
RT	CUM/ISC300	8.3	2011	ULSD	-	DPF+SCR	UDDS, AQMD RTC

CNG 5&6- associated high ethane and propane, details in karavalakis et al., 2013 ; RT -Refuse Truck

**Table 8 Vehicle matrix describing the vehicle type, make and model, fuel used, after treatment technology, operating conditions and test cycle.**

## 4.4 Results & Discussions

### 4.4.1 NOx Emissions

NOx emissions are the primary regulatory concern in the southern California basin. Figure 20, Figure 21 and Figure 22 represent NOx emissions in g/mile from buses and refuse trucks tested on CBD and refuse cycles. All measurements were within 5% uncertainty and were statistically significant in case of replicate test runs. All the newer manufacture years on all cycles had lower NOx emissions from their older counterparts. The stoichiometric engines equipped with a TWC showed significantly lower emissions in comparison to the lean burn engines, the phenomenon also observed by other study<sup>75</sup>. The stoichiometric conditions provide optimum operating efficiency promoting NOx reductions while the natural gas vehicle equipped with an oxidation catalyst does not provide catalytic reduction of NOx burning on lean conditions. Previous studies<sup>18</sup> have seen that lean-burn engines run richer as their MN is decreased which leads to the oxidation of more fuel, higher combustion temperatures, and increased cylinder

pressures. In the CBD cycle the stoichiometric ISL-G8.9 Cummins (CUM/ISLG-280/2009) and the John Deere C-Gas Plus buses (JD/6081H/2009, JD/NG/2004) were operated on different grades of the CNG fuel, the fuel effects are best described in the another study<sup>16</sup>. The ISL-G8.9 Cummins (CUM/ISLG-280/2009) was also equipped with a cooled EGR, reducing combustion temperature facilitating NOx reductions. The combustion temperature is reduced by introducing the inert exhaust gas back into the combustion chamber, reducing the overall combustion temperature<sup>17</sup>. The cooled EGR showed lower NOx emissions in the case of diesel engines operated on the refuse truck cycle. The diesel trucks equipped with SCR showed the lowest emissions in the refuse truck category. A more detailed discussion relating to the real-time SCR temperature and the NOx emission profile is dealt with, in the next section of the chapter. In case of the refuse trucks the William H. Martin and the AQMD refuse cycles both simulate the refuse hauler operation. The UDDS cycles (both hot and cold) closely represent certification cycles, as described in Chapter 2. The main observation on the UDDS cycles was that the cooled EGR equipped vehicles had higher NOx emissions in comparison to the SCR equipped vehicles. The SCR vehicles showed lower emissions even on the cold start UDDS cycle, demonstrating efficient control technology. Among all the refuse trucks only one of them was a CNG truck (2001 Cummins 8.3L C Gas Plus, lean burn, SI (spark ignited) fitted with an oxidation catalyst) operated on several different grades of the gas. While this study is aimed at emission factors as a whole from a particular cycle, fuel effects on the WHM cycle on the Cummins 8.3L C gas plus engine is elaborately discussed in<sup>19</sup>. The lean burn engine has higher NOx for the refuse cycle in comparison

with the diesel refuse trucks. Table 9 provides more detailed emission factors in g/kg fuel, g/mile and g/hour for NO<sub>x</sub> emissions.

#### **4.4.2 NO<sub>x</sub> emissions from SCR equipped diesel trucks:**

The SCR equipped vehicles in this study were the two diesel refuse trucks. The temperature profiles monitored on the refuse truck cycle for the refuse trucks showed that the temperature peaks after the first main double peak of the transit portion of the cycle and then slowly declines throughout the remainder of the transit portion and during the curbside portion. Temperatures during the compaction portion of the cycle showed a slight increase, but overall they similar to those near the end of the curbside segment. Figure 23 shows how the cumulative NO<sub>x</sub> varies over a refuse truck cycle for the Cummins ISX 11.9 engine equipped with SCR. The NO<sub>x</sub> is shown as function of accumulated power (brake horse power hour). NO<sub>x</sub> emissions over the refuse truck cycle showed a stronger dependency on the driving operation. Approximately 1/3rd of the cumulative NO<sub>x</sub> emissions were from the first 200 seconds of operation when the post-DPF temperature (SCR inlet temperature) was below 250°C, with an average emission rate of 0.72 g/hp-h. For the main part of the cycle, after the initial peak and including the curbside pickup portion of the cycle, relatively little NO<sub>x</sub> was produced, with an average emission rate of 0.11 g/bhp-h. The greatest percentage of NO<sub>x</sub> was formed during the latter stages of the cycle, when the compaction portion of the cycle was conducted. The average post-DPF temperature was around 250°C during the compaction portion of the cycle and the average emission rate was 0.99 g/bhp-h. The cold start catalyst temperatures were lower than the hot start catalyst temperatures and thus, showed much

higher NOx emissions. Figure 25 shows the Cummins ISX 11.9 liter engine's NOx accumulated mass emissions for a cold and hot start UDDS. The cold start catalyst temperatures started at 10°C and 230°C for the hot start tests. The bsNOx for the first ½ mile, 1 mile, and from 1 to 11miles are computed and shown in the figure. The amount of emissions accumulated in 1 mile of the cold start UDDS are equivalent to 32 miles of the hot start UDDS for the Cummins ISX 11.9 engine. This difference in emission rates can be attributed to the SCR catalyst temperature. The SCR must be at a certain minimum exhaust temperature to promote hydrolysis of urea into ammonia (NH<sub>3</sub>) which then reduces NOx into nitrogen (N<sub>2</sub>) and water (H<sub>2</sub>O)<sup>20</sup>. As a result, the efficiency of SCR is dependent on driving conditions as that affects the exhaust temperature and urea dosing strategy<sup>21</sup>. Figure 24 describes the emissions for SCR equipped vehicles when the catalyst temperature is >250<sup>0</sup> C. At temperatures > 250<sup>0</sup>C the urea in the SCR catalyst gets activate in order to reduce NOx to N<sub>2</sub>. SCR vehicle that spent a larger percentage of time at >250<sup>0</sup> C had lower NOx emissions in.

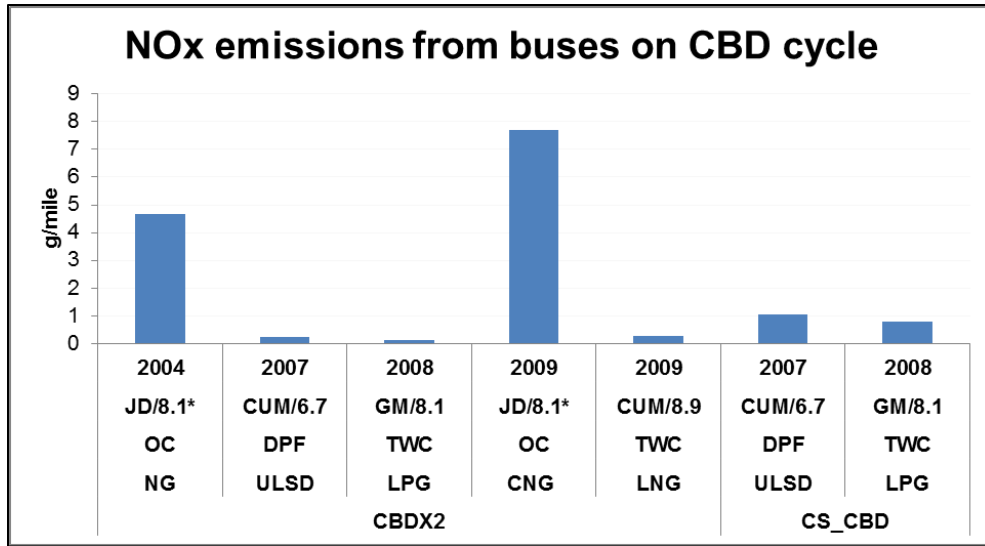


Figure 23 NOx emissions in g/mile for buses on the CBD cycle; \* indicates NOx/10

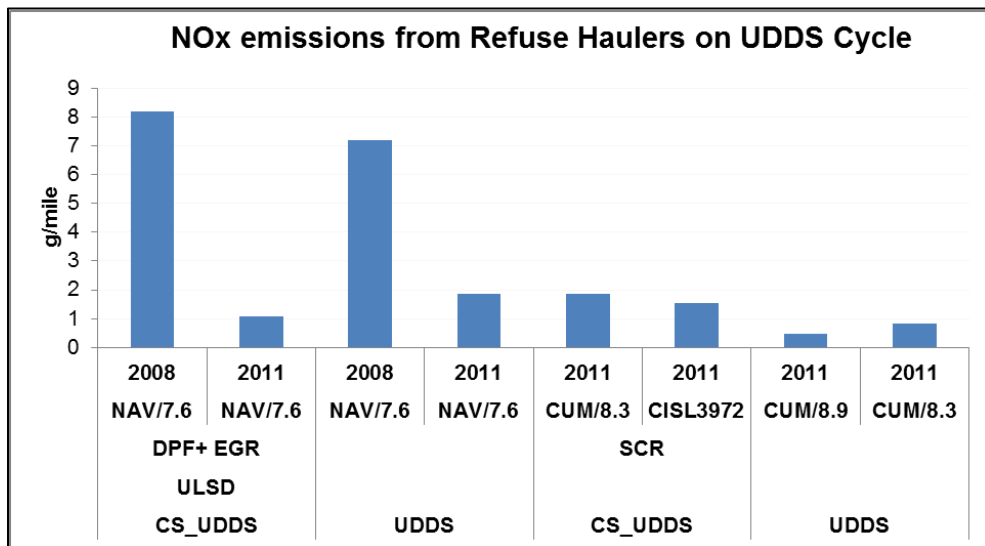
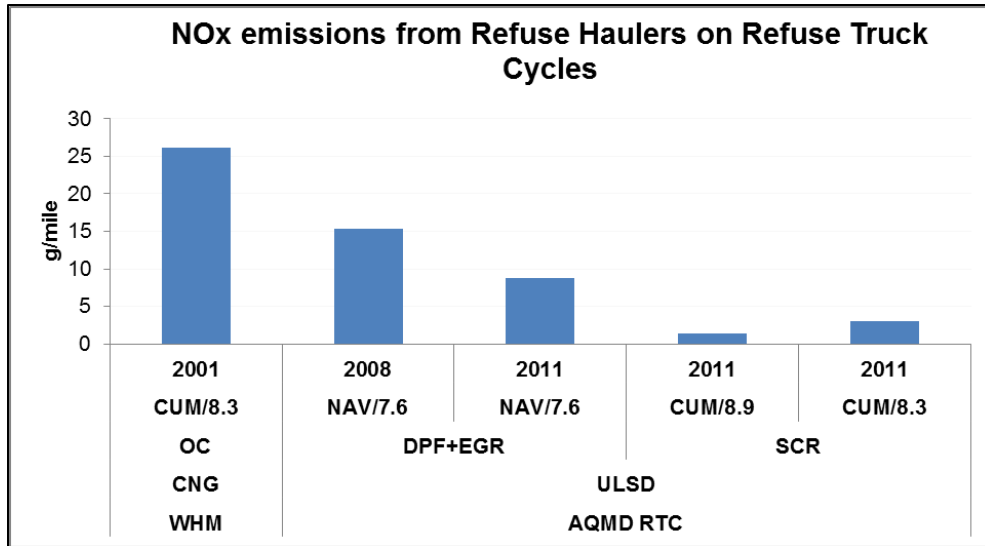
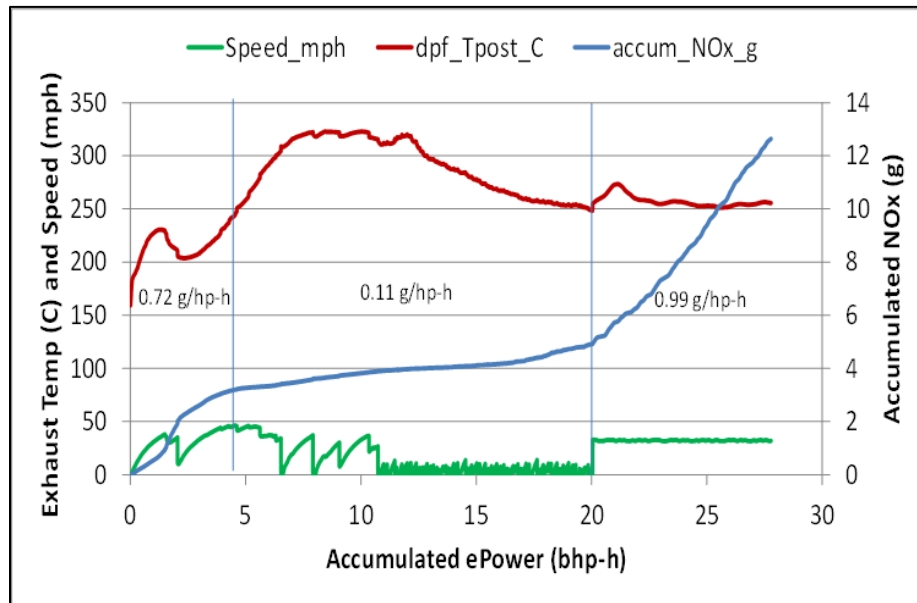


Figure 24 NOx emissions in g/mile from refuse trucks on hot and cold UDDS cycle





**Figure 25 NOx emissions in g/mile from refuse trucks on RTC (Refuse Truck Cycles- William H. Martin and AQMD RTC)**



**Figure 26 Cummins ISX 11.9 liter engine's cumulative NOx emissions in grams on the secondary y-axis; Exhaust temperature in °C and Speed in mph on the primary y-axis as a function of accumulated power (brake horse power hour) on x-axis**

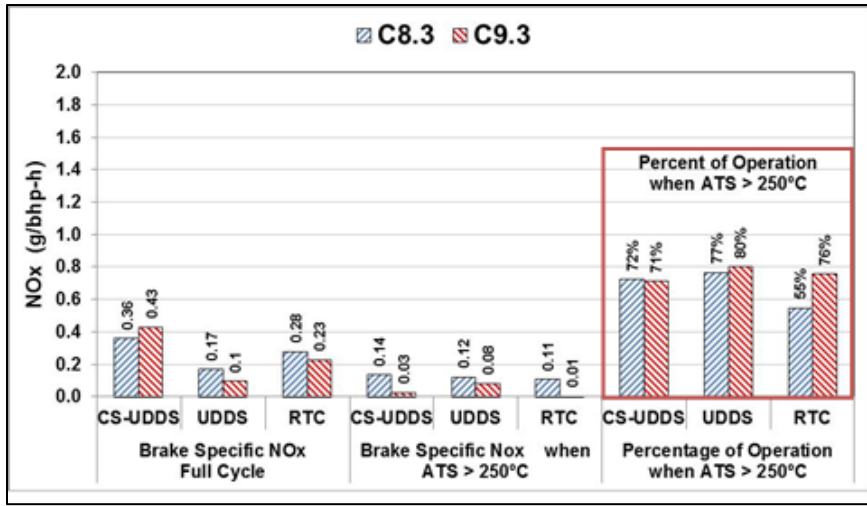


Figure 27 Brake specific NOx emissions for SCR temperature > 250 °C and percent time of the cycle when the ATS was > 250 °C for the SCR equipped vehicles

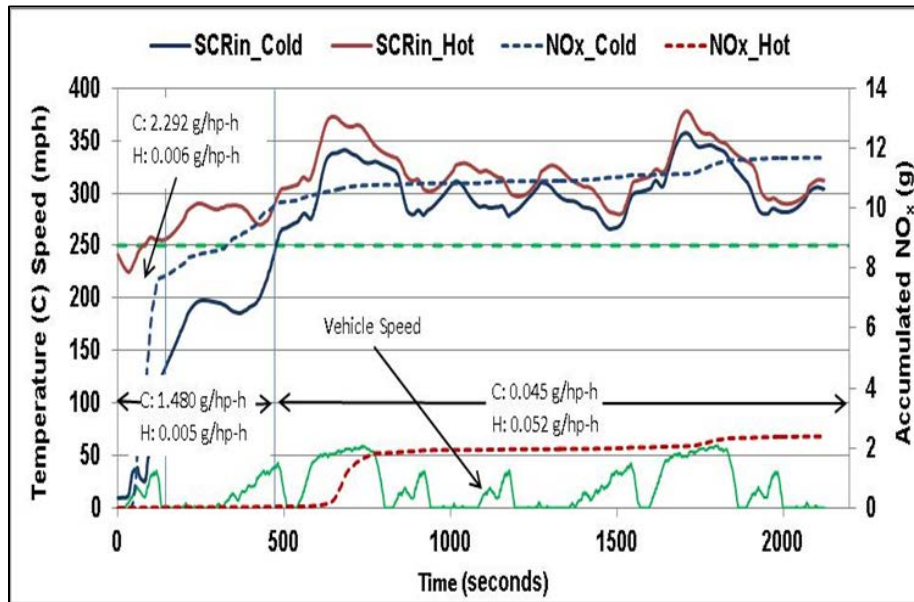


Figure 28 Cummins ISX 11.9 liter engine's NOx accumulated mass emissions for a cold and hot start UDDS cycle

#### 4.4.3 PM Emissions

This section describes PM<sub>2.5</sub> emissions in grams per mile for buses and refuse trucks. The uncertainties of measurements were within 5% for all test runs. Overall the PM<sub>2.5</sub> emissions were at or lower than 10 mg/mile. The total PM mass emissions were lower than the tunnel background PM on an absolute level. The very low levels of PM mass emissions in case of NG vehicles can be attributed to the fact the main composition of NG is methane which has a simple chemical structure and contains hydrocarbons which have a lower molecular weight than that in diesel. Therefore NG has a reduced tendency to form localized areas of rich combustion and generate unburned and partially oxidized hydrocarbons with lower molecular sizes in the exhaust <sup>22</sup>. In the case of the CBD cycle all of the vehicles had very low PM emissions. The diesel school bus equipped with a DPF had the lowest PM, followed by the GM LPG school bus equipped with a TWC. Although, mixed results were seen, where in the 2009 John Deere burning lean equipped with an oxidation catalyst had lower emissions than the Cummins ISL engine burning stoichiometric fuel equipped with a TWC. While, the 2004 John Deere equipped with an OC and burning lean had very slightly higher PM than the Cummins with a TWC. Both these scenarios were observed by other studies, where the former situation was consistent with <sup>25</sup> and the latter with <sup>24, 23</sup>. These differences in the PM emissions can be attributed to the changes in fuel composition and characteristics of combustion such as the peak flame temperature.

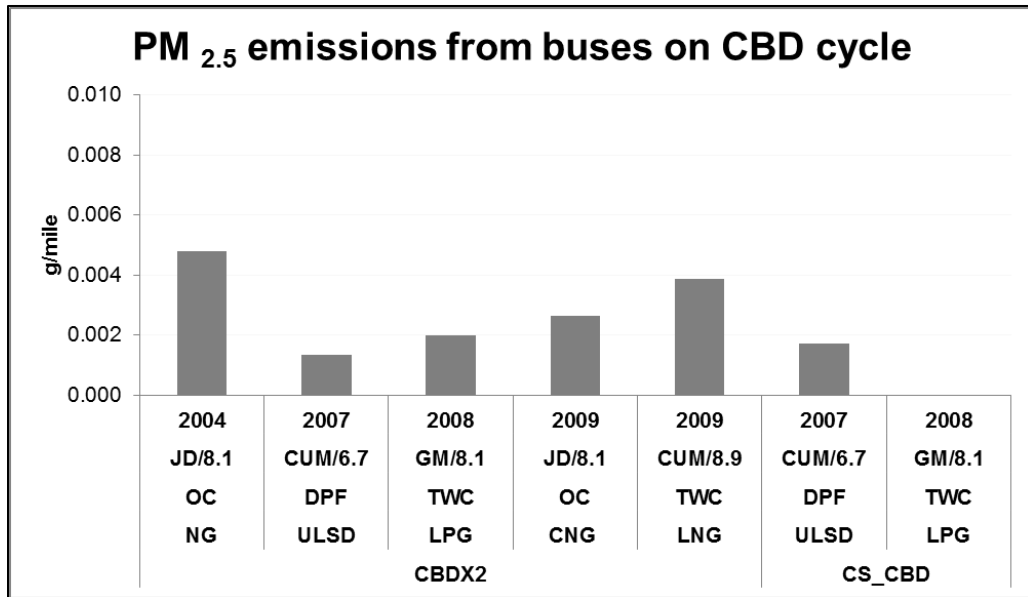


Figure 29 PM<sub>2.5</sub> emissions in g/mile from the CBD cycle

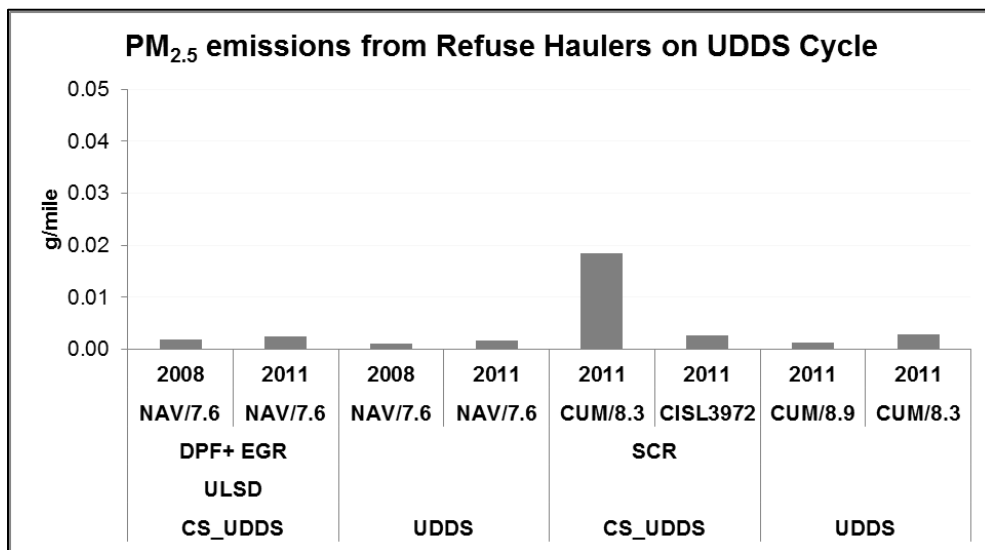
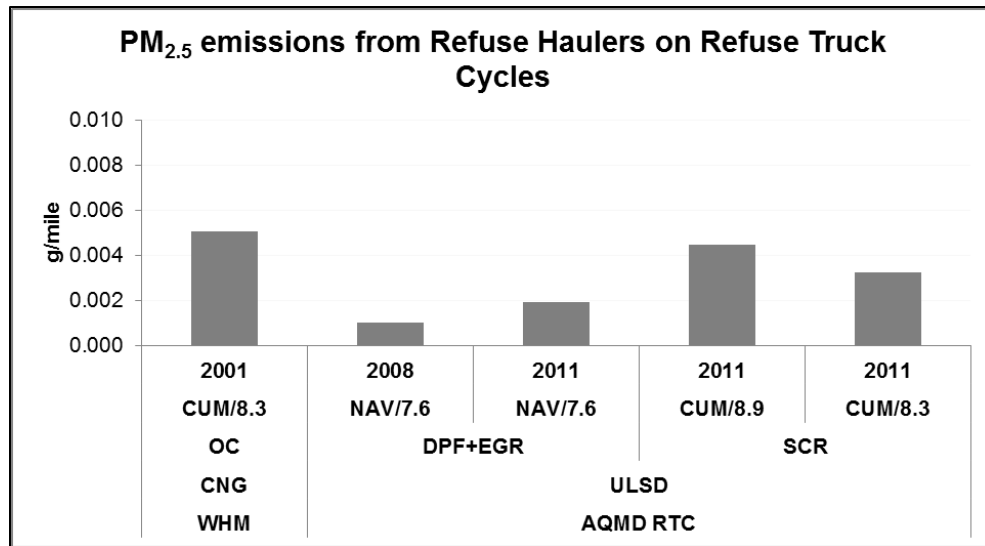


Figure 30 PM<sub>2.5</sub> emissions in g/mile from refuse trucks on hot and cold UDDS cycles



**Figure 31 PM<sub>2.5</sub> emissions in g/mile refuse trucks on RTC (Refuse Truck Cycles- William H. Martin and AQMD RTC)**

#### 4.4.4 THC, NMHC, CH<sub>4</sub> and CO emissions

Table 9 gives a detailed picture about the emission factors for the criteria pollutants and no-regulated emissions. THC emissions were significantly lower for the stoichiometric engines with a Three Way Catalyst (TWC) than the lean burn engines with an OC (Oxidation Catalyst). With that being said, older vehicles had higher emissions than the newer ones, mainly because the older engines were designed to meet an older certification requirement. The reductions in THC emissions from engines equipped with a TWC can be attributed to higher conversion efficiency of methane, (major constituent of hydrocarbon emissions) owing to the catalyst material. The catalyst is mainly made from precious metals and increasing composition of the metals can yield a higher efficiency of conversion in a stoichiometric TWC engine in comparison of a lean burn OC engine, as seen by <sup>26</sup>. The higher THC emissions could also be a result of fuel content, specifically

methane. The effect of fuel composition on THC emissions from the JD 2004, CNG engine burning lean and C-ISLG 2009, NG, TWC, stoichiometric engine are discussed clearly in <sup>16</sup>. They report that higher THC emissions are seen for the gases with higher methane contents for the lean burn engines is probably because THC emissions are predominately methane with lower levels of heavier hydrocarbons. The reductions in THC emissions for the low methane gases could also be due to more complete oxidation of the fuel as the adiabatic flame speeds and combustion temperatures are increased. Similar observations were reported by <sup>19</sup>, in their results for the 2002 Cummins 8.3L C Gas Plus, lean burn, SI (spark ignited), engine operated on the WHM refuse cycle. The THC emissions from ULSD diesel engines equipped with an EGR or a SCR were considerably low and were at background levels. NMHC emissions for the stoichiometric engines were lower than lean burn engines owing to higher conversion efficiency for the TWC compared to OC <sup>[25, 26]</sup>. It must be noted that the NMHC emissions in lean burn engines is dependent on the chemical makeup of the fuel itself i.e. if the fuel contains higher levels of NMHC's it would naturally yield higher NMHC's <sup>[16]</sup>. CH<sub>4</sub> emissions for the stoichiometric engines with the TWC were lower than that of lean burn engines. This could be attributed to the ability of the TWC to convert CH<sub>4</sub> emissions <sup>[26]</sup>. The diesel engines had virtually no CH<sub>4</sub> emissions and were at the range of instrument noise. Table 9 also shows values for equivalent CH<sub>4</sub> values for all the vehicle types and cycles. They were lower than CO<sub>2</sub> values suggesting that the global warming potential of these vehicles were dominated by CO<sub>2</sub> emissions and not that of CH<sub>4</sub>.

CO emissions are present in the Table 9 where in the CO emissions were higher for stoichiometric engines than the lean burn engines. The CO emissions from the diesel vehicles were lowest for all the cycles, in comparison to the NG vehicles because of cleaner combustion. The richer operating conditions of the stoichiometric combustion compared to lean burn combustion causes the former to produce higher CO emissions. As less amount of oxygen is available to oxidize CO to CO<sub>2</sub> during combustion the stoichiometric engine produces higher CO <sup>[15]</sup>.

#### **4.5 Conclusions**

This chapter evaluates the range of emissions from buses and refuse trucks operating on cycles which simulate the exact real-world driving conditions of these vehicles. These selected vehicles are representative of the buses and refuse haulers in the southern Californian region. The test vehicles and fuels were mainly natural gas, propane and diesel equipped with either stoichiometric burn three way catalyst or lean burn oxidation catalyst in case of natural gas and cooled EGR or SCR in case of diesel. Overall the NOx emissions were higher for lean burn NG engines in comparison to stoichiometric engines. The NOx emissions followed a typical trend where the newer vehicles showed lower emissions than the older vehicles. The NOx from SCR vehicles greatly depended on factors like the cycle driven, engine load and temperature of the SCR catalyst. Given that the SCR is working in its optimum temperature conditions, the vehicles equipped with SCR catalyst showed the lowest NOx among all the technologies, cycles and fuels used. The PM<sub>2.5</sub> emissions were all low and were below 10mg/mile. Diesel vehicles had the

least amount of PM in comparison to other NG engines. The vehicles equipped with TWC generally had lower PM than the lean burn OC engines, unless otherwise was seen in which case the engines had a NO<sub>x</sub> /PM trade off situation. THC, NMHC and CH<sub>4</sub> emissions were higher in lean burn engines while the CO emissions were higher for the stoichiometric engines. CO<sub>2</sub> was still a dominant contributor of greenhouse gases for all the NG vehicles. THC, NMHC, CH<sub>4</sub> and CO emissions were all very low as generally seen with diesel engines. The growing use of NG as an alternate to diesel and gasoline definitely has its advantages when it comes to mitigating emissions. This chapter provides a very detailed understanding of the emissions factors from these vehicles under very different driving conditions.



Cycle	Fuel	ATS	Vehicle	Year	g/mile							
					THC	CH4	NMHC	CO	Nox	CO2	NH3	PM
CBDX2	NG	OC	JD/8.1	2004	21	16	4	0.12	5	1692	0	0.005
CBDX2	ULSD	DPF	CUM/6.7	2007	0.01	0.02	-0.01	-0.12	0.25	3089.30	0.06	0.001
CBDX2	LPG	TWC	GM/8.1	2008	0.30	0.20	0.13	9.82	0.10	1515.68	0.50	0.002
CBDX2	CNG	OC	JD/8.1	2009	21.32	17.50	0.00	0.14	7.68	2769.73	0.03	0.003
CBDX2	LNG	TWC	CUM/8.9	2009	0.49	0.61	0.00	8.48	0.25	1686.05	1.29	0.004
CS_CBD	ULSD	DPF	CUM/6.7	2007	0.03	0.03	0.01	-0.03	1.04	3117.44	0.07	0.002
CS_CBD	LPG	TWC	GM/8.1	2008	0.77	0.25	0.56	16.03	0.77	1728.07	0.45	0.000
WHM	CNG	OC	CUM/8.3	2001	8.21	6.50	0.00	0.69	26.14	1253.58	0.02	0.005
AQMD RTC	ULSD	DPF+EGR	NAV/7.6	2008	0.02	0.05	-0.02	-0.24	15.31	4888.48	0.07	0.001
AQMD RTC	ULSD	DPF+EGR	NAV/7.6	2011	2.99	1.29	1.90	9.06	8.84	4631.10	0.02	0.002
AQMD RTC	ULSD	SCR	CUM/8.9	2011	-0.02	0.03	-0.05	-0.67	1.36	5326.45	0.05	0.004
AQMD RTC	ULSD	SCR	CUM/8.3	2011	-0.15	0.05	-0.19	-0.31	3.03	5732.00	0.11	0.003
CS_UDDS	ULSD	DPF+ EGR	NAV/7.6	2008	0.01	0.01	0.00	0.00	8.19	2412.05	0.03	0.00
CS_UDDS	ULSD	DPF+ EGR	NAV/7.6	2011	0.36	0.37	0.04	1.90	1.06	1810.62	0.01	0.00
UDDS	ULSD	DPF+ EGR	NAV/7.6	2008	0.00	0.01	-0.01	0.06	7.20	2355.58	0.03	0.00
UDDS	ULSD	DPF+ EGR	NAV/7.6	2011	1.13	0.45	0.74	1.86	1.84	1940.57	0.03	0.00
CS_UDDS	ULSD	SCR	CUM/8.3	2011	0.28	0.02	0.27	-0.11	1.87	3035.37	0.12	0.02
CS_UDDS	ULSD	SCR	CISL3972	2011	0.00	0.01	-0.01	-0.19	1.52	2589.92	0.05	0.00
UDDS	ULSD	SCR	CUM/8.9	2011	-0.03	0.01	-0.04	-0.13	0.47	2824.66	0.04	0.00
UDDS	ULSD	SCR	CUM/8.3	2011	-0.03	0.01	-0.05	-0.23	0.81	2818.03	0.05	0.00

**Table 9 Emission factors for the Buses and Refuse Trucks operated on CBD, WHM and AQMD-RT Cycl**

## References:

1. Gamas, E. D.; Diaz, L.; Rodriguez, R.; Lopez-Salinas, E.; Schifter, I.; Ontiveros, L. Exhaust emission from gasoline and LPGpowered vehicles operating at the altitude of Mexico City. *J. Air Waste Manage. Assoc.* 1999, 49, 1179–1189 ; Chang, C. C.; Lo, J. G.; Wang, J. L. Assessment of reducing ozone forming potential for vehicles using liquefied petroleum gas as an alternative fuel. *Atmos. Environ.* 2001, 35, 6201–6211.
2. Chang, C. C.; Lo, J. G.; Wang, J. L. Assessment of reducing ozone forming potential for vehicles using liquefied petroleum gas as an alternative fuel. *Atmos. Environ.* 2001, 35, 6201–6211
3. Ristovski, Z. D.; Jayaratne, E. R.; Morawska, L.; Ayoko, G. A.; Lim, M. Particle and carbon dioxide emissions from passenger vehicles operating on unleaded petrol and LPG fuel. *Sci. Total Environ.* 2005, 345, 93–98.
4. Lim, M. C. H.; Ayoko, G. A.; Morawska, L.; Ristovski, Z. D.; Jayaratne, E. R.; Kokot, S. A comparative study of the elemental composition of the exhaust emission of cars powered by liquefied petroleum gas and unleaded petrol. *Atmos. Environ.* 2006, 40, 3111–3122
5. Lim, M. C. H.; Ayoko, G. A.; Morawska, L.; Ristovski, Z. D.; Jayaratne, E. R. Influence of fuel composition on polycyclic aromatic hydrocarbon emissions from a fleet of in-service passenger cars. *Atmos. Environ.* 2007, 41, 150–160.

6. Cho HM, He B-Q. Spark-ignition natural engines-a review. *Energy Conversion and Management* 2007;48:608e18.
7. Turrio-Baldassarri L, Battistelli CL, Conti L, Crebelli R, De Berardis B, Iamiceli AL, et al. Evaluation of emission toxicity of urban bus engines: compressed natural gas and comparison with liquid fuels. *Science of the Total Environment* 2006;355:64e77.
8. Nylund N, Erkkila K, Lappi M, Ikonen M. Transit bus emission study: comparison of emissions from diesel and natural gas buses. Research Report PRO3/P5150/04. Finland: Technical Research Centre VTT Processes, [http:// www.vtt.fi/inf/pdf/jurelinkit/VTTNylund.pdf](http://www.vtt.fi/inf/pdf/jurelinkit/VTTNylund.pdf); 2004.
9. Jayaratne ER, Ristovski ZD, Meyer N, Morawska L. Particle and gaseous emissions from compressed natural gas and ultralow sulphur diesel-fuelled buses at four steady engine loads. *Science of the Total Environment* 2009;407:2845e52
10. Jayaratne ER, He C, Ristovski ZD, Morawska L, Johnson GR. A comparative investigation of ultrafine particle number and mass emissions from a fleet of on-road diesel and CNG buses. *Environmental Science and Technology* 2008;42:6736e42.
11. Holmen BA, Ayala A. Ultrafine PM emissions from natural gas, oxidation catalyst diesel and particle trap diesel heavy-duty transit buses. *Environmental Science and Technology* 2002;36:5041e50.

12. Arvind Thiruvengadam,, Marc C. Besch, Daniel K Carder, Adewale Oshinuga, and Mridul Gautam. Influence of Real-World Engine Load Conditions on Nanoparticle Emissions from a DPF and SCR Equipped Heavy-Duty Diesel Engine. [dx.doi.org/10.1021/es203079n](https://doi.org/10.1021/es203079n) | Environ. Sci. Technol. 2012, 46, 1907–1913
13. Herner, D. J.; Hu, S.; Robertson, H. W.; Huai, T.; Collins, F. J.; Dwyer, H.; Ayala, A. Effect of advanced aftertreatment for PM and NO<sub>x</sub> control on heavy-duty diesel truck emissions. Environ. Sci. Technol. 2009, 43, 5928–5933.
14. Strots, O. V.; Santhanam, S.; Adelman, J. B.; Griffin, A. G.; Derybowski, M. E. Deposit formation in urea-SCR systems. SAE 2009, 2009-, 01–2780.
15. Yoon S, Collins J, Thiruvengadam A, Gautam M, Herner J, Ayala A. Criteria pollutant and greenhouse gas emissions from CNG transit buses equipped with three-way catalysts compared to lean-burn engines and oxidation catalyst technologies. J Air Waste Manag Assoc 2013; 63(8):926e33.
16. Maryam Hajbabaei , Georgios Karavalakis , Kent C. Johnson , Linda Lee ,Thomas D. Durbin. Impact of natural gas fuel composition on criteria, toxic, and particle emissions from transit buses equipped with lean burn and stoichiometric engines. Energy 62 (2013) 425e434.
17. Zhang F, Okamoto K, Morimoto S, Shoji F. Methods of increasing the BMEP (power output) for natural gas spark ignition engines. SAE Technical Paper; 1998. 981385.

18. Feist MD. Fuel composition testing using DDC series 50G natural gas engines; August 2006. Final report prepared by Southwest Research Institute for the Southern California Gas Company, Report No. 11657.
19. Georgios Karavalakis, Maryam Hajbabaei, Thomas D. Durbin, Kent C. Johnson, Zhongqing Zheng, Wayne J. Miller. The effect of natural gas composition on the regulated emissions, gaseous toxic pollutants, and ultrafine particle number emissions from a refuse hauler vehicle. *Energy* 50 (2013) 280e291
20. Majewski, W. A., Khair, M. K. Diesel Emissions and Their Control; SAE International: Warrendale, PA, 2006.
21. Chandan Misra, John F. Collins, Jorn D. Herner, Todd Sax, Mohan Krishnamurthy, Wayne Sobieralski, Mark Burntitzki, and Don Chernich. In-Use NOx Emissions from Model Year 2010 and 2011 Heavy-Duty Diesel Engines Equipped with Aftertreatment Devices. [dx.doi.org/10.1021/es4006288](https://doi.org/10.1021/es4006288) | *Environ. Sci. Technol.* 2013, 47, 7892–7898
22. Walkowicz K, Proc K, Wayne S, Nine R, Campbell K, Wiedemeier G. Chassis dynamometer emission measurements from refuse trucks using dual-fuel natural gas engines. SAE Technical Paper; 2003 (2003-01-3366).
23. Feist M, Landau M, Harte E. The effect of fuel composition on performance and emissions of a variety of natural gas engines. SAE Technical Paper; 2010 (2010-01-1476)

24. Nylund N, Erkkila K, Lappi M, Ikonen M. Transit bus emission study: comparison of emissions from diesel and natural gas buses [Internet]. p. Research Report PRO3/P5150/04.
25. Yoon S, Collins J, Thiruvengadam A, Gautam M, Herner J, Ayala A. Criteria pollutant and greenhouse gas emissions from CNG transit buses equipped with three-way catalysts compared to lean-burn engines and oxidation catalyst technologies. *J Air Waste Manag Assoc* 2013;63(8):926e33
26. Einewall P, Tunestål P, Johansson B. Lean burn natural gas operation vs. Stoichiometric operation with EGR and a three way catalyst. *SAE Technical Paper*; 2005 (2005-01-0250)
27. Cocker DR, Shah S, Johnson K, Miller JW, Norbeck J. Development and application of a mobile laboratory for measuring emissions from diesel engines. I regulated gaseous emissions. *Environmental Science and Technology* 2004;38: 2182e9.
28. Huai T, Durbin TD, Miller JW, Pisano JT, Sauer CG, Rhee SH, et al. Investigation of the formation of NH<sub>3</sub> emissions as a function of vehicle load and operating condition. *Environmental Science and Technology* 2003;37:4841e7.

## 5 Technology Has Significantly Lowered Emissions from Yard Tractors over 10 years

### 5.1 Introduction

Cargo handling equipment (CHE) is the one of the largest contributors to the emissions inventory of port related operations in the Port of Long Beach and Port of Los Angeles. The emissions from the CHE's rank the third highest after the ocean going vessels and heavy duty diesel trucks. Cargo handling equipment comprises all of those vehicles used in loading and unloading cargo from ocean going vessels, trains and trucks, and includes tractors, top handlers, side picks, sweepers, dozers and cranes. From the ARB state survey in 2004 <sup>1</sup>, the yard tractors represented over 60% of the units and about 66% of the NOx and PM emissions in the ports of LA and Long Beach.

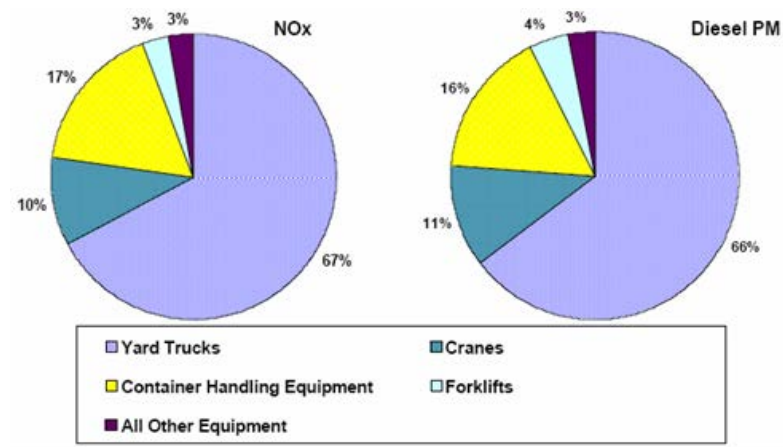


**Figure 32 NOx and Diesel PM Emission Distributions at California Ports**

Yard tractors, are also known as terminal tractors, yard trucks yard hustlers or yard goats, are powered with diesel engines and are designed for the movement of containers: to/from

ships/trains, on/off terminals, to/from RTG cranes or on/off stacks. Yard tractors alone contribute 65% of the state-wide and about 80% of the port region NOx and PM from CHEs.

This chapter establishes emission factors for Yard Tractors built to meet tier 0 to tier 3 emission standards. The vehicle pool tested was selected based on a previous survey by ARB survey that identified the most representative yard tractors in the port regions. This will be the first work in literature to directly measure and report Yard Tractor emissions.

## **5.2 Vehicle Matrix**

There are about 1500 yard tractors operating in the port regions. The ARB survey<sup>1</sup> was used to identify representative tractors on the basis of engine manufacturer and manufacture year. The survey included different types of CHEs at port terminals, their annual use, information about general equipment operating conditions, and engine information (make and model of the engine, horsepower, annual hours of use, any control equipment associated with it, etc.). Table 10 summarizes the distribution of yard tractors based on their make and manufacturer in the port regions. The largest market share of YTs belonged to Cummins and in that the 5.9L and 8.3L engines were most widely used. Furthermore, the Cummins 5.9L engine comprised 14% and 9% respectively of the total YTs in service in the ports. Likewise the 8.3L represented 26% of the total inventory with the most common years, 1991 and 2001, comprising 9% and 5% of the total inventory, respectively. The YTs studies in this chapter are listed in Table 11 and represent >1000 in-use units of yard tractor population.



<b>Yard Truck Make/Size</b>	<b>Total number</b>	<b>% of Total</b>
CUMMINS 5.9L	687	54%
CUMMINS 8.3L	331	26%
Other CUMMINS	180	14%
CATERPILLAR	3	<1%
DETROIT DIESEL	57	5%
OTHER MAKES	8	1%
<b>TOTAL</b>	<b>1266</b>	<b>100%</b>

**Table 10 Diesel Engine Manufacturer for Yard Tractors <sup>1</sup>**

<b>MF Year</b>	<b>VEHICLE</b>	<b>Disp. L</b>	<b>FUEL</b>	<b>ATS</b>	<b>NOx Cert. g/bhp-h</b>	<b>PM Cert. g/bhp-h</b>
1995	CUMMINS/BG	6.7	LNG	DOC		
1997	CUMMINS/C	8.3	Baseline Technology		4	0.1
			Baseline Technology+LZ retrofit	DPF		
2000	CUMMINS/B	5.9	Baseline Technology		6.9	0.41
			Baseline Technology+LZ retrofit	DPF		
2001	CUMMINS/C	8.3	Baseline Technology		5.8	0.41
			Baseline Technology+LZ retrofit	DPF		
2001	CUMMINS/C	8.3	ULSD	DOC/CCV/DPF	6.9	0.4
2003	CUMMINS/C	8.3	ULSD	DOC/CCV/DPF	4.95	0.15
2004	CUMMINS/ISB	5.9	ULSD	DPF	2.4	0.1
2004	CUMMINS/QSB	5.9	ULSD	DPF	4.95	0.15
2004	CUMMINS/WP/BLPG	5.9	LPG	DPF		
2005	CUMMINS/ISB	5.9	ULSD	DOC/CCV/DPF	2.4	0.1
2005	CUMMINS/CG 250	8.3	LNG	TWC/DPF	1.8	0.01
2005	CATERPILLAR/C7	7.2	CARB DIESEL	DPF		
2008	CUMMINS/ISL	8.9	LNG	TWC/DPF		

**Table 11 Vehicle matrix showing the yard tractor manufacturer, manufacture year, fuels used and after treatment technology.**

The first engine listed in the table was a 1995 Cummins LNG engine with a three way catalyst. The next three engines are intended to represent baseline non-road engines with mechanical fuel injection from MF year 1997, 2000 and 2001. An additional engine from 2001 is included operating on ultralow sulfur diesel instead of the CARB diesel like its previous counterparts. The engines from 2004 and 2005 represented tier 1 emission standard engines. The QSB was low-emission engine intended for off-road applications and included electronic controls and both charge air cooled and turbochargers. The ISB was modern low-emission engine, except this one

was designed for on-road applications and therefore required to meet the more stringent on-road standard. Therefore, the ISB included electronic controls and a cooled EGR subsystem and a turbocharger with variable geometry. The BLPG- 195 engine with 3-way catalyst is made by Cummins Westport was tested as it was, reported to have very low emissions. The subsequent engines were newer engines designed to meet tighter certification standards.

### **5.3 Test Cycles and Emissions measurements**

The ISO cycle <sup>2</sup> similar to the ARB 8-Mode Cycle which is specially designed to certify off-road vehicles and diesel-powered off-road industrial equipment was used as the operating cycle for all the yard tractors. The cycle consists of 8 modes as shown in Figure 30. This drive cycle represents the driving pattern of most of the off-road vehicles such as industrial drilling rigs, construction equipment including wheel loaders, bulldozers, and off-highway trucks including yard tractors, material handling equipment, fork-lift trucks, and road maintenance equipment. An engine map was generated for yard tractors (engine torque/power versus revolutions per minute (RPM) for the engine in the vehicle) to enable use of this cycle. Emissions sampling and measurements were performed using the Code of Federal Regulations (CFR): *Protection of the Environment*, Section 40, Part 86. Real-time and integrated measurements of criteria pollutants were measured using a mobile emissions collection lab which housed the instrumentation. NO<sub>x</sub> emissions measurements on a real-time basis were performed by chemiluminescence, total hydrocarbons were measured using a heated Flame ionization detector. Particle samples were extracted from the primary dilution tunnel, diluted further in a secondary dilution system and collected on Teflon filters for the PM mass. Detailed description of the mobile emissions lab and emissions collection procedures is provided elsewhere <sup>91</sup>.

<b>Mode number</b> (cycle B)	1	2	3	4	5	6	7	8	9	10	11
<b>Mode number</b> (cycle C1)	<b>1</b>	<b>2</b>	<b>3</b>		<b>4</b>	<b>5</b>	<b>6</b>	<b>7</b>			<b>8</b>
<b>Speed</b> <sup>1)</sup>	Rated speed					Intermediate speed					Low-idle speed
<b>Torque</b> <sup>1)</sup> , %	100	75	50		10	100	75	50			0
<b>Weighting factor</b>	0,15	0,15	0,15		0,1	0,1	0,1	0,1			0,15

**Figure 33 Test Modes, Torque and Weighting Factors for the ISO-8178-C1 Cycle**

## 5.4 Discussions

In this section the history of emissions from yard tractors is discussed. As the years passed the emissions regulations became tighter which ensued the engine manufacturers to meet those stringent standards by adopting different strategies. The strategies for emission control involve the use of improved engine design, the use of after treatment technologies, retrofit of old existing engine technologies with that of a newer improved one and the use of alternate fuels in place of diesel fuels. The discussions in this section will be subdivided based on –

1. Yard tractor emissions benefits from fuel emulsification
2. Yard tractor emissions from advanced engine technology (> Tier 2)
3. Yard tractor emissions from engines fuelled with alternate fuels

### 5.4.1 Yard Tractor emissions from engine retrofits

This sub section evaluates the emissions benefits of water fuel emulsification on emissions. CARB diesel (baseline fuel) and Chevron’s Proformix Lubrizol emulsified fuel were tested on three engines 2001 MY Cummins C8.3L, 2000 MY Cummins B5.9L and 1997 MY Cummins C8.3L as shown in Figure 31. The retrofit incorporating an

emulsified fuel has emissions reductions benefit shown in Table 12. The emulsified fuel used in the yard tractors across the ports of LA and LB and is “water-in-fuel” or diesel blend that utilizes Lubrizol’s PuriNOx technology to lower NOx emissions it is a homogeneous, white emulsion of diesel fuel, water and chemical additives. The addition of water to fuel increases atomization of the diesel/air charge within the cylinder and lowers peak combustion temperature. The net result of these processes is reduced NOx, particulate matter and other emissions. Low amount of water addition, the amount of emitted NO and NOx increases. As the percentage of water in the emulsion increase the amount of emitted NO and NOx decreases. The reduction of NO and NOx with increases water content refers to the vaporization and sensible water heat reduces the local adiabatic flame temperature <sup>4</sup>. The addition of a DOC along with the retrofit fuel technology can bring added emission reduction advantage as the organic carbon fractions are seen to be further reduced by 65% and the elemental carbon fraction ~10%. Although another study found that the water emulsion fuels emitted higher CO<sub>2</sub> than pure diesel because of the increasing amount of oxygen atoms in mixture<sup>4</sup>.

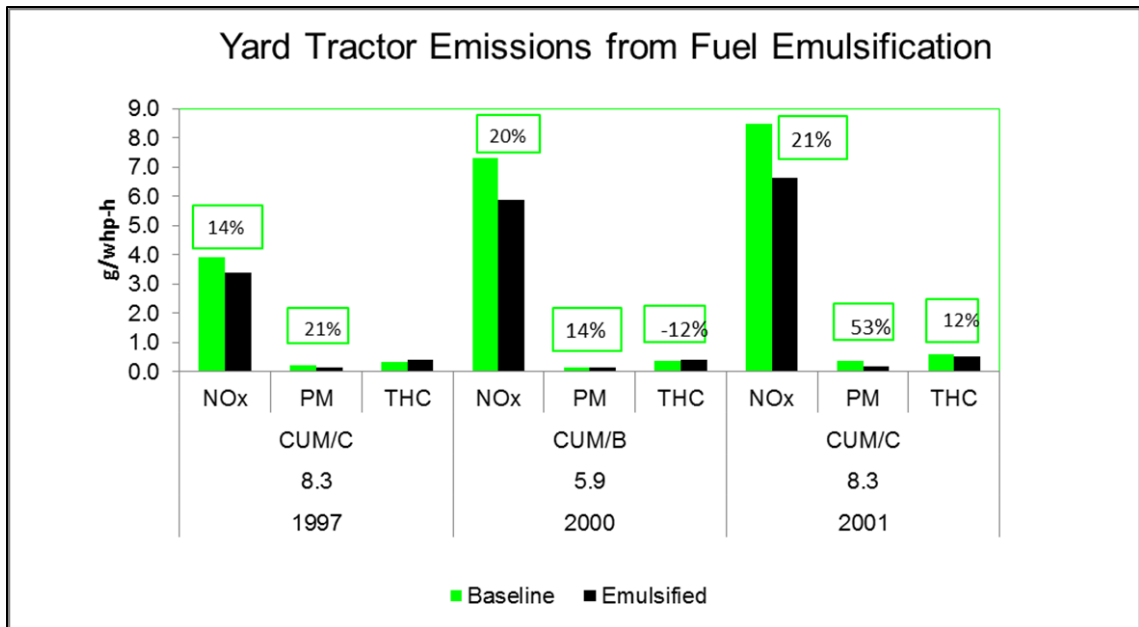


**Figure 34 Emissions from baseline (CARB diesel) and retrofit technology (emulsified diesel) from Yard tractors; repeat tests were within 2% of uncertainty.**

MY	Vehicle	Technology	Emissions g/whp-h			% Change in Emissions		
			NOX	PM	THC	NOX	PM	THC
1997	CUMMINS/C/8.3L	Baseline	3.92	0.19	0.33	-	-	-
		Baseline/LZ	3.38	0.15	0.4	14%	21%	-21%
2000	CUMMINS/B/5.9L	Baseline	7.3	0.14	0.34	-	-	-
		Baseline/LZ	5.86	0.12	0.38	20%	14%	-12%
2001	CUMMINS/C/8.3L	Baseline	8.47	0.34	0.59	-	-	-
		Baseline/LZ	6.65	0.16	0.52	21%	53%	12%

**Table 12 Emissions and percent change in emissions for NOx, PM and THC emissions from Baseline (CARB diesel) and retrofit (Emulsified diesel Lubrizol); +indicates benefit and – indicates dis-benefit.**

#### 5.4.2 Yard Tractor emissions from improved engine technology

Yard tractor emissions from different engines incorporating advanced engine technology are represented in the Figure 32. Starting from the tier 1 Cummins 8.3L 2001 engine the emissions are highest and as the newer advanced engines were used the emissions

reduced to meet the certification standards. PM emissions were all low and near certification standards owing to the DPF. The Cummins 8.3L 2003 engine was designed to meet the tier 2 emissions standards. Both of these engines had a closed crankcase ventilation system along with a diesel oxidation catalyst and a diesel particulate filter. The next two engines were a 2004 off-road (QSB 5.9L), and a 2004 on-road engine (ISB 5.9L). Both are similar engines and have a similar displacement the former has an off-road engine and the latter an on-road engine. The on-road ISB engine was using an EGR emissions control strategy to meet on-road standards that were more stringent than Tier-2 off-road standards required for the industrial QSB engine. The 2004 ISB engine certified to 2.4 g/bhp-hr for NO<sub>x</sub> plus NMHC and 0.10 g/bhp-hr for PM on the FTP cycle and a 2004 QSB engine is certified to Tier II values of 8.8 g/bhp-hr for NO<sub>x</sub> plus NMHC and 0.27 g/bhp-hr for PM on the CARB Off-Road or ISO-8178 C1 cycle. The ISB engine additionally had an EGR after treatment technology. The controlled replacement of O<sub>2</sub> by CO<sub>2</sub> in an EGR acts mainly by lowering the O<sub>2</sub> concentration leading to a lower local peak temperature in the combustion zone and, therefore, lowering NO<sub>x</sub> levels<sup>5, 6</sup>. The Caterpillar engine being the most new engine in this category showed the least emissions. All of the engines were equipped with a DPF enabling the PM emissions to be very low<sup>7</sup>. Additionally the DPF accompanied by a DOC reduces the hydrocarbon emissions substantially.<sup>8</sup>

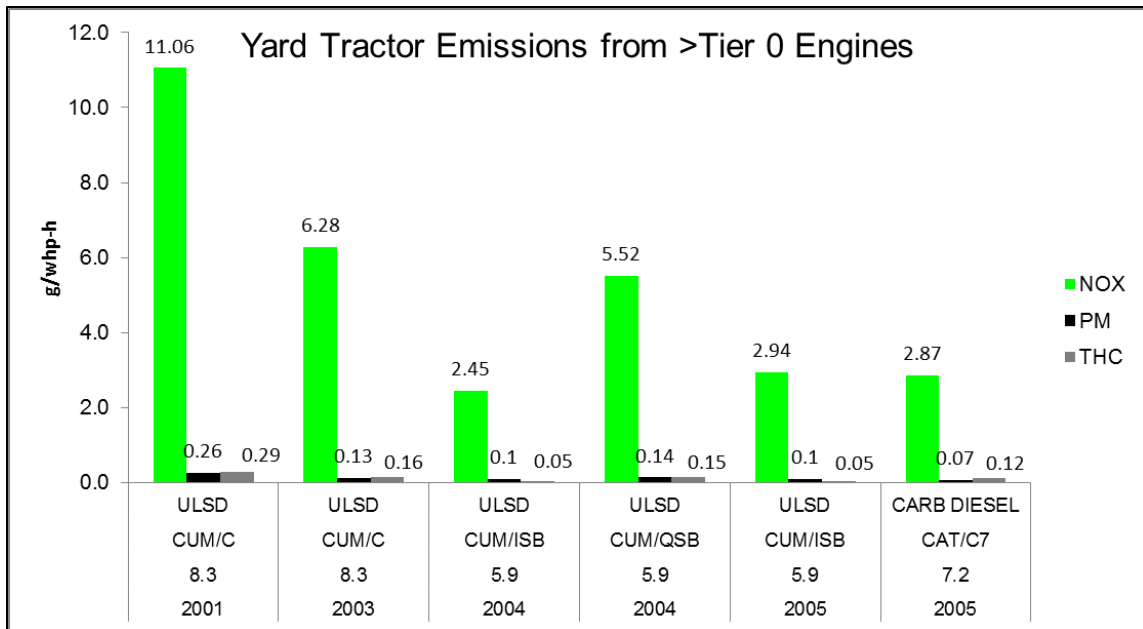


**Figure 35 Yard Tractor emissions from different engine technologies, repeat tests were within 2% of uncertainty.**

#### 5.4.3 Yard tractor emissions from engines fuelled with alternate fuels

Emissions from yard tractors operating on LNG and LPG fuels are shown in the Figure 33. The older engines had higher emissions no matter which fuel. Among the diesel and the alternate fuel yard tractors the latter had the lowest NOx emissions of all the vehicles in this study. The LNG and LPG fuelled yard tractors have very low PM emissions in comparison to diesel. Natural gas vehicles, generally, produce lower levels of NOx, CO (carbon monoxide), and NMHC (non-methane hydrocarbon) emissions<sup>9, 10, 11</sup>. LPG fuels similar to LNG have low emission advantages<sup>12, 13, 14, 15</sup>. The fuel composition is an important characteristic that governs the nature of emissions w.r.t. LNG vehicles<sup>16</sup>. The 1995 lean burn Cummins 6.7 L yard tractor with a diesel oxidation catalyst had the highest NOx of all the yard tractors using alternate fuels. The oxidation catalyst does not provide catalytic reduction of NOx burning on lean conditions and the lean-burn engines

run richer as their molecular number is decreased which leads to the oxidation of more fuel, higher combustion temperatures, and increased cylinder pressures <sup>17</sup>. Whereas, mixed results were seen on the yard tractors burning stoichiometric along with the presence of a three way catalyst. The stoichiometric burns provide optimum operating efficiency promoting NO<sub>x</sub> reductions in comparison to lean burn engines. In view of this fact, the 2008 Cummins ISL 8.9L yard tractor showed the lowest NO<sub>x</sub> emissions among all the yard tractors. The high THC emissions from the 2005 Cummins 8.3L yard tractor are not clear. In order to explore the possibility of any abnormalities with the fuel, samples from this yard tractor were analyzed to find the methane content between 92 to 99%, with a Wobbe Number of 1315 to 1320, well within California's motor vehicle natural gas specifications. Perhaps, the authors speculate the high methane content may be yielded higher THC emissions in which case the catalyst efficiency of the TWC may have been low.



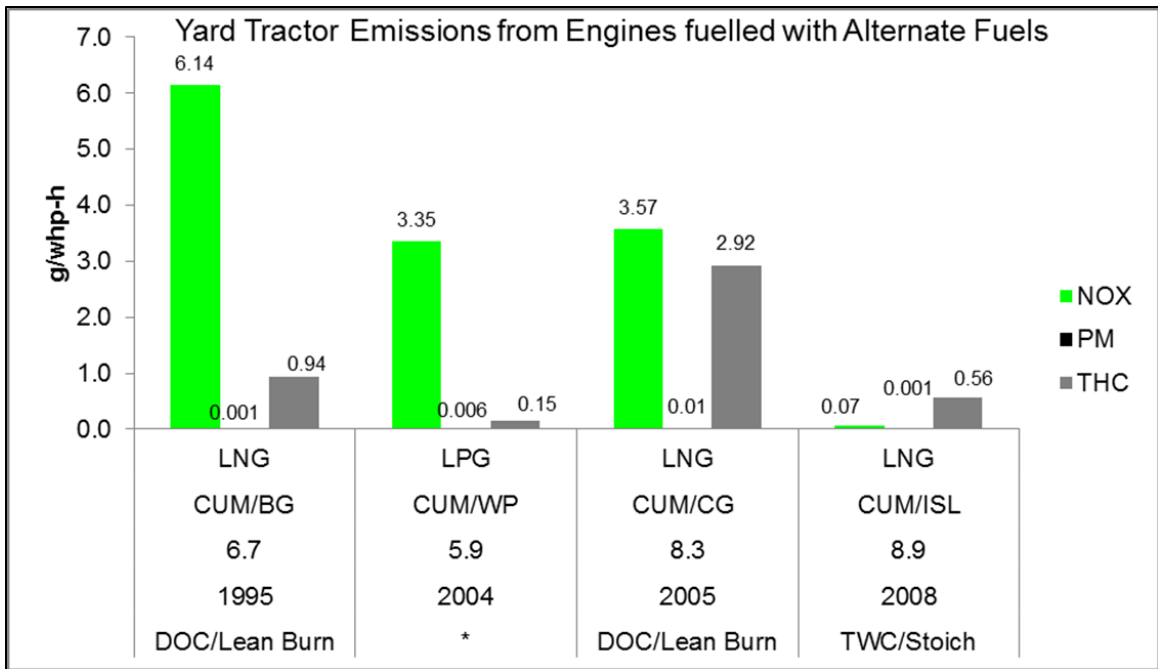


**Figure 36 Yard Tractor emission from using alternate fuels, repeat tests were within 2% of uncertainty.**

\* indicates that the vehicle was equipped only with DPF and no catalyst

## 5.5 Conclusions

Yard tractors are the workhorse of the cargo handling equipment (CHE) and there are over 1,000 in the Ports of Los Angeles and Long Beach region. Their high numbers and frequent use, make them the primary contributor to the emissions inventory from cargo handling equipment. Over 50% of the NOx and PM emissions from CHEs can come from yard tractors. This paper is one of its kinds mainly focusing on the emissions trend from yard tractors over a decade. The emissions from the yard tractors starting from the older tractors and fuels that were at the ports from 2001(baseline inventory) to eight years later in 2008 is shown in this paper. The emissions trend has varied over the years owing to different strategies like the use of advanced engine/fuel technologies and alternate fuel

geared towards meeting certification requirements. The emissions shown in this study are in terms of wheel horse power instead of brake horse power. Due to power losses in the drive train plus other losses due to auxiliary units, the brake engine load will be higher than the wheel load. The specific emission factors, in g/hp-hr, presented in this paper are calculated using the load at the wheel (whp) instead of the engine load (bhp). Therefore, the emission factors measured in vehicle chassis testing (brake horse power) are typically higher than those measured in equivalent engine testing. With this in mind the measured values are very close to the certification values, especially when one accounts for the 10 to 20+% difference between wheel-hp and brake-hp. The g/whp-h emission factors for the yard tractors over decade are shown in the Figure 34. It is clear that with the advancement in engine and fuel technology the yard tractor emissions have reduced by over a factor of 6 starting oldest yard tractor to the newest in the study. This information is crucial in order to provide a basis for the emissions inventory for emissions specially arising from Yard tractors in the port regions. Additionally this information will contribute towards understanding the projection of emissions from the yard tractor if a major change is desired fuel or technology wise for the yard tractor fleet in the port regions.

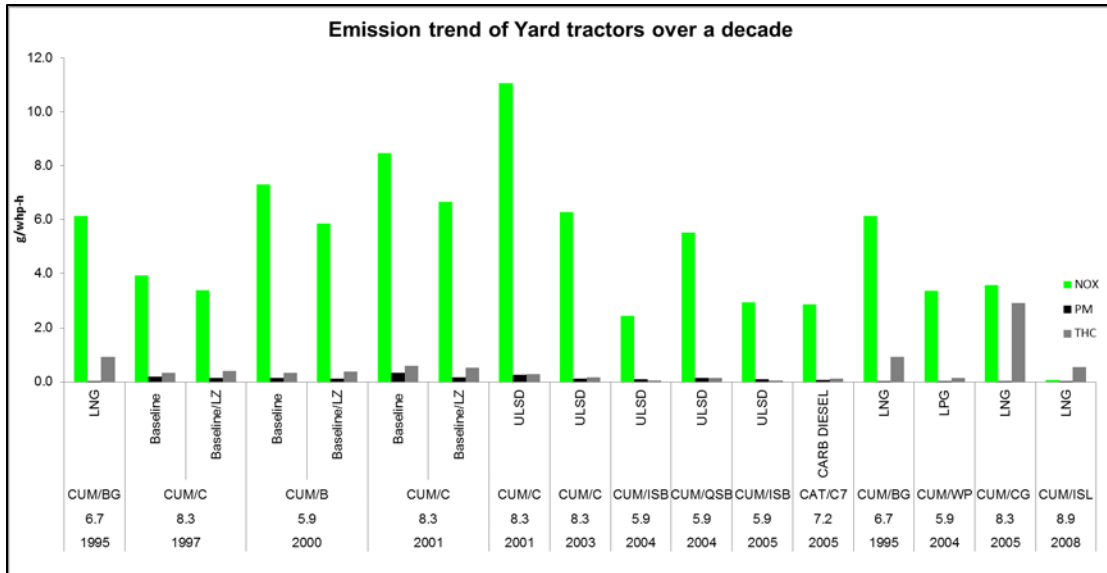


Figure 37 Yard tractor emission trend over a decade.

**References:**

1. California Environmental Protection Agency, Air Resources Board Staff Report, Stationary Source Division, Emissions Assessment Branch: Initial Statement of Reasons for Proposed Rulemaking & Adoption of the Proposed Regulation for Mobile Cargo Handling Equipment at Ports and Intermodal Rail Yards, October 2005.
2. International Standard Organization ISO 8178-4 Reciprocating internal combustion engines - Exhaust emission measurement -Part 4:Test cycles for different engine applications, First edition 1996-08-15
3. Cocker III, D. R., Shah, S., Johnson, K., Miller, J. W., Norbeck, J., Development and Application of a Mobile Laboratory for Measuring Emissions from Diesel Engines. I Regulated Gaseous Emissions, Environ. Sci. Technol.,2004, 38,2182-2189
4. A. Alahmer, J. Yamin, A. Sakhrieh, M.A. Hamdan., Engine performance using emulsified diesel fuel. Energy Conversion and Management 51 (2010) 1708–1713
5. Ladommatos, N., Abdelhalim, S. M., Zhao, H., & Hu, Z. (1998). The effects of carbon dioxide in exhaust gas recirculation on diesel engine emissions.Proceedings of the I MECH E Part D Journal of Automobile Engineering, 212, 25–42.
6. Zheng, M., Reader, G. T., & Hawley, J. G. (2004). Diesel engine exhaust gas recirculation—a review on advanced and novel concepts. Energy Conversion & Management, 45, 883–900

7. Majewski, W. A, and Khair, M. K., Diesel Emissions and Their Control, SAE International, 2006
8. Johnson, T. V., “Diesel Emission Control in Review”, SAE 2006-01-0233
9. Turrio-Baldassarri L, Battistelli CL, Conti L, Crebelli R, De Berardis B, Iamiceli AL, et al. Evaluation of emission toxicity of urban bus engines: compressed natural gas and comparison with liquid fuels. Science of the Total Environment 2006;355:64e77.
10. Nylund N, Erkkila K, Lappi M, Ikonen M. Transit bus emission study: comparison of emissions from diesel and natural gas buses. Research Report PRO3/P5150/04. Finland: Technical Research Centre VTT Processes, <http://www.vtt.fi/inf/pdf/jurelinkit/VTTNylund.pdf>; 2004.
11. Jayaratne ER, Ristovski ZD, Meyer N, Morawska L. Particle and gaseous emissions from compressed natural gas and ultralow sulphur diesel-fuelled buses at four steady engine loads. Science of the Total Environment 2009;407:2845e52
12. Gamas, E. D.; Diaz, L.; Rodriguez, R.; Lopez-Salinas, E.; Schifter, I.; Ontiveros, L. Exhaust emission from gasoline and LPGpowered vehicles operating at the altitude of Mexico City. J. Air Waste Manage. Assoc. 1999, 49, 1179–1189 ; Chang, C. C.; Lo, J. G.; Wang, J. L. Assessment of reducing ozone forming potential for vehicles using liquefied petroleum gas as an alternative fuel. Atmos. Environ. 2001, 35, 6201–6211.

13. Chang, C. C.; Lo, J. G.; Wang, J. L. Assessment of reducing ozone forming potential for vehicles using liquefied petroleum gas as an alternative fuel. *Atmos. Environ.* 2001, 35, 6201–6211
14. Ristovski, Z. D.; Jayaratne, E. R.; Morawska, L.; Ayoko, G. A.; Lim, M. Particle and carbon dioxide emissions from passenger vehicles operating on unleaded petrol and LPG fuel. *Sci. Total Environ.* 2005, 345, 93–98.
15. Lim, M. C. H.; Ayoko, G. A.; Morawska, L.; Ristovski, Z. D.; Jayaratne, E. R.; Kokot, S. A comparative study of the elemental composition of the exhaust emission of cars powered by liquefied petroleum gas and unleaded petrol. *Atmos. Environ.* 2006, 40, 3111–3122
16. Maryam Hajbabaie , Georgios Karavalakis , Kent C. Johnson , Linda Lee , Thomas D. Durbin. Impact of natural gas fuel composition on criteria, toxic, and particle emissions from transit buses equipped with lean burn and stoichiometric engines. *Energy* 62 (2013) 425e434
17. Feist MD. Fuel composition testing using DDC series 50G natural gas engines; August 2006. Final report prepared by Southwest Research Institute for the Southern California Gas Company, Report No. 11657

## 6 Summary of the Dissertation

Chapter 1 examined a total of forty-nine burns conducted at the Missoula Fire Sciences Lab consisting of nine fuel types; i.e., chamise scrub oak, ceanothus, maritime chaparral, coastal sage scrub, California sage brush, manzanita, oak savanna, and oak woodland and masticated mesquite. The chemical characterization performance of the high resolution Time-of-flight Aerosol Mass Spectrometer (HR-ToF-AMS) for during flaming, mixed and smoldering phases of biomass burning was assessed. Correlations between HR-ToF-AMS and offline chemical characterizations following standardized methods are provided for levoglucosan, organic carbon, and particle bound PAHs, and inorganic ions, providing direct insight into the performance of the HR-ToF-AMS for these species. The HR-ToF-AMS was found to perform well for organics carbon and levoglucosan (consistent negative 30% bias) while chloride, sulfate, and nitrates performed poorly due to the formation of refractory salts in the biomass plumes. PAHs were greatly overestimated by the HR-ToF-AMS, possibly due to surface ionization effects.

Chapter 2 on the efficiency of the NO<sub>x</sub> control technologies, given a number of control technologies were employed during this regulatory transition period. Contrary to earlier reports, NO<sub>x</sub> emissions for HDDTs with only cooled EGR more than double for the Near Port operations as compared to the Regional driving. During the Near Port cycle, the engine usually operated outside the Not-to-Exceed (NTE) zone, thus allowing emissions higher than certification. With Selective Catalytic Reduction (SCR) control, emissions

increased up to four times for the Near Port operations, again driven by the temperature when the urea was added and the NTE regulatory provisions. Other criteria pollutants did not exhibit these differences. Given the magnitude of the NO<sub>x</sub> differences and importance in the SIP inventories, the results clearly show that NO<sub>x</sub> emissions should be made following real world driving cycles. A secondary finding was the importance of the NTE zones in understanding differences from certification values.

Chapter 3 focused on providing a broader comparison of regulated emissions over a range of different vehicle technologies and applications for buses and refuse haulers. The cycles that were used for in-use testing of these vehicles also covered wide range of scenarios of driving, therefore providing a realistic idea about the emissions factors.

Chapter 4 discussed the history of yard tractor emissions over a span of 10 years. This study was one of its kinds, focusing mainly on yard tractor emissions, as they play a major role in contributing to the port region emissions inventory. Data was presented on Tier 0 engines and on engines with control technologies including: emulsified fuels, CNG (both original and retrofit), LPG, diesel oxidation catalysts, diesel particle filters. Emissions measurements were made using UCR's mobile lab meeting federal standards while the vehicles were operated following both steady-state and transient driving cycles. The resultant impact of this concerted effort to reduce the impact of yard tractors on the nearby neighborhoods was made clear.



## A. APPENDIX

Laboratory characterization of PM emissions from combustion of wildland biomass fuels  
S. Hosseini<sup>1</sup>, S. P. Urbanski<sup>2</sup>, P. Dixit<sup>1</sup>, Q. Li<sup>1,\*</sup>, I. Burling<sup>3</sup>, R. Yokelson<sup>3</sup>, M.  
Shrivastava<sup>4</sup>, H. Jung<sup>1</sup>, D. R. Weise<sup>5</sup>, W. Miller<sup>1</sup>, D. Cocker<sup>1</sup>

### Introduction

Fresh smoke from wildland biomass burning is a complex mixture of gases and aerosols. The amount and composition of fire emissions depend on a wide range of parameters related fuel type, packing ratio, fuel composition, chemical composition, fuel moisture, fire behavior (e.g. relative amount of smoldering and flaming) [*Andreae and Merlet, 2001; Akagi et al., 2011*]. While wildland fuels are composed primarily of cellulose, hemicelluloses, and lignin, the composition and quantity of trace elements vary by plant species, soil type, and ambient air mass, deposition of sea-salt and anthropogenic nitrogen and sulfur deposition [*Albini, 1976, Fenn, 1991; Hardy et al., 1996; McKenzie et al., 1996; Yokelson et al., 2011*]. Local climate and meteorological conditions influence both plant structure and moisture-conserving strategies, which in turn influence fire behavior and smoke emissions when these fuel types are burned.

While the mean June-August temperatures are similar (15-27 °C), the southwestern (SW) United States tends to be drier (34-69 cm annual precipitation) than the more humid southeastern (SE) United States (114-160 cm) and the seasonality of precipitation is different (23-30 cm December-February for both regions, < 3 cm and 30-42 cm June-

August for the SW and SE, respectively<sup>1</sup>. However, some plants and plant communities have developed similar structure and foliar characteristics such as chaparral in California and pocosin in North Carolina [Christensen, 2000; Keeley, 2000]. Prescribed burning is a vegetation management tool used to manage wildlife habitat, remove wildland fuel accumulation to reduce the potential for severe wildfire, and to mimic the natural role of fire [Chandler *et al.*, 1983]. Recent modeling studies have analyzed the potential use of prescribed burning as a tool to reduce carbon dioxide emissions [Narayan *et al.*, 2007; Wiedinmyer and Hurteau, 2010]. Due to a variety of reasons, prescribed burning is used extensively in the SE in contrast to limited use in chaparral and oak ecosystems in the SW. Between 2002 and 2011 the annual average area treated with prescribed burning was 599 kHa in the southeastern U.S. (SE: Alabama, Arkansas, Florida, Georgia, Louisiana, Mississippi, North Carolina, South Carolina, Tennessee, and Virginia) and 134 kHa in the southwestern U.S. (SW: Arizona, California, Colorado, New Mexico, Nevada, and Utah) (NIFC, 2012). During the same period, wildfires burned an average of 854 kHa yr<sup>-1</sup> in the SW and 215 kHa yr<sup>-1</sup> in the SE (NIFC, 2012).

While prescribed burning is an important land management tool, emissions from prescribed fires and wildfires can have a significant detrimental impact on air quality by degrading visibility and increasing ambient concentrations of fine particulate matter (PM<sub>2.5</sub>, aerosol with an aerodynamic diameter  $\leq 2.5 \mu\text{m}$ ), ozone (O<sub>3</sub>) More generally,

---

<sup>1</sup> Climatological statistics derived from data developed by National Climatic Data Center using US Climate Division Dataset Mapping Page and 1981-2010 base period (<http://www.esrl.noaa.gov/psd/data/usclimdivs/>) accessed 24 Apr 2012.

emissions from biomass combustion can have a substantial influence on local-to-global scale chemical and physical properties of the atmosphere through short- and long-range transport [Crutzen and Andreae, 1990; Fishman et al., 1991]. Smoke aerosols can alter the radiation budget of the earth, cloud properties and climate [Reid et al., 1998; Haywood et al., 2003; Kaufman and Fraser, 1997; Hobbs et al., 1997]. Epidemiological studies have linked mass concentration of PM<sub>2.5</sub> to human morbidity and mortality [Pope et al., 2009]. Wildland firefighter exposure studies have reported exposures to CO, particulates, and silica at levels near or higher than recommended occupational exposure levels [Materna et al., 1992], other studies report that smoke exposure occasionally approaches legal and recommended exposure levels [Reinhardt and Ottmar, 1997]. Because of the different nature of the work, firefighters generally were exposed to more smoke on prescribed fires than on wildfires [Reinhardt and Ottmar, 2004]. Additionally, toxic gases [Roberts et al., 2011] are emitted and several PAHs present in wood-smoke are known to be carcinogenic and/or associated with mutagenicity [Roberts and Corkill, 1998; Ramdahl and Becher, 1982]. Wildland firefighter exposure studies have reported exposures to CO, particulates, and silica at levels near or higher than recommended occupational exposure levels [Materna et al., 1992], other studies report that smoke exposure occasionally approaches legal and recommended exposure levels [Reinhardt and Ottmar, 1997]. Because of the different nature of the work, firefighters generally were exposed to more smoke on prescribed fires than on wildfires [Reinhardt and Ottmar, 2004].

Limited data is available regarding particulate emissions from the combustion of fuels commonly burned by prescribe fires and wildfires in the U.S. Little emissions data exist for fuels common to the SW United States, specifically those classified as chaparral. The USFS has classified approximately 5.7 million hectares (17%) of the vegetation in California as brush, 1.62 million hectares of southern and central California are covered with the shrub complex known as chaparral. To assess the potential effects of biomass burning on the atmosphere, it is necessary to provide reliable emission factors (EF) and combustion parameters to emission inventory algorithms that provide emission input to atmosphere – chemistry transport models and smoke dispersion models. The objective of our study is to determine particulate matter EF for the combustion of fuels representative of ecosystems commonly managed with prescribed burning in SW and SE U.S. EF were determined by measuring particulate and gas phase emissions from the burning of fuels in the large scale combustion facility at U.S. Forest Service (USFS) Missoula Fire Sciences Laboratory. The current study presents only a subset of results and the other results from lab and field components are published elsewhere [*Burling et al.*, 2010; *Hosseini et al.*, 2010; *Burling et al.*, 2011; *Veres et al.*, 2010; *Roberts et al.*, 2010].

## Experimental Methods

### Fuel type description

Samples of vegetation representing important wildland fuel types on Department of Defense installations in the southwestern and southeastern U.S. were harvested in the field and shipped to the U.S. Forest Service Fire Sciences Laboratory (FSL) in Missoula,

MT in January 2009. These fuel types commonly occur in these two regions. The fuels were stored and then burned in the FSL combustion facility in February 2009.

The species composition and chemistry of vegetation comprising each fuel type studied and provides the three-letter fuel code used for fuel type in this paper. This list encompasses 9 and 4 fuel types from the SW and SE that were provided by the United States Forest Service (USFS). Further details regarding the fuels are provided in *Burling et al.*, [2010].

Fuels were analyzed for chemical composition by first grinding the plant tissues (wood and foliage) into a uniform coarse material using a Thomas Model 4 Wiley® Mill<sup>2</sup>. The samples were further ground to extremely fine particles using a mortar grinder. Approximately 5g of each fuel sample was analyzed for C, H, N, S, and O using a combustion technique [McGeehan and Naylor, 1988] on a Thermo Fisher Scientific FlashEA 1112 Series Elemental Analyzer. The vegetation components comprising the fuel beds were also analyzed by an outside laboratory (University of Idaho Analytical Sciences Laboratory) for Cl, K, and Na content (Table 1). The content of Cl, K, and Na varied greatly with location of origin and plant type (see Table 1). Because we did not measure fuel consumption by vegetation component, we cannot quantitatively link element loss in the fuels to the particle and gas-phase emissions. However, we have estimated lower and upper limits on element release for each fuel type and aggregated

---

<sup>2</sup> The use of trade names is provided for informational purposes only and does not constitute endorsement by the U.S. Department of Agriculture.

these limits to provide a representative value for each location (see Table 1). The purpose of these representative values is to illuminate the role of fuel chemistry in aerosol element emissions they are not intended for developing quantitative relationships.

#### Combustion Facility and Burn procedure

Experiments were conducted at the U.S. Forest Service's combustion facility at the Fire Sciences Laboratory (FSL) in Missoula, MT. The facility is a large air-conditioned chamber that measures  $12.5\text{ m} \times 12.5\text{ m} \times 22\text{ m}$  in height. A 3.6 m inverted funnel opening approximately 2 m above the floor captures the smoke from fires on a continuously weighed fuel bed. The smoke is then directed through a 1.6 m diameter exhaust stack that exhausts through the ceiling. The room is pressurized slightly to ensure complete entrainment of fire emissions. A large sampling platform surrounds the stack at 17 m elevation where an Open Path Fourier Transform Infrared Spectrometer (OP-FTIR) and a suite of particle instrumentation were located. The smoke at the height of sampling platform is well-mixed and has the same temperature and mixing ratios across the stack diameter [Christian *et al.*, 2003; Christian *et al.*, 2004]. The fuel bed was an aluminum frame with wire mesh and removable heat-resistant 1.27 cm Kaowool M Board that was removed depending on the physical characteristics of the vegetation. Two electronic balances continuously recorded the mass of the fuel. The stack exhaust fan speed was 1.5 and 3.0 m/s for majority of the burns. Nearly all of the fires were ignited with a propane torch, a small number were ignited using isopropyl alcohol in addition to the torch. Additional information on the FSL combustion facility may be found in [Christian *et al.*, 2004].

## Measurement system and sample analysis

Three filter sampling systems (FS1, FS2, UCR) simultaneously pulled the smoke sample from the exhaust stack through a cyclone, and then onto quartz and Teflon filters. The cut-off sizes and set flow rates are as follows: two cyclones with cut-off diameters of 2.5 and 3.5  $\mu\text{m}$  were installed on the FS1 and FS2 lines operating at 30 and 28 lpm, respectively. A 2.5  $\mu\text{m}$  impactor ( $PM_{2.5}$ ) distributed the smoke samples between filter samplers QF1,2 and TF1,2 at 25, 23, 27, and 22 lpm (UCR), respectively. For 43 of the 77 burns, FS2 was loaded with Teflon filters while FS1 was loaded with a quartz filter. However, for 24 of the burns FS1 and FS2 were loaded with Teflon filters. QF1,2 and TF1,2 were always loaded with quartz and Teflon filters, respectively. Since duplicate measurements were made by UCR and the USFS (FS1 and FS2), the two subsets were ultimately combined to form the larger data set that is used in this study. UCR used 47 mm Quartz (2500QAT-UP Tissuquartz™, Pall Corporation, NY) preconditioned at 600 °C for 5 hours and pre-weighed 47 mm Teflo® (2 $\mu\text{m}$  pore, Pall Corporation, NY) filters.

In addition to the sampler system described previously, several particulate phase instruments were also located on the platform: an Aerodyne High Resolution Time of Flight Aerosol Mass Spectrometer (HR-TOF-AMS), an Ultrafine Condensation Particle Counter (UCPC Model 3776, TSI Inc.), a Scanning Mobility Particle Sizer (SMPS), a Fast Mobility Particle Sizer (FMPS Model 3091, TSI Inc.), Aerodynamic Particle Sizer (APS Model 3321, TSI Inc.), a Micro-Orifice Uniform Deposit Impactor (MOUDI), and a Dekati® Mass Monitor (DMM).

A single 1.0 cm × 1.5 cm punch from each quartz filter was analyzed for elemental and organic carbon by both UCR and the USFS with a Sunset Laboratory (Forest Grove, OR) Thermal/Optical Analyzer following NIOSH 5040 reference method (1996) [*Birch and Cary, 1996*]. Pre- and Post-experiment Teflon filter weights were obtained following Code of Federal Regulations [*CFR40 1065, 2005*].

Following gravimetric analysis, elemental composition of the deposited material on the Teflon filters was determined using by X-ray fluorescence (XRF). The USFS samples were analyzed by Chester Labnet (Tigard, OR) using U.S. EPA Method IO-3.3. The UCR samples were analyzed by the South Coast Air Quality Management District (SCAQMD, Diamond Bar, CA) using a PANalytical Epsilon 5® Energy Dispersion X-Ray Fluorescence (EDXRF) equipped with dual anode (Scandium/Tungsten) X-ray tube. Each filter was analyzed ten separate times using ten different excitation conditions under vacuum. The instrument software deconvoluted and calculated the concentration for each element in µg/m<sup>3</sup>. For the EDXRF technique, Analytical quality control was determined by testing NIST Standard Reference Material 2783. Most USFS Teflon filters were analyzed by XRF method for 29 burns, while UCR analyzed one filter for each fuel type.

A set of 47-mm Teflon substrates was used for Ion Chromatography (IC) analysis following California Air Resources Board Method MLD 142. The filters were extracted by sonication into deionized water and small amount of isopropyl alcohol. Aliquots of the extract were then filtered and analyzed on a Dionex DX-120 ion chromatograph. The



analysis yielded concentrations of the following ions: sulfate, nitrite, fluoride, chloride, bromide, sodium, ammonium, potassium and calcium.

The 47-mm quartz substrates were spiked with  $^{13}\text{C}$  labeled levoglucosan (purchased from Cambridge Isotope Laboratories Inc., Andover, MA) and select deuterated PAHs. The  $^{13}\text{C}$  spike volume was calculated based on the organic carbon content of each filter ( $\mu\text{g}/\text{filter}$ ), whereas the PAH spike volume was maintained constant at 100  $\mu\text{L}$  on each filter. The filters were extracted using dichloromethane and acetone (50:50) by a Dionex® Automated Solvent Extractor 200 (ASE). Half of the extracted volume was used for levoglucosan analysis and the other half for the PAH analysis.

The half of the extracted sample used for PAH analysis was concentrated to 5 mL by rotary evaporation using a BUCHI-3000 evaporator. The sample was further concentrated to 1.5 mL with a nitrogen stream. This final volume was transferred to amber wide crimp top vials, sealed and analyzed on a Agilent® 5973 GC-MS equipped with a Programmable Temperature Vaporizer (PTV) large volume inlet (7683 Series).

The other half of the extracted sample was concentrated to 5 mL by rotary evaporation using a Buchi® R-3000 Rotary evaporator. This sample was further evaporated to 250 $\mu\text{L}$  aliquot using nitrovap. 50  $\mu\text{L}$  of the aliquot was carefully transferred into an amber vial and nitrovaped to dryness. The sample was then derivatized for 2 hours at 70°C with 50 $\mu\text{L}$  of N,O-bis(trimethylsilyl) trifluoroacetamide and 25 $\mu\text{L}$  of pyridine (obtained from Sigma-Aldrich Chemle GmbH, Switzerland). The sample was subsequently re-diluted to a specific calculated volume based on expected LV concentration, transferred to an

amber wide crimp top vial, sealed and analyzed on the GC-MS. The mass spectrum of levoglucosan tritrimethylsilyl ether exhibited only a small molecular ion (m/z 378) with fragments due to loss of CH<sub>3</sub> (m/z 363), CH<sub>5</sub>Si (m/z 333), C<sub>6</sub>H<sub>17</sub>OSi<sub>2</sub> (m/z 217) and C<sub>7</sub>H<sub>18</sub>OSi<sub>2</sub> (m/z 204, base peak). Fragments 217 and 333 were used for quantification.

The general fire behavior (i.e. the relative amount of flaming and smoldering combustion) was characterized using Modified Combustion Efficiency (MCE) based on CO and CO<sub>2</sub> concentrations measured by OP-FTIR (further details in *Burling et al.* [2010]). The MCE is defined as the fire-integrated excess ratio of CO<sub>2</sub> to CO plus CO<sub>2</sub> (*Ward, D. E. and Radke* [1993]:  $= \frac{\Delta CO_2}{\Delta CO + \Delta CO_2}$ ). It was assumed that the background concentrations of CO and CO<sub>2</sub> were constant during the burns and were equal to their 1-min averaged concentration prior to ignition.

## Results and Discussion

77 fuel beds were burned in an 18 day period in February 2009. Mean temperature and relative humidity in the facility during this period were 23.7 °C (s.d. = 2.0) and 15.2% (s.d. = 3.5), respectively. While in storage, the samples lost much of the moisture normally contained in the plant tissues so the samples that were burned did not represent the moisture content of the living vegetation when normally burned during either a prescribed burn or wildfire. Moisture content of the SW fuels ranged from 4 to 33%; moisture content in living chaparral ranges from 70-160% over the normal growing cycle [*Countryman and Dean*, 1979]. Similarly, moisture content of the SE fuels ranged from 3 to 32%; moisture content in living evergreen pocosin shrubs ranged from about 70 to

250% [Blackmarr and Flanner, 1975]. The arrangement of the fuels significantly affected the fuel consumption. Initially, five chamise/scrub oak and three ceanothus fuel beds were arranged vertically; however, the fire failed to spread well resulting in low fuel consumptions of 3% to 52% (average: 26%). The remaining fuel beds were arranged horizontally, which greatly increased fuel consumption to ~90% for the rest of the burns. A total of 77 fires (71 from SE and SW fuel beds) were conducted at the Missoula FSL combustion facility in February 2009.

#### Determination of the mix of Combustion Processes

Modified Combustion Efficiency (MCE) [Ward, D. E. and Radke, 1993; Yokelson et al., 1996], calculated for each burn, was used to ascertain the relative amount of combustion processes (e.g., smoldering, and flaming; average MCE )The average of fire-integrated MCE values for all burns is  $0.94 \pm 0.002$  (median: 0.942; range: 0.868 - 0.975) indicating that all the burns had a mix of flaming and smoldering with high MCE indicating relatively more flaming. The coefficient of variation of MCE in this study is much smaller than some previous studies (e.g. 0.5% vs. 3.1% McMeeking 2009).

#### Fuel Moisture versus MCE

Fuel Moisture (FM) may weakly affect the average burn MCE was produced combining data from this study with a selected other lab studies: Weise et al. [1991] for California chaparral, Keene et al. [2006] for African savanna, and McMeeking et al. [2009] for a wide variety of U.S. domestic fuels. The plot shows that all these studies have consistent MCE-FM results. The upper bound of MCE for FM>20% stays relatively flat around 0.95 while the lower bound decreases with increasing FM. Upper and lower bounds both

sharply converge to  $MCE=1$ , when  $FM < 20\%$ . The downward and upward triangles in indicate heading and backing fires, respectively [Keene *et al.*, 2006]. As can be seen for  $FM$  up to 20%,  $MCE$  appears to be bound by the fire propagation dynamics (backing/heading fire). Backing/heading fires represent two limiting combustion cases: A heading fire has larger flames, spreads faster and leaves more un-burned fuel behind while a backing fire has smaller flames, slower propagation rates and has higher combustion completeness [Ward, 1998; Peterson and Leenhouts, 1997]. For example, Lobert *et al.* [1991] observed a 40% increase in the  $CO/CO_2$  ratio going from a backing fire to a heading fire for laboratory savanna grass burns. The propagation factor (heading/backing fire) does not seem to be the dominant factor in  $MCE$  values for  $FM > 30\%$ , since after this point the  $MCE$  is seemingly not bound by backing/heading fire data points.

#### Total Particulate Emissions

##### Particle Matter Mass Emission Factors

The EFs in the current study are calculated based on the carbon mass-balance method [Ward *et al.*, 1979; Yokelson *et al.*, 1999; Burling *et al.*, 2011]. The average emission factors for  $PM_{2.5}$  (g  $PM_{2.5}$  per kg dry biomass burned  $EF_{PM_{2.5}}$ ) measured in this study are plotted versus average  $MCE$ . Also included are data points from previous studies that examined similar fuels, as well as trend lines from earlier lab and airborne studies. Hereafter, we will use notation of  $EF \text{ g/kg} < MCE >$  for reporting emission factor and  $MCE$ .

The laboratory study of McMeeking 2009 reported an average EFPM2.5 for chaparral fuels of  $11.6 \pm 15.1 \text{ g kg}^{-1} <0.909 \pm 0.029>$  that includes  $7.8 \pm 1.2 \text{ g kg}^{-1} <0.913 \pm 0.012>$ ,  $6.5 \pm 4.2 \text{ g kg}^{-1} <0.914 \pm 0.030>$ , and  $23.5 \pm 25.9 \text{ g kg}^{-1} <0.899 \pm 0.030>$  for cea, chs, and man, respectively. The current study has lower PM emissions for chs and man, mainly attributed to the higher MCEs (for these specific fuels) in this study. However, cea is higher in the current study, likely due to lower combustion temperatures from the poorly combusted fuel bed. The EFPM2.5 response to MCE in our study (slope = 248.8, is 80% of that reported by *McMeeking et al.* [2009] (slope = 311.1, Figure 9 of *McMeeking et al.* [2009] for EFPM2.5).

Size-resolved PM mass speciation using a micro-orifice uniform deposit impactor (MOUDI) was obtained for 6 burns. The size distribution of PM peaked in the particle accumulation mode with an aerodynamic diameter that ranged (depending on fuel type shown in parentheses) between the 8th stage (2yr/CL and 1 yr/CL;  $0.18 \mu\text{m}$  cut-size) and 10th stage (oas, cea, cuh, and mes;  $0.056 \mu\text{m}$  cut-size). The PM mass in the size range  $3.2\text{-}18\mu\text{m}$  varied between 2-18% of the PM3.2 mass with an average of  $10\% \pm 6\%$ . The ratio of EFPM3.5 to EFPM10 was 1.00-1.07; this is consistent with the PM10 to PM2.5 mass ratio of 1.09 of *McMeeking et al.* [2009]. For quality control purposes, we correlated the total accumulated mass on the MOUDI stages against the Teflon filter mass on the same fire. The total accumulated MOUDI mass was 27% higher than the Teflon filters mass (g),  $r^2=0.99$ ). According to *Reid et al.* [2005], coarse-mode particles can contribute to 10-20% of the total collected PM mass consistent with the current study.

### Particulate Matter Number Emission Factors

The number emission factor was measured and reported separately for two instruments: the ultra-fine CPC Model 3772, TSI Inc. (measuring size range: 2.5nm-3 $\mu$ m) and the Dekati® Mass Monitor (DMM) (measuring size range: 0-1.2 $\mu$ m). CPC Average EFPN were calculated to be  $(5.2\pm 2.7)\times 10^{15}$ ,  $(4.7\pm 1.3)\times 10^{15}$ , and  $(7.8\pm 1.9)\times 10^{15}$  for fuels from the chaparral group, FHUA (SW), and camp Lejeune (SE), respectively. Similarly, average DMM EFPN were  $(5.3\pm 1.6)\times 10^{15}$ ,  $(3.7\pm 1.2)\times 10^{15}$ ,  $(6.5\pm 2.2)\times 10^{15}$  for fuels from chaparral group, FHUA (SW), and camp Lejeune (SE), respectively. These EFPN are in agreement with the estimate of *Andreae and Merlet* [2001] that suggest an EFPN of  $3.4\times 10^{15}$  particles per kg of fuel burned for Aitken nuclei/condensation nuclei aerosol. Differences between particle number emission factors from different fuel types in the current study are explained based by their respective MCEs. In general, the lower SE MCE values compared with higher SW MCE values result in the higher SE particle number emission factors compared with SW fuels.

The airborne EFPN<sub>3 $\mu$ m}</sub> of  $(3.0\pm 1.7)\times 10^{16}$  of *Sinha et al.* [2003] (CPC TSI 3025A) from 10 savanna fire smoke plumes in Africa with very little aging was an order of magnitude higher than this study. The rapid production of ozone and organic acids observed in their airborne FTIR measurements indicate ongoing photochemistry in the plume suggesting the possibility of new particle formation. An airborne study of Amazonian deforestation, *Guyon et al.* [2005], measured an EFPN<sub>3 $\mu$ m}</sub> of  $4.6\times 10^{14}$ - $1.1\times 10^{16}$  particles/kg fuel burned covering the wide range of lab and field study values.

The EFPN by the CPC versus the EFPN by the DMM. As shown, there is a relatively large coefficient of variation (with  $r^2=0.63$ ) in comparing the CPC and DMM. The overall particle number emission factor of CPC is observed to be about 82% of the DMM. As shown in a previously published article from this study [*Hosseini et al.*, 2010], the geometric mean diameter of particles decreases as the fire evolves from flaming phase into smoldering phase. It is noted that the DMM requires a robust size distribution to accurately invert the electronic signals to number concentrations leading to greater variability in number count and possible biases in absolute number concentrations. Therefore, varying PN size distributions and different particle size ranges of the two instruments gave rise to the discrepancy; the ultrafine CPC 3776 has a particle size lower detection limit of 2.5 nm and the DMM has a size range of 0 to 1.2  $\mu\text{m}$ .

Similar to the observed dependency of PM mass on MCE, the linear correlation of EFPN of CPC and DMM with MCE is obtained. As shown, MCE and EFPN are weakly anti-correlated ( $r_{\text{CPC}}^2=0.27$ ,  $r_{\text{DMM}}^2=0.33$ ) which shows some natural variability and may reflect the wide range of fuel types of this study. The regression lines in this study are comparable to previous field studies. The airborne study of *Guyon et al.* [2005] who observed biomass burning of Amazonian forests reported a regression line of  $\text{EFPN} = (-2.80 \times \text{MCE} + 2.76) \times 10^{16}$  that is 37% of the EFPN observed in this study. The *Janhall et al.* [2010] review paper, based on airborne measurements of biomass burning of three fuel types (forest, savanna, and grass), estimates a regression line of  $\text{EFPN} = (-3.46 \times \text{MCE} + 3.44) \times 10^{16}$ , about half the EFPN measured in the current study. These differences are easily attributed to coagulation losses of nucleation mode particles on short time

scales [Reid *et al.*, 1998; Akagi *et al.*, 2012; Reid *et al.*, 2005]. Moreover, the regression line calculated by Janhall *et al.* [2010] uses data points acquired from a Passive Cavity Aerosol Spectrometer Probe (PCASP), which has a lower cut-size of 100nm compared to the cut-size of 2.5 nm in the current study.

#### Particle Component Emission Factors

##### Organic and Elemental Carbon Thermal Optical Analysis

Integrated EFOC, g carbon/kg fuel burned, for all the burns are plotted as function of MCE (Figure -b). EF OC is observed to negatively correlate with MCE ( $r^2=0.72$ ). Lit/FB from SE fuels emitted the highest amount of OC per kg fuel burned ( $10.60\pm 3.64$  g kg<sup>-1</sup>  $\langle 0.894\pm 0.017 \rangle$ ), and oas/FHUA from SW the lowest ( $0.44\pm 0.10$  g kg<sup>-1</sup>  $\langle 0.971\pm 0.004 \rangle$ ). Comparisons of literature EFOC must account for MCE since OC emission factors are highly dependent on MCE. McMeeking *et al.* [2009] reports EFOC of 1.8  $\langle 0.913 \rangle$ , 1.5  $\langle 0.914 \rangle$ , and 7.1  $\langle 0.899 \rangle$  g/kg dry fuel for chaparrals cea, chs, man, respectively, similar to values but slightly overestimated by the proposed EFOC vs. MCE line (Figure -b). Andreae and Merlet [2001] suggest EFOC of 3.4 g kg<sup>-1</sup>  $\langle 0.94 \rangle$  for savanna and grassland that agrees well with the given EFOC-MCE linear fit. Overall, SE fuels generally led to higher EFOC compared to SW fuels at similar MCEs. The only exception is cuh/CL of SE, which was similar to SW fuels.

Integrated EFEC as a function of MCE is plotted in Figure -a. The EFEC (g/kg) ranged from 0.47 g kg<sup>-1</sup>  $\langle 0.965 \rangle$  to 1.54 g kg<sup>-1</sup>  $\langle 0.944 \rangle$  for SW fuels and from 0.41 g kg<sup>-1</sup>  $\langle 0.954 \rangle$  to 1.51 g kg<sup>-1</sup>  $\langle 0.945 \rangle$  for SE fuels, respectively. The highest EFOC in SE and SW group is from cas/FHL and uh/CL, respectively; the lowest EFEC for SE and SW



were cuh/CL and oaw/FHUA. No EFEC ecosystem dependency was observed. Further, *Andreae and Merlet* [2001] suggest an EFEC of  $\sim 0.48 \text{ g kg}^{-1}$   $\langle \sim 0.94 \rangle$  for savanna and grassland fuels that is comparable with the average of chaparral fuels in this study  $1.08 \text{ g kg}^{-1}$   $\langle 0.945 \rangle$ . The correlation between EFEC and MCE is much weaker ( $r^2=0.10$ ) than correlation between EFOC and MCE.

Intense flaming significantly increases the fraction of elemental carbon (EC) emissions in the total PM carbon emissions (TC). The relationship between the EC/TC ratio and average MCE. EC/TC was lower than 0.15 for MCEs smaller than 0.93, while this value strongly rose to 0.7 for MCEs larger than 0.95. The results are consistent with previous studies (e.g. as shown in the figure: *McMeeking et al.* [2009], and *Christian et al.* [2003]). *Reid et al.* [2005] suggests values between 0.05 and 0.18 for flaming, and 0.03 to 0.075 for smoldering. However, *Reid et al.* define smoldering as  $\text{MCE} < 0.9$ ; furthermore, their EC/TC numbers mostly originate from field studies, which rarely achieve  $\text{MCE} < 0.95$  compared to up to 0.98 achieved in the lab where EC/TC rises quickly. Even accounting for MCE, field EC/TC values are lower than lab EC/TC. For example, the airborne study of *Sinha et al.* [2004] sampled fires from African savannah grasses. They measured EC/TC ratios of 0.135  $\langle 0.959 \rangle$  and 0.255  $\langle 0.976 \rangle$  for miombo woodland and dambo grass gland fires, respectively. During the flaming phase in our experiment, we observed temperatures up to  $\sim 70 \text{ }^\circ\text{C}$  at the instrumentation platform level; it is possible that the NMOC require more time to condense to the particle phase, as indicated by the lower EC/TC ratios of airborne studies.

EC/TC ratio increases rapidly as MCE increases past 0.94. The same fact can be seen in Figure 9 (a)-(b) of *McMeeking et al.* [2009]. *Reid et al.* [2005] also noted through investigation of previous studies on fires from savanna/grass/cerrado, tropical forest, etc. for phases of flaming/smoldering set forth that the black carbon content of PM during flaming can be a factor of 5 higher than during smoldering.

Compared to *McMeeking et al.*, 2009, current study has nearly seven times higher adsorption artifacts for  $OC > 500 \mu g/m^3$  and almost twice higher for  $0-100 \mu g/m^3$  and the data is more scattered as well. The mass fraction of artifact exponentially,  $0.146+0.355e^{-0.004x}$  and  $0.021+0.173e^{-0.012x}$ , decreased with increase in concentration of smoke for the current and *McMeeking et al.* studies, respectively. *McMeeking et al.* [2009] used significantly less amount of fuel for each burn and this might have led to cooler diluted smoke, enhanced partitioning of gas into particle phase, and subsequently less artifacts, while in the current study the weight of the fuel bed varied between 250 and 5,500 grams averaging  $2470 \pm 1090$  g.

*McMeeking et al.* [2009] reported an exponential function for the ratio of carbon artifacts (SVOCs) collected on the back filter to front filter OC. a plot of artifacts (SVOC) collected on the back shows

#### Particle Inorganic Content

#### Particle Inorganic Content Metals: X-ray Fluorescence (XRF) Analysis

Teflon filters collected on 50 different burns were analyzed for Cl, Br, Si, P, S, and metals (atomic mass number Na-Pb). The dominant elements, by mass fraction, in order

of decreasing median ranking by burn were K, Cl, Na, S, Zn, Mg, Si, and Ca with potassium the dominant element in 47 of the 50 filters analyzed. In the vast majority of burns with XRF data (28 of 50) the elements K, Cl, Na, and S comprised >90% of the inorganic elemental mass. As discussed in *Akagi et al.* [2011], the properties of particles emitted by biomass burning can change rapidly after emission. The cooling/dilution regime experienced by emissions in the laboratory may be very different from that realized by emissions of a “real fire” burning in the natural environment. It is possible the contribution of semi-volatile organic compounds to organic particle formation and growth is not as efficient in the lab environment. However, the amount of elemental carbon and metals cannot change after emission. Therefore, the EF of inorganic elements measured in our laboratory burns are applicable to fires in the natural environment; however, the mass percentages are likely overestimated due to incomplete condensation of gas-phase SVOC.

The mass of all inorganic elements as a percent of total PM<sub>2.5</sub> mass ranged from 1-56% and varied strongly with fuel type and source location. The mass percent for K, Cl, Na, and S are shown in figure. Fuels harvested from SW consistently produced particles with higher K and Cl mass fractions than the fuels from SE. By source location, the average K and Cl mass percent for SW fuels was: VAFB: K = 17.1(± 4.0)%; Cl = 16.4(± 5.3)%, FHL: K = 10.5(± 5.1)%; Cl = 4.9(± 3.4)%, and FHUA: K = 13.7(± 3.0)%; Cl = 6.9(± 1.3)% for FHUA. The particulate mass fractions of these elements are higher than in previous reports, which may be due to incomplete condensation of gas-phase NMOC as plume cools. However, *Chang-Graham et al.* [2011] noted unusual metallo-organic

species noted detected previously in biomass burning aerosol and hypothesized that land use practice on the military bases where the fuels were collected could contribute. Further, the ratios between metals and metals and EC should not be affected by any possible temperature artifacts.

The PM mass fractions of Cl, K, (and also Na for VAFB), and the sum of all inorganics produced by the southwestern fuels are on the upper end of values found in the literature. The studies reviewed by *Reid et al.* [2005], which covered a wide-range of biomass (South American grassland, African savanna, Cerrado, and North American temperate forest, and tropical broadleaf forest) reported that inorganic trace species emissions were highly variable and accounted for ~5-15% of PM mass. Of 10 studies reviewed by *Reid et al.* [2005], the percent of PM mass consisting of K ranged from 0.4-18% and the Cl mass percent ranged from 0.2-11%. *Andreae and Merlet* [2001] recommend particulate K emission factors that correspond to 6%, 3%, and 1-3% of their recommended EFPM2.5 for savanna/grassland, tropical forest, and extra-tropical forest biomass, respectively. In the laboratory study of *McMeeking et al.* [2009], results for a large variety of fuels, classified according to five broad vegetation groups (montane, rangeland, chaparral, southeast U.S. coastal plain, boreal) produced average mass percents of K and Cl that each ranged from ~0.3-6%. At the less generalized classification of fuel type, the results of *McMeeking et al.* [2009] differ widely, with the mass percentages of K and Cl varying between 0.1-19.4% and 0.1-18.4%, respectively. In a laboratory study of fuels from Indonesia and Africa, the sum of K and Cl typically accounted for only a few percent of PM mass, with the exception of invasive fire-maintained along-along grass from

Indonesia which generated PM that was ~28% Cl and ~19% K by mass *Christian et al.* [2003]. Only two studies reported PM mass fractions of K and Cl for fuels similar to our southwestern fuels. *McMeeking et al.* [2009] found that the fraction of PM<sub>2.5</sub> mass comprised by K and Cl ranged from 1.6-9.5% and 0.4-6.1%, respectively for the chaparral varieties ceanothus, chamise, manzanita and sagebrush. In another laboratory study, K and Cl made up ~24% and ~10%, respectively, of total PM mass emitted by sagebrush combustion [*Chen et al.*, 2007].

Emission factors for K, Cl, Na, and S in PM<sub>2.5</sub> are provided EF for K, Cl, and Na varied significantly by fuel. Fuels from VAFB and FHL had the largest EF<sub>K</sub>, EF<sub>Cl</sub>, and EF<sub>Na</sub> (with VAFB being significantly larger than FHL), while the fuels from the southeast had the smallest. EF<sub>K</sub>, EF<sub>Cl</sub>, and EF<sub>Na</sub> were highest for the fuels from VAFB and FHL and lowest for the southeast fuels. The oas and oaw fuels from FHUA had EF<sub>K</sub>, EF<sub>Cl</sub>, and EF<sub>Na</sub> similar to the southeast fuels, while EF<sub>K</sub> and EF<sub>Cl</sub> for mes was comparable to that measured for the Pacific coast fuels (VAFB and FHL). The differences can be explained largely by the chemical composition of the vegetation making up the fuels. The VAFB and FHL fuels had representative Cl, K, and Na in contrast, the SE fuels and FHUA oas and oaw had concentrations of these elements that were very low. The chemistry of the mes from FHUA was an outlier, high in Cl and K, but low in Na. The high Cl and K for the mes fuel were largely due to the desert broom component, a shrub species that has been identified as a possible element hyper-accumulator.

We may compare our chaparral metal/halogen results with *McMeeking et al.* [2009] which reports chaparral emissions for K, Cl, Na, and S. Our chaparral average EFK of 0.652 g kg<sup>-1</sup> is similar to *McMeeking et al.* [2009] (EFK = 0.50 g kg<sup>-1</sup>), while our EFCl is about three times as large (0.471 g kg<sup>-1</sup> vs. 0.20 g kg<sup>-1</sup>) and our EFNa differs greatly (0.143 g kg<sup>-1</sup> vs. 0 g kg<sup>-1</sup>). Considering the strong link we observed between the element content of the fuels and their respective particle EF, it is likely the differences in EF are due to fuel chemistry. *McMeeking et al.* [2009] do not report fuel chemistry; however, it is possible the Cl and Na content of the fuel samples burned their study was significantly less than that in our study. Among the southwestern fuels, those with an ‘oak’ wood component (chs of California, oas and oaw of Arizona) produced particles with K (9.4±3.2%) and Cl (2.4±1.1%) mass fractions that were significantly lower than that of the other 6 fuels types studied from this region (average 18.0±4.4% and 11.9±5.5%) – see figure.. Inter-fuel differences for both elements are significant at the p <0.001 level. These observations, along with the lack of a significant correlation with MCE, indicate that location and vegetation composition both influence the chemical composition of fuels. We believe both factors are responsible for the difference in EFCl and EFNa observed between our study and *McMeeking et al.* [2009] The Cl content in vegetation and chloride deposition has been observed to show a strong gradient with distance from the Pacific coast [*McKenzie et al.*, 1996]. Since our chaparral fuels were sampled at coastal sites, while, *McMeeking et al.* [2009] studied chaparral harvested 150 km east of Los Angeles, the fuels used in the later study would be expected have a lower content of Cl, Na, and other sea-salt elements.

The percentage of particulate mass as K or S was weakly correlated with MCE ( $r^2 = 0.20$  for K and  $r^2 = 0.40$  for S), while the Cl and Na mass fractions had no correlation. The lack of a significant correlation between inorganic particulate emissions and MCE is consistent with the findings of *McMeeking et al.* [2009] and *Christian et al.* [2003] although *Ward and Hardy et al.* [1996] found EF<sub>K</sub> (flaming) was roughly 10× higher than EF<sub>K</sub> (smoldering). The *Ward and Hardy et al.* [1991] study were all from fires of the same fuel type; whereas this and the other studies cited were across many different fuel types. It is possible that the fuel variations may mask any MCE dependence for these studies.

The particulate emissions of Cl and gas-phase HCl (EF<sub>HCl</sub>) were not correlated with MCE and we suspect their variability is driven by fuel composition. Any underlying dependence of PM Cl and HCl emissions on combustion behavior, in particular the partitioning of evolved fuel Cl between the gas and particulate phase, if present, may be masked by wide variations in fuel Cl content. The EFs of particulate Cl to HCl as a function of MCE was observed to account for the variability of the fuel Cl content. No significant correlation between the ratio EF<sub>PMCl</sub>/EF<sub>PMHCl</sub> and MCE (plot not shown) was observed, a result that indicates combustion behavior (as represented by MCE) is not an important factor in Cl partitioning between these two species.

#### Ionic Inorganic species

Inorganic ion species emission factors are provided in figure at the end.. Similar to the emission factor of crustal elements, potassium and chloride were the most abundant ions and were strongly correlated with each other (slope=1.03;  $r^2=0.89$ ). Fuels from

southwest, compared to the fuels from southeast, emitted much higher amounts of  $\text{Cl}^-$ ,  $\text{K}^+$ ,  $\text{SO}_4^{2-}$ ,  $\text{Na}^+$  per unit mass of fuel burned. This is consistent with our results from the previous section. The mass concentration of nitrite, nitrate, and ammonium for most of filters was below detection limit. These species grow rapidly post emission as reported elsewhere [Yokelson *et al.*, 2009; Akagi *et al.*, 2012].

Chlorine was the most abundant inorganic species in the PM<sub>2.5</sub> aerosol, accounting for 0.4-24.5% of the soluble inorganic mass concentration. McMeeking *et al.* [2009] found that chlorine accounted for 2-9% of PM<sub>2.5</sub> mass for several of the same fuels burned in this study including chaparral and sagebrush. Similar to our study, they observed high  $\text{Cl}^-$  mass fraction (60% of inorganics).  $\text{EFCl}^-$  varied from 0 to 1.23 g/kg of fuel burned depending on the fuel type and source location. The study average was  $0.34 \pm 0.35$  g/kg. The  $\text{EFCl}^-$  reported were 1-2 g/kg, 0-1.8 g/kg, 0-1.8 g/kg, and 0-3.2 g/kg from Andreae and Merlet [2001], Christian *et al.* [2003], Keene *et al.* [2006], and McMeeking *et al.* [2009], respectively.

Sulfate emission factors ranged from 0 to 0.22 g  $\text{SO}_4^{2-}$ /kg fuel and were weakly correlated with MCE ( $r^2=0.48$ ). Also comparing XRF to IC results, it can be inferred that ~89% of the particulate sulfur element is in the form of  $\text{SO}_4^{2-}$ . Sinha *et al.* [2003] estimated an average 0.16 g sulfate per kg of fuel burned for savanna fires, while Andreae and Merlet [2001] recommended 0.37 g/kg.  $\text{EFSO}_4^{2-}$  is affected by the age of smoke and the nutrient content of the fuel [Yokelson *et al.*, 2009]. As a smoke plume ages, the  $\text{SO}_2(\text{g})$  oxidizes in aqueous phase to  $\text{H}_2\text{SO}_4$  and then partners with positive ions



such as potassium and ammonium in the particles, thereby increasing aerosol  $\text{SO}_4^{2-}$  percent mass over time. In the airborne studies of northern tropics deforestation, *Yokelson et al.* [2009] showed that sulfate mass concentration can increase 3 times during a time interval of ~1hr. In their study, sulfate made up to 1.5% of PM1 mass from nascent smoke, while in our study it made up to 7.5% of PM2.5 mass for very fresh smoke. The sulfate content differences are attributed to the different sulfur content of the fuel. In our study, sulfate was also weakly correlated with MCE ( $r^2=0.48$ ).

Non-soil, non-sea-salt Potassium (often denoted “nsnss-K”) is an important tracer of biomass burning aerosol [*Andreae and Merlet, 2001*]. Potassium was the second-most abundant ionic species in this study varying between 0.03 to 1.40 g/kg fuel burned. The emission factor of potassium from XRF was 12% higher than the ionic K from Ion Chromatography (IC) ( $r^2=0.83$ ) indicating the vast majority of potassium is in ionic form. Our results are consistent with the laboratory studies of *McMeeking et al.* [2009] and *Christian et al.* [2003] that reported emission factor of 0.03 to 1.50 g/kg for a variety of US domestic fuels, and 0.02 to 1.29 g/kg for African, Indonesian fuels. However, we report  $\text{EFK}^+$  that is twice the  $\text{EFK}^+$  that *McMeeking et al.* [2009] obtained for chaparral.

Among all the southeastern and southwestern fuels, fuels from VAFB had the highest mass percent of ionic inorganic species ranging from ~9-62%, while emissions from Camp Lejeune fuels had the lowest amount of inorganic PM (~2-15%). Other than fuel source location, fuel type also affected the ionic species emissions. For example, among the fuel from VAFB, fuel code 'man' has the least amount of  $\text{Cl}^-$  ( $301.03 \pm 97.73$  mg/kg

fuel burned), while fuel code 'cas' from the same location has the greatest amount (1405.99±457.22 mg/kg fuel burned). These observations coupled with the lack of significant correlation with MCE suggest that fuel composition and vegetation type play the dominant role in emissions of ionic species. Very little to lower than detection limit amounts of calcium, ammonium, bromide, and nitrite were found. These species plus fluoride comprise the remainder of the inorganic ions. No dependency on MCE was observed for any these ions. A slight correlation between Na<sup>+</sup> and MCE (r<sup>2</sup>=0.19) without any regional dependency was observed.

#### Elemental Analysis of the PM filters

##### Mass Balance

PM<sub>2.5</sub> mass was reconstructed based on OC, EC, metals, and water-soluble ions from Ion Chromatography (IC) analysis. The relation that is considered here is as follows:

$$EF_{PM_{2.5}} = EF_{EC} + EF_{OM} + \sum EF_{XRF} + \sum EF_{IC} \quad \text{Eq. 1}$$

where the terms of the right hand side are the sum of emission factors of elemental carbon (EF<sub>EC</sub>), organic mass (EF<sub>OM</sub>=factor×EFOC), elemental crustal material (∑ EF<sub>XRF</sub>), and inorganic salts (∑ EF<sub>IC</sub>) for the *i*th burn.

Mass reconstruction followed *Levin et al.* [2010]; Cl<sup>-</sup> was paired to K<sup>+</sup> as KCl, excess K<sup>+</sup> was then balanced with K<sub>2</sub>SO<sub>4</sub> and KNO<sub>3</sub>, whereas, excess Cl<sup>-</sup> was balanced with NH<sub>4</sub>Cl and NaCl. Any remaining ions were explicitly accounted for in the salt group. Following

the IMPROVE protocol [Pitchford *et al.*, 2007], an assumption was made to consider all Ca and Al from XRF analysis as CaO and Al<sub>2</sub>O<sub>3</sub>.

The EF of organic matter (EFOM) was estimated by multiplying the organic carbon emission factor by a factor of 1.52 to account for associated O, H, and N. This OM/OC value minimizes the difference between the actual and the constructed PM masses, is within the range recommended by Reid *et al.* [2005], and is consistent with the OM/OC ratio acquired by the AMS in this study [Qi *et al.*, 2012]. Additionally, the value is similar to the factors of 1.5 and 1.55 used by Levin *et al.* [2010] and McMeeking *et al.* [2009], respectively. A coefficient of determination of 0.94 is observed).

#### Emission Factors of Levoglucosan

Levoglucosan (1,6-anhydro- $\beta$ -D-glucose), a tarry anhydro sugar and by-product of pyrolysis of cellulose, is a well-established biomass burning marker (Shafizadeh and Fu, 1973; Shafizadeh *et al.*, 1979; Shafizadeh, 1984; Simoneit *et al.*, 1999). Cellulose itself accounts for 40-45% of wood's dry weight and is composed of linear chains of D-glucose linked by  $\beta$ -1,4-glycosidic bonds with a degree of polymerization of up to ~15000 unit [Pettersen, 1984].

Emission factors of levoglucosan (LG) versus MCE are listed in). This subset of data encompasses 43 burns. Measured emission factors for levoglucosan vary substantially with fuel type. For the 15 fuel types of this study, EFLG varied over two orders of magnitude. On average, fuels from 'Camp Lejeune' emitted the highest amount of levoglucosan per kg fuel burned, while the lowest per mass LG emissions were from the

Chaparral fuels. The reported values from the current study are within the range reported by *Schauer et al.* [2001] for residential wood burning, average EFs of 1375, 706, and 1940 mg/kg fuel for pine, oak, and eucalyptus, respectively. The LG/OC ratios for the three fuel groups were  $4.24 \pm 0.90$ ,  $4.30 \pm 1.41$ , and  $5.73 \pm 0.83$  mg/g for Chaparral, FHUA, and CL, respectively. *Sullivan et al.* [2008] during the FLAME studies measured an average LG/OC value of 520 mg/g for their 73 burns. *Engling et al.* [2006] reported values from 36 to 1368  $\mu\text{g}/\text{mg}$  OC. The current study values are 2-3 times lower than reported LG/OC ratios for 'man' and 'chs' [*Sullivan et al.*, 2008] of 8.8-11.4 and 6.3-10.6 mg/g, respectively. In general, fuels from SE emitted more LG per unit weight of fuel compared to the SW fuels. MCE alone is unable to account for the differences observed between these studies. Lab experiments suggest that presence of salts, specially salts containing K, Li, Ca significantly reduces LG pyrolysis yields [*Richards and Zheng*, 1991; *Eom et al.*, 2012]. Thus, higher K/PM ratios in this study suggest lower EFLG. As shown in, a sharp decrease in LG production is observed at K/PM ratio of  $\sim 0.03$ . Moreover, *Ward and Hardy* [1991] found that potassium emissions were high during high temperature flaming phase. Hence, potassium could not be identified a predictive factor for determining EFLG that varied two orders of magnitude.

The PM mass fractions of levoglucosan in this study were  $1.56 \pm 0.50$  (FHL),  $1.76 \pm 0.44$  (FHUA),  $5.73 \pm 0.83$  (CL), and varied largely between burns from 0.3 for 'cos' (lowest) to 9.5% for 'cuh' (highest). SE fuels had the highest levoglucosan PM mass fraction ranging from 3% ('cuh') to 9.5% ('2yr'), while SW fuels varied between 0.3% ('cos') and 3.2% ('cea'). No correlation between mass fraction of levoglucosan in PM and MCE was found

in contrast to previous findings of *Dhammapala et al.* [2007] for wheat and Kentucky blue grass (only based on three samples).

#### Emission Factor of Particle-Phase PAHs

The major emissions of particle-phase PAHs from southwestern fuels are benzo[k] fluoranthene, pyrene, benzo[a] fluoranthene, chrysene, benzo[a] pyrene, fluoranthene, phenanthrene, and fluorene, which contribute approximately 80% of total particle-phase PAHs for both chaparral and FHUA groups. Pyrene and benzo[k] fluoranthene alone made up 13-20% of PAH emissions. Chaparral and FHUA had a mean emission factor of 6550 and 1720  $\mu\text{g}/\text{kg}$ . The highest observed amount of total PAHs per kg fuel burned was 11300  $\mu\text{g}/\text{kg}$  from 'cos' and the lowest was 1300  $\mu\text{g}/\text{kg}$  from 'oas'. In general, Chaparral fuels emitted approximately 4 times higher amount of PAHs than FHUA fuels.

The mass fraction of PAH in the PM varied from 0.03%(chs) to 0.54%(cos) and averaged 0.20% and 0.26% mass of PM for chaparral and FHUA fuels, respectively. Despite having less PAH per kg fuel burned, FHUA resulted in higher fraction of PM in PAHs compared to the Chaparral group.

It has been suggested that the ratio of certain diagnostic ratios for PAHs are useful in determining combustion source [*Gonkalves et al.*, 2011; *Wang et al.*, 2009; *Alves et al.*, 2010]. The ratios of Fla/(Py+Fla) and Ph/(Ph+Ant) as suggested by *Wang et al.* [2009] and Ind/(Ind+Benzo[ghi]P) by *Gonkalves et al.* [2011] are shown in the bottom of for all the fuel types and the two fuel groups. The ratio Fla/(Py+Fla) was  $0.40\pm 0.04$  for Chaparral group and  $0.20\pm 0.10$  for FHUA group. The FHUA ratios are similar to those

reported from combustion of cereal straw (0.50-0.53) [Hays *et al.*, 2005], shrubs (0.54-0.60) [Wang *et al.*, 2009], and agricultural residue (0.46-0.63) [Goncalves *et al.*, 2011]. 'mes' and 'oas' did not fall within the range of suggested ratios for the ratio of Fla/(Py+Fla). The Ph/(Ph+Ant) ratio averaged  $0.72 \pm 0.17$  (except for 'mch') and was consistent with the range reported by above-mentioned studies. 'mes' and 'oas' from FHUA significantly has higher Ph/(Ph+Ant) ratios ( $\sim 0.9$ ) close to the values seen cooking emissions/engine exhaust [He *et al.*, 2004; Rogge *et al.*, 1993; Schauer *et al.*, 1999], which in addition to a differing fuel type, the disparity might be due to the high MCE values. Most of the studies used by [Wang *et al.*, 2009] are combustion processes involving mostly smoldering (based on small EC/TC ratios). Therefore, the range of suggested diagnostic ratios might not be robust due to the overlap of suggested ranges between different emission sources [Goncalves *et al.*, 2011] and also not covering the wider range of possible MCE values (e.g. higher MCEs were observed in the current study). Ind/(Ind+Benzo[ghi]P) was  $0.40 \pm 0.04$  for both fuel groups. Our data is close to lower end of evaluated values from the study of [Hays *et al.*, 2005] for cereal straw. Chinese cooking [He *et al.*, 2004] and automobile and trucks [Rogge *et al.*, 1993] have ratios of 0.19 and 0.04-0.09, respectively.

## Conclusions

We report detailed particle-phase emission measurements from combustion of different vegetation types typically managed with fire on military bases in the southwest US. Since these fuels burn periodically (prescribed or wildfire), the results of this study will help to better understand and manage air quality impacts in neighboring areas. Emission factors

for numerous species are provided as a function of MCE. At a certain FM, all observed MCEs were limited between two heading and backing fire MCEs. Due to lack of sufficient data, it was impossible to model the fire behavior; more effort is needed for characterizing the MCE.

On average, the SE fuels emitted more PM mass (10.8 g/kg fuel burned) compared to SW fuels (3.83 g/kg fuel burned) consistent with lower MCE for SE fuels. No regional trend was observed after accounting for MCE. Some of the observed differences between field and lab results for similar MCE may be attributable to the smoke temperature, fuel bed differences as discussed in more detail elsewhere [Yokelson *et al.*, 2012]) and also timescale of the MCE measurement (field is on order of hours, laboratory on order of a few minutes). Due to the non-linear emissions behavior with MCE, comparison of fire-integrated values from lab and field studies might result in unexpected and unexplainable differences.

The SE and SW fuels showed large regional dependency in their emission factors for particle inorganics. The PM mass fraction of chlorine and potassium in the SW fuels was on the high end of values reported in the literature. Any correlation between these emission rates with MCE was masked by large variations due to fuel composition. Chlorine alone accounted for 0.4-24.5% of the water-soluble mass fraction. Sulfate correlated weakly with MCE. Comparison of XRF and IC results indicates the vast majority (~88%) of sulfur and potassium are present as  $\text{SO}_4^{2-}$  and  $\text{K}^+$ , respectively. Inorganic species contributed 9-62% and 2-15% of PM mass for SW and SE fuels,

respectively. No correlation was observed between MCE and calcium, ammonium, bromide, and nitrate.

Levoglucosan/OC ratios were observed to be a function of the fuel type with little to no correlation with MCE. Finally, the emission factor of 15 PAHs totaled 1 - 11 mg/kg burned for SW. 80% of measured particle phase PAHs was attributed to benzo[k] fluoranthene, pyrene, benzo[a] fluoranthene, chrysene, benzo[a] pyrene, fluoranthene, phenanthrene, fluorene. Pyrene and benzo[k] flouranthene constituted 13-20% of particle-phase PAHs emissions. Previously published PAH diagnostic ratios were not observed to be good markers for our biomass burning samples.



Levoglucosan (LG) emission factors (mg/kg fuel burned), and also fraction of LG in the PM, Organic Carbon (OC) and Organic Mass (OM) (wt%)

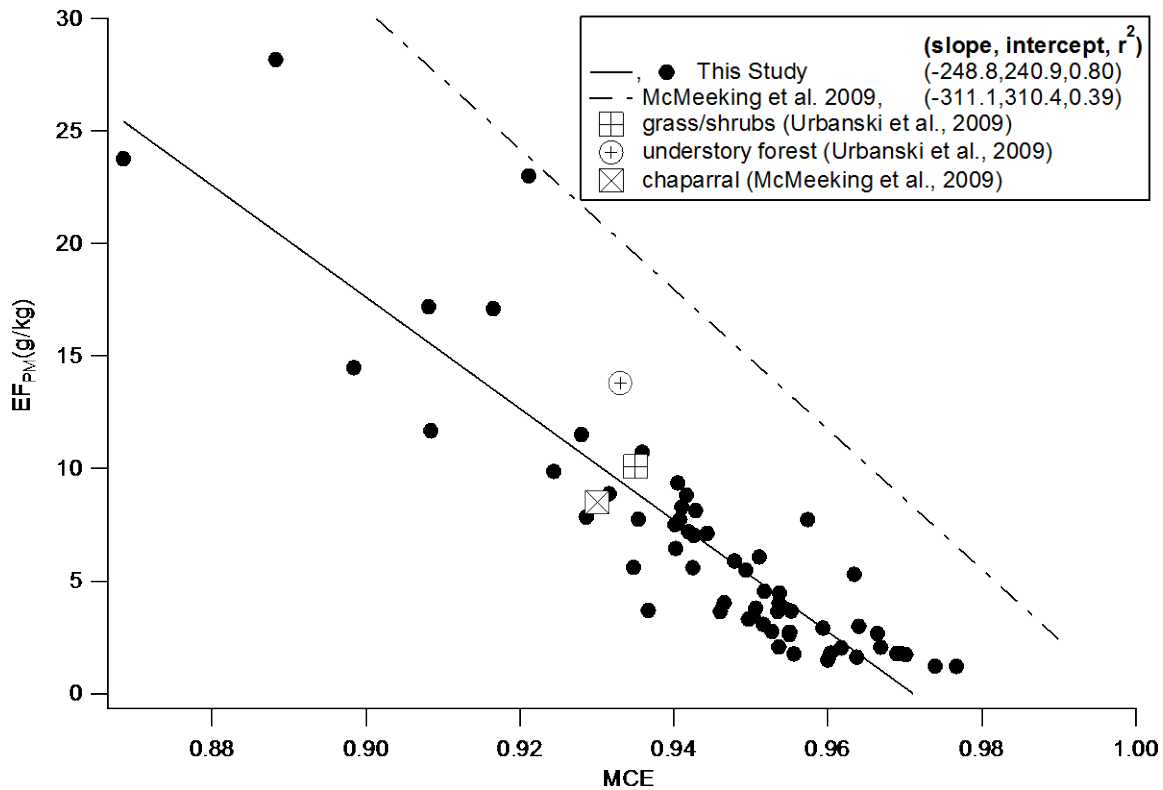
<b>Fuel type</b>	<b>EF<sub>LG</sub></b>	<b>LG/PM</b>	<b>LG/OM</b>	<b>LG/OC</b>	<b>EC/TC</b>
<b>Southwest</b>					
cea	187.4±172.2	3.19±2.42	6.24±3.14	4.1±2.1	36±23
chs	234.0±117.7	3.03±1.24	6.44±3.05	4.2±2.0	38±8
cas	25.2±9.3	0.37±0.17	1.46±0.13	1.0±0.1	58±7
cos	19.7±6.4	0.31±0.08	1.53±0.47	1.0±0.3	63±9
man	30.2±10.3	0.79±0.21	3.71±1.13	2.4±0.7	47±9
mch	79.2±42.7	1.64±1.18	6.05±2.86	4.0±1.9	44±18
<b>Chaparral ave.</b>	95.9±35.6	1.56±0.50	4.24±0.90	2.8±0.6	48±6
mes	28.9±10.9	0.75±0.08	2.07±0.37	1.4±0.2	44±1
oas	29.1±13.6	1.80±0.67	4.31±0.91	2.8±0.6	52±8
oaw	58.6±35.1	2.74±1.12	6.53±4.12	4.3±2.7	42±15
<b>FHUA ave.</b>	38.9±13.1	1.76±0.44	4.30±1.41	2.8±0.9	46±6
<b>Southeast</b>					
lit	1089.8±507.2	5.76±1.65	5.76±1.65	3.8±1.1	10±6
1yr	888.0±521.7	6.92±0.33	6.92±0.33	4.5±0.2	8±4
2yr	1272.5±545.9	9.52±1.04	9.52±1.04	6.2±0.7	6±4
poc	208.3±142.2	4.03±1.11	4.03±1.11	2.6±0.7	17±8
cuh	50.2±6.8	3.02	3.02	2.0±0.0	37
uh	337.0±135.7	5.14±3.46	5.14±3.46	3.4±2.3	32±9
<b>Camp Lejeune ave.</b>	641.0±155.1	5.73±0.83	5.73±0.83	3.7±0.5	18±3

PAH presents emission factors in  $\mu\text{g}$  per kg fuel burned and diagnostic ratios for particle phase PAHs

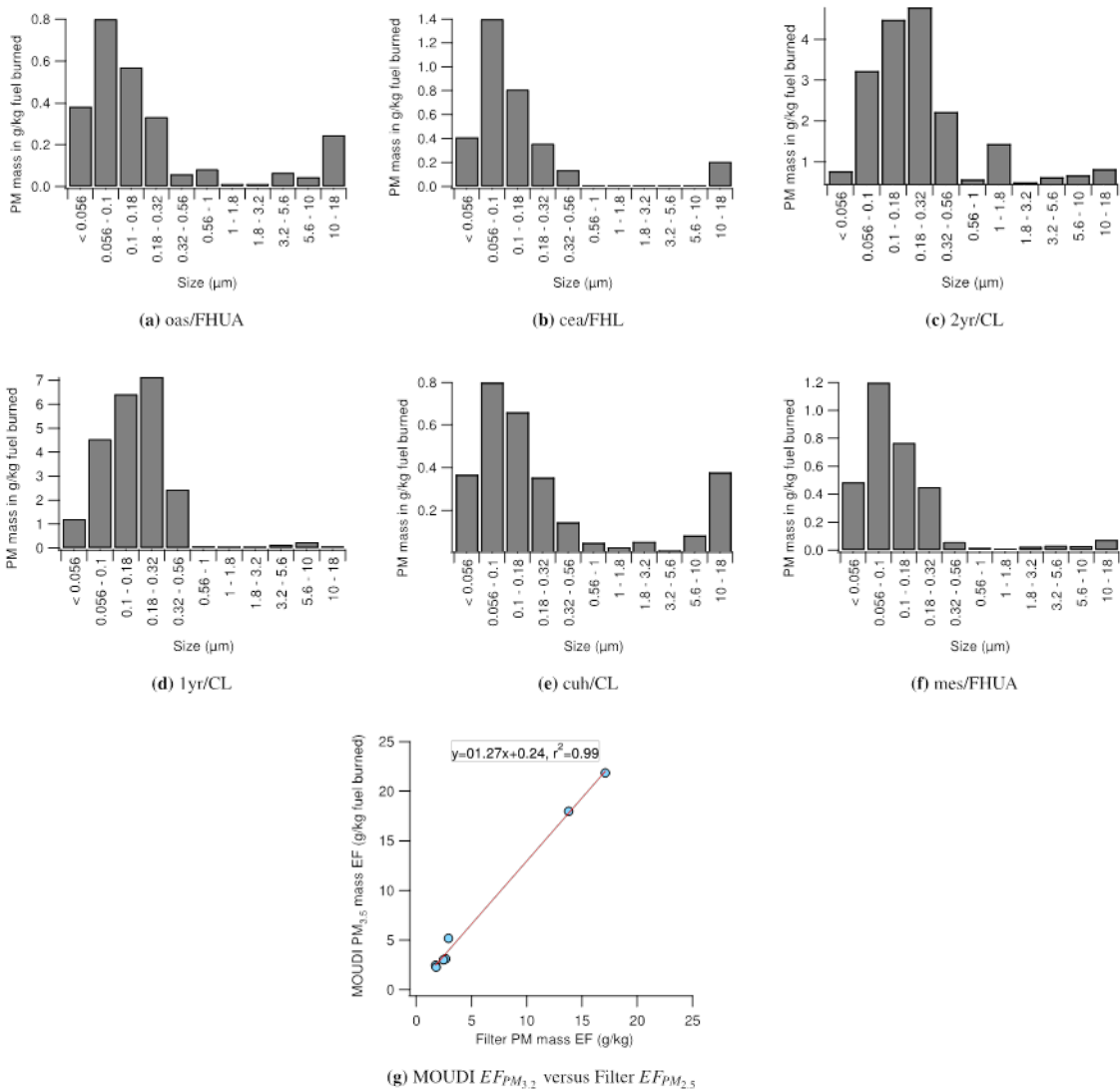
Fuel type	cea	chs	cas	cos	man	mch	Chaparal Ave.	mes	oas	oaw	FHUA Ave.
Acy {2} <sup>ab</sup>	297.2 ± 338.6	144.3 ± 137.5	77.8 ± 42.1	270.8 ± 149.9	19.2 ± 12.6	27.9	139.5 ± 66.2	35.5 ± 26.6	36.1 ± 49.0	82.2 ± 84.3	51.2 ± 33.7
Ace {2}	144.0 ± 97.7	126.8 ± 146.3	26.6 ± 26.9	7.4 ± 4.2	11.0 ± 13.9	3.7	53.2 ± 29.8	25.2±1 7.7	29.6±3 9.4	37.9±4 5.2	30.9±2 0.8
Fle {2}	329.7±3 50.1	391.4±4 76.0	84.2±81 .9	20.8±5.2	43.9 ±53.0	97.4	161.2±9 9.8	68.4±7 7.8	145.5± 134.5	128.6± 156.8	114.2± 73.6
Ph {3}	1434.5± 1270.8	1055.1± 1045.7	301.1±2 01.6	234.4±53 .5	244. 6±17 1.8	133. 6	567.2±2 78.0	116.3± 89.9	214.6± 160.9	113.5± 193.1	148.2± 89.0
An {3}	197.5±2 83.1	78.0±74 .5	148.1±1 66.6	94.5±59. 3	156. 7±23 0.4	136. 7	135.2±6 8.7	11.1±9. 0	8.7±5.1	79.3±1 28.9	33.0±4 3.1
Fla {3}	492.2 ± 171.7	558.3 ± 549.5	1041.9 ± 343.5	1156.1 ± 17.1	176. 7 ± 124. 8	257. 8	613.8 ± 113.7	103.6 ± 96.6	88.5 ± 36.2	181.8 ± 309.3	124.6 ± 108.7
Py {4}	664.2 ± 426.6	738.0 ± 976.6	1480.4 ± 170.2	1433.2 ± 121.3	345. 8 ± 162. 3	447	851.4 ± 183.0	418.1 ± 420.1	256.3 ± 149.7	273.3 ± 243.0	315.9 ± 169.3
B[a]A {4}	778.9 ± 430.0	338.2 ± 302.4	1524.2 ± 707.5	1550.7 ± 74.4	223. 8 ± 119. 8	432. 5	808.1 ± 148.8	280.1 ± 283.4	134.0 ± 71.6	172.7 ± 161.5	195.6 ± 111.3
Chr {4}	269.6 ± 273.5	225.9 ± 202.9	1478.4 ± 686.8	1425.2 ± 225.6	238. 4 ± 167. 8	432. 5	678.3 ± 136.1	258.1 ± 213.4	133.8 ± 70.2	171.6 ± 159.7	187.8 ± 91.9
B[b]F {4}	216.3 ± 213.1	164.5 ± 182.2	591.8 ± 341.9	823.7 ± 213.2	145. 4 ± 108. 1	151. 9	348.9 ± 83.8	107.8 ± 98.6	37.0 ± 13.8	105.1 ± 116.0	83.3 ± 51.0
B[k]F {4}	1164.6 ± 809.6	256.8 ± 241.8	3232.0 ± 3144.1	2156.5 ± 135.6	537. 6 ± 563. 0	612. 4	1326.7 ± 551.1	228.4 ± 182.6	145.9 ± 43.1	266.6 ± 461.8	213.6 ± 166.2
B[a]P {5}	130.2 ± 80.4	59.9 ± 52.9	713.2 ± 937.3	433.0 ± 37.8	28.2 ± 10.0	75.2	240.0 ± 157.2	29.6 ± 25.8	22.7 ± 1.9	405.7 ± 682.1	152.7 ± 227.5
Ind {5}	104.4 ± 163.9	118.3 ± 123.7	342.5 ± 110.2	582.1 ± 167.1	42.4 ± 28.2	102. 3	215.3 ± 48.0	37.3 ± 27.5	23.2 ± 5.3	8.2 ± 12.0	22.9 ± 10.2

Fuel type	cea	chs	cas	cos	man	mch	Chaparal Ave.	mes	oas	oaw	FHUA Ave.
D[ah]A {5}	59.0 ± 68.8	12.1 ± 10.5	113.7 ± 59.4	149.9 ± 44.8	13.4 ± 7.5	26.5	62.5 ± 17.0	13.5 ± 9.1	10.7 ± 3.5	8.7 ± 7.8	11.0 ± 4.1
B[ghi]P {4}	199.6 ± 276.0	136.8 ± 119.1	534.2 ± 172.2	993.2 ± 268.1	47.5 ± 31.7	164.6	346.0 ± 73.2	53.9 ± 39.3	34.1 ± 10.7	12.5 ± 20.6	33.5 ± 15.2
<b>Sum</b>	6481.9	4404.4	11690.1	11331.5	2274.6	3102	6547.3	1786.9	1320.7	2047.7	1718.4
<b>Diagnostic ratios</b>											
Fla/(Py+Fla)	0.43	0.43	0.41	0.45	0.34	0.37	0.40	0.2	0.26	0.40	0.28
Ph/(Ph+Ant)	0.88	0.93	0.67	0.71	0.61	0.49	0.72	0.91	0.96	0.59	0.82
Ind/(Ind+Benzo[ghi]P)	0.34	0.46	0.39	0.37	0.47	0.38	0.40	0.41	0.40	0.40	0.40

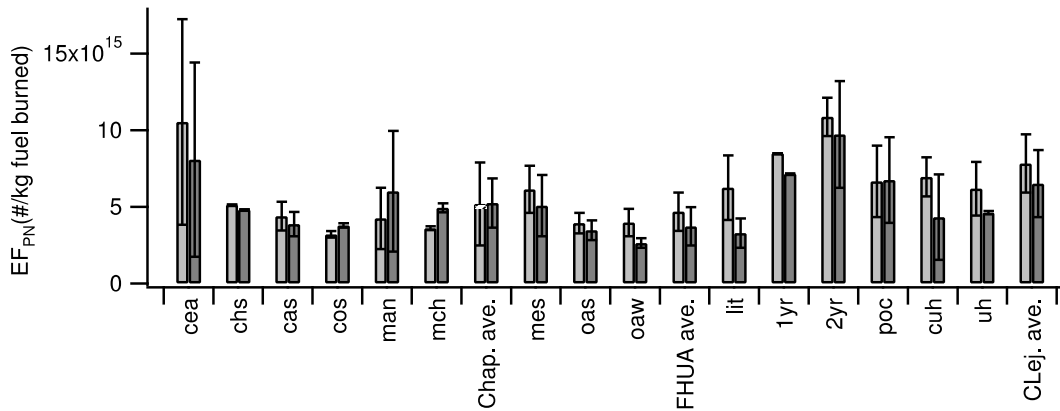
<sup>a</sup> Abbreviations: Acy(acenaphthylene), Ace(acenaphthene), Fle(flourene), Ph (phenanthrene), An (anthracene), Fla (fluoranthene), Py (pyrene), B[a]A (benz[a]anthracene), Chr (chrysene), B[b]F (benzo[b]fluoranthene), B[k]F (benzo[k]fluoranthene), B[a]P (benzo[a]pyrene), B[ghi]P (benzo[ghi]perylene), Ind (indeno[1,2,3-cd]pyrene), D[ah]A (dibenz[ah]anthracene) <sup>b</sup> No. of fused aromatic ring



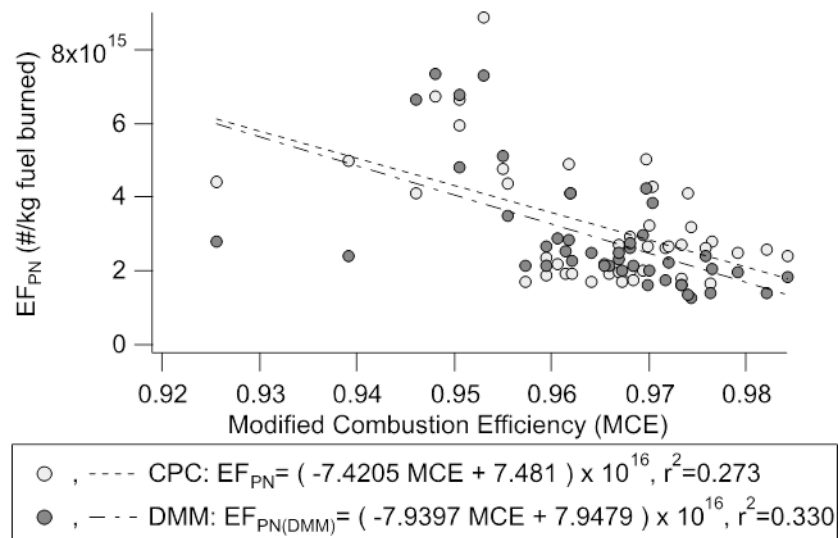
Particulate Matter (PM<sub>2.5</sub>) as a function of Modified Combustion Efficiency (MCE). Black solid circles are EF for PM<sub>2.5</sub> measured for this study. Solid and dashed lines represent the linear regression of PM<sub>2.5</sub> onto MCE for this and other studies, respectively indicated on the plot for laboratory, ground-based and airborne field measurements.



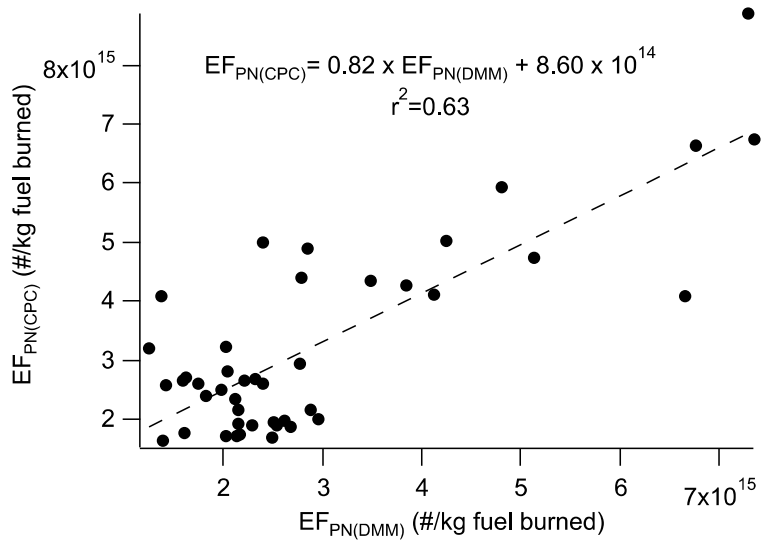
Size-resolved mass emission factors obtained through the MOUDI/filter setup (a)-(f); in sub-figure (g) the mass emission factors of PM<sub>3.5</sub> from the six sampled MOUDIs are graphed versus their corresponding mass emission factors acquired from the filter measurements



Particle number emission factors measured by CPC and DMM as function of fuel type



Particle number emission factors –EF<sub>PN</sub> (#/kg fuel burned) vs. Modified Combustion Efficiency (MCE) for all southwestern and southeastern fuel types acquired by two different working principal instruments, butanol-based CPC (solid dark gray circles) and particle-charge based DMM (solid light gray circles) are shown here. The best linear fit also is depicted using the dashed lines.



This graph illustrates the difference between measured particle number emission factors of butanol-based CPC and DMM; the slope is 0.82 and as shown DMM gives ~20% higher EFPN

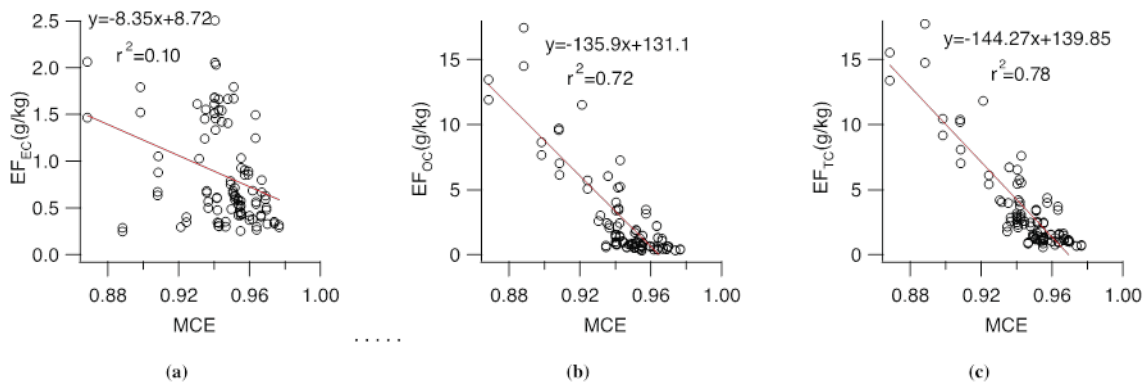
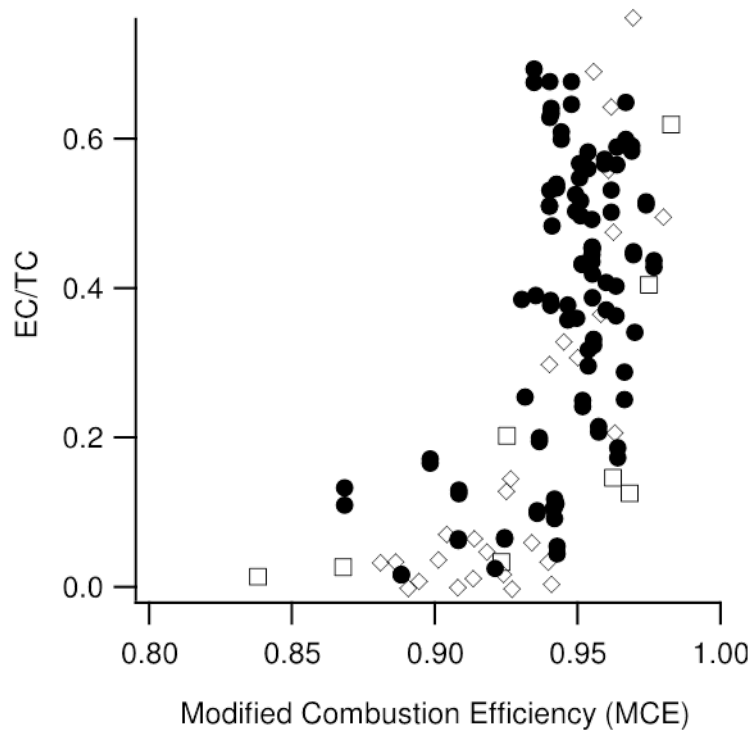
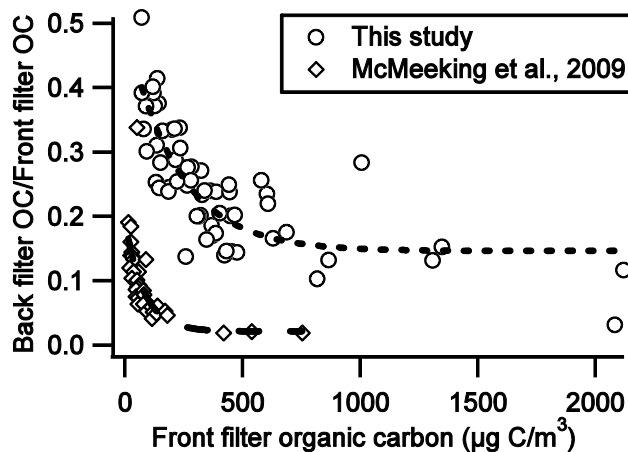


Figure Fire-integrate PM2.5 emission factors plotted versus MCE for (a) elemental carbon(EC) (b) organic carbon(OC) (c) total carbon(TC)



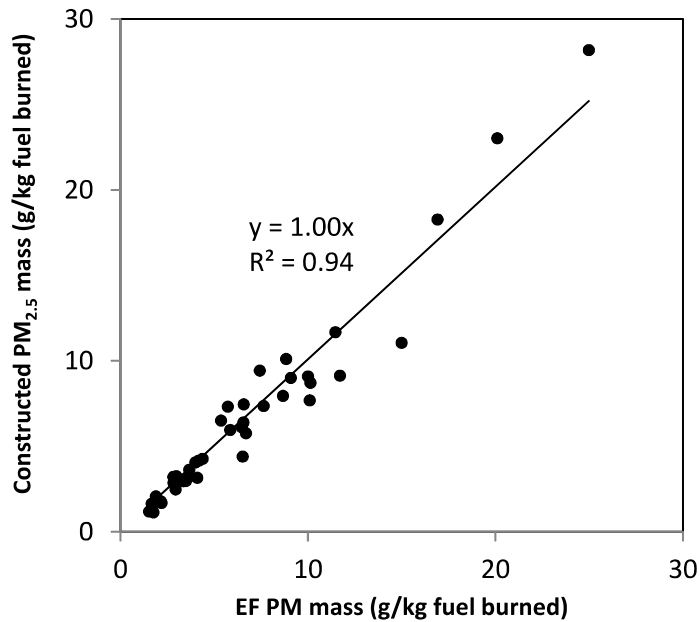
Particle elemental carbon to total carbon ratio (EC/TC) plotted versus modified combustion efficiency (MCE). Solid circles represent EC/TC measured in this study. Also shown are: open diamond, McMeeking et al. 2009, and open box, Christian et al. 2003



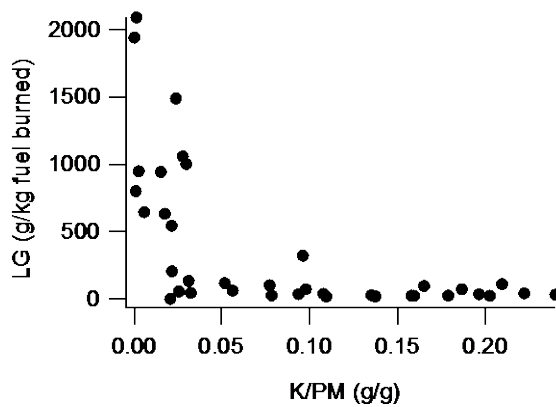
Mass fraction of semi-volatile organic compounds (SVOCs) in total collected Organic Carbon (OC); Open circles are data from this study (best exponential fit:







Reconstructed PM<sub>2.5</sub> mass emission factor (g/kg fuel burned) versus gravimetric PM<sub>2.5</sub> mass emission factor. Solid line represents the regression line with slope of 1 and correlation coefficient of 0.94.



Levoglucosan emission factor (g/kg fuel burned) plotted versus potassium to PM mass ratio (g/g) for the SW and SE fuels

## **B. APPENDIX**

The **Not-To-Exceed (NTE)** standard promulgated by the United States Environmental Protection Agency (EPA) ensures that heavy-duty engine emissions are controlled over the full range of speed and load combinations commonly experienced in use. NTE establishes an area (the “NTE zone”) under the torque curve of an engine where emissions must not exceed a specified value for any of the regulated pollutants. The NTE test procedure does not involve a specific driving cycle of any specific length (mileage or time). Rather it involves driving of any type that could occur within the bounds of the NTE control area, including operation under steady-state or transient conditions and under varying ambient conditions. Emissions are averaged over a minimum time of thirty seconds and then compared to the applicable NTE emission limits.

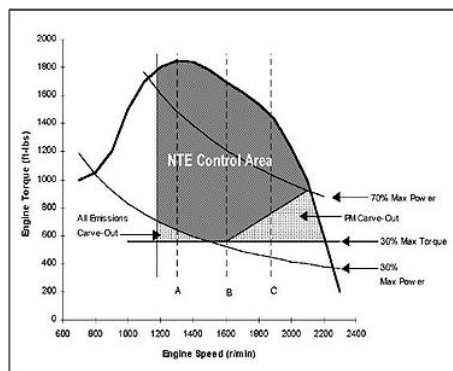
Current requirements to achieve engine operation in the "NTE Zone"

When all of the following conditions are simultaneously met for at least 30 seconds, and engine is considered to be operating in the NTE zone.

1. Engine speed must be greater than 15% above idle speed
2. Engine torque must be greater than or equal to 30% of maximum torque.
3. Engine power must be greater than or equal to 30% of maximum power.
4. Vehicle altitude must be less than or equal to 5,500 feet (1,700 m).
5. Ambient temperature must be less than or equal to 100 °F (38 °C) at sea level to 86°F at 5,500 feet (1,700 m).

6. Brake specific fuel consumption (BSFC) must be less than or equal to 105% of the minimum BSFC if an engine is not coupled to a multi-speed manual or automatic transmission.
7. Engine operation must be outside of any manufacturer petitioned exclusion zone.
8. Engine operation must be outside of any NTE region in which a manufacturer states that less than 5% of in-use time will be spent.
9. For Exhaust gas recirculation (EGR) equipped engines, the intake manifold temperature must be greater than or equal to 86-100 degrees Fahrenheit, depending upon intake manifold pressure.
10. For EGR-equipped engines, the engine coolant temperature must be greater than or equal to 125-140 degrees Fahrenheit, depending on intake manifold pressure.
11. Engine after treatment systems' temperature must be greater than or equal to 250 degrees Celsius.

#### Visual representations of NTE Zone



Example NTE Control Area for Heavy-Duty Diesel Engine With 100% Operational Engine Speed Less Than 2400 rpm

The NTE test, as defined in CFR 86.1370-2007, establishes an area (NTE control area) under the torque curve of an engine where emissions must not exceed a specified emission cap for a given pollutant. The NTE cap is set at 1.25 times the FTP emission limit as described in the subsection above. For 2005 model year heavy-duty engines, the NTE emission cap for NMHC plus NO<sub>x</sub> is 1.25 times 2.5 grams per brake horsepower-hour, or 3.125 grams per brake horsepower-hour. The basic NTE control area for diesel engines has three basic boundaries on the engine's torque and speed map. The first is the upper boundary that is represented by an engine's maximum torque at a given speed. The second boundary is 30 percent of maximum torque. Only operation above this boundary is included in the NTE control area. The third boundary is determined based on the lowest engine speed at 50 percent of maximum power and highest engine speed at 70 percent of maximum power. This engine speed is considered the "15 percent operational engine speed". The fourth boundary is 30% of maximum power

#### Controversy and deficiency regarding NTE standards

A controversial issue is the applicability of the NTE limits to the real-world driving. In order for NTE standards to apply, the engine needs to remain within the NTE zone (limits include operation at a minimum of 30% of rated power) for at least 30 seconds. Concerns arose that performing this action could prove to be difficult, as each time the driver removes the foot from the accelerator pedal, or shifts gears on vehicles with manual transmission, the engine leaves the NTE zone.

In urban or suburban driving, this happens relatively often, to the point that NTE standards are applicable only a very small portion of the operation or, in some cases, not at all. The probability of the engine remaining within the NTE zone for over 30 seconds also decreases with the advent of high-power engines. For example, if the power required to maintain a motorcoach or an over-the-road truck at highway cruising speed is somewhere around 150 hp (110 kW), the probability that a 475 hp (354 kW) engine will consistently operate at loads above 30%, without “dips” to lower power levels, can be relatively small.

These concerns were confirmed by studies carried out by West Virginia University (WVU) under the Consent Decrees. WVU found that “remaining for 30 seconds within the NTE zone can be quite difficult. The resulting low NTE availability poses a problem as many measurements within the NTE area have to be rejected along with those from outside the NTE area. The question arises if in this way all real-life emissions are sufficiently ‘well reflected’ in the NTE test results”

## C. APPENDIX

### Central Business District (CBD)

The Central Business District (CBD) Cycle is a chassis dynamometer testing procedure for heavy-duty vehicles (*SAE J1376*). The CBD cycle represents a “sawtooth” driving pattern, which includes 14 repetitions of a basic cycle composed of idle, acceleration, cruise, and deceleration modes. The following are characteristic parameters of the cycle:

- Duration: 560 s
- Average speed: 20.23 km/h
- Maximum speed: 32.18 km/h (20 mph)
- Driving distance: 3.22 km
- Average acceleration:  $0.89 \text{ m/s}^2$
- Maximum acceleration:  $1.79 \text{ m/s}^2$

Vehicle speed over the duration of the CBD cycle is shown in Figure A-1.

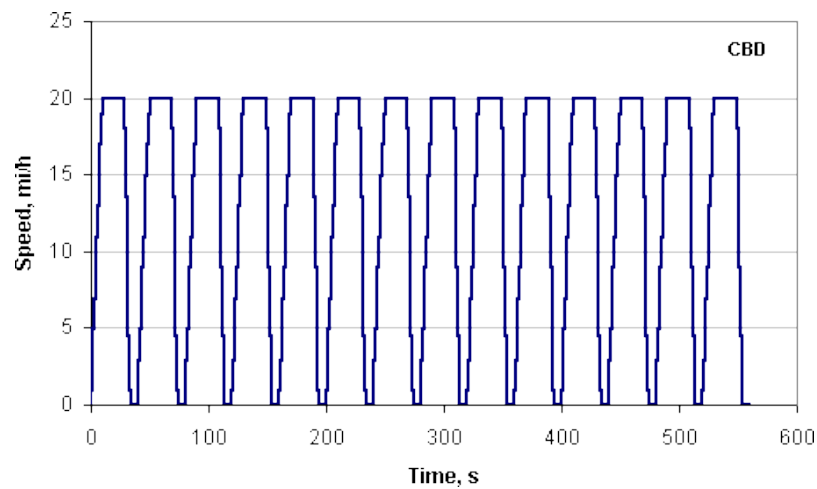


**Figure A-1.** CBD Driving Cycle

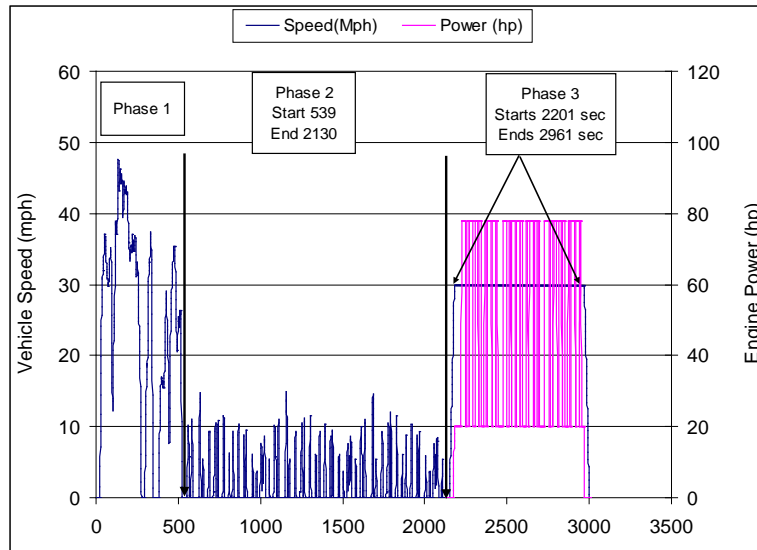
## AQMD refuse truck cycle

The waste haulers cycle will be tested using the AQMD refuse truck cycle (AQMD-RTC). This cycle was developed by West Virginia University to simulate waste hauler operation and is a modification of the William H. Martin Refuse Truck Cycle. The original William H. Martin (WHM) refuse truck cycle was created from data logged from sanitation trucks operating in Pennsylvania. The modified cycle consists of a transport segment (phase 1), a curbside pickup segment (phase 2), and a compaction segment (phase 3), see Figure A-2. The modified cycle will be used for this study since this represents the operation of refuse haulers in the SC AQMD district.

The transient phase starts runs for 538 seconds, the curbside phase runs from 1591 seconds where it starts at 539 and ends at 2130 seconds. The final phase is a compaction cycle that runs from 2201 to 2961 and is 760 seconds long.

The compaction load is simulated by applying a predetermined torque to the drive axel while maintaining a fixed speed of 30 mph. Previous studies by WVU have used an engine load varying between 20 hp to 80 hp for the compaction load, as shown in the right hand side of Figure A-2. To perform the compaction cycle the vehicle is accelerated up to 30 mph where no emissions are collected. Once steady state load conditions are achieved the emissions collection starts and then the varying load is applied. The emissions collection stops before the vehicle is decelerated back to zero speed.





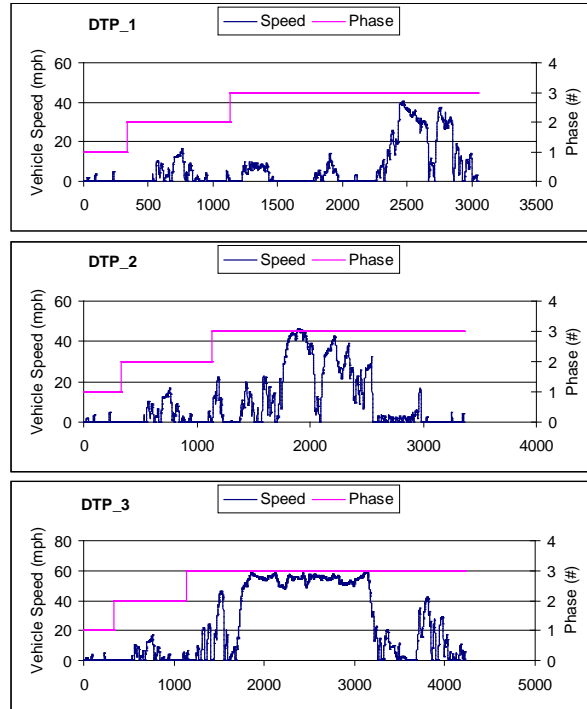
### AQMD Refuse Truck Cycle (AQMD-RTC)

#### Drayage Truck Port (DTP) cycle

The port cycle was developed by TIAX, the Port of Long Beach and the Port of Los Angeles. Over 1,000 Class 8 drayage trucks at these ports were data logged for trips over a four-week period in 2010. Five modes were identified on the basis of several driving behaviors average speed, maximum speed, energy per mile, distance, and number of stops. These behaviors are associated with different driving conditions such as queuing or on-dock movement, near-dock, local or regional movement, and highway movements. The data were compiled and analyzed to generate a best fit trip. The best-fit trip data was then additionally filtered (eliminating accelerations over 6 mph/s) to allow operation on a chassis dynamometer. The final driving schedule is called the drayage port tuck (DPT) cycle and is represented by 3 modes where each mode has three phases to best represent near dock, local, and regional driving as shown in Table A-5 and Figure A-3. Figure A-4

shows the preconditioning cycles that will be performed for the first test of the day. This will be accomplished after warming up the vehicle and chassis dynamometer.

### Drayage Truck Port cycle by mode and phases



Drayage truck port cycle near dock (DTP\_1), local (DTP\_2), and regional (DTP\_3)

Drayage Truck Port cycles	Phase 1	Phase 2	Phase 3
Near-dock (2 to 6 miles)	Creep	Low Speed Transient	Short High Speed Transient
Local (6 to 20 miles)	Creep	Low Speed Transient	Long High Speed Transient
Regional (20+ miles)	Creep	Low Speed Transient	High Speed Cruise

## D. APPENDIX

Non-regulated emissions of Port vehicles, on Port Cycles

THC, CH<sub>4</sub>, NMHC, and CO emissions for the Near Dock port cycle

Category	Vehicle		Emission Factor (g/mi)			
	Engine	MY	THC	CH <sub>4</sub>	NMHC	CO
VIII	C8.3p	2010	0.04	0.03	0.02	-0.41
VIII	C11.9	2011	0.06	0.09	-0.02	-0.50
VIII	V12.8	2011	0.34	0.06	0.29	0.65
VII	N12.4b	2011	0.36	0.10	0.28	3.21
VII	N12.4c	2011	0.24	0.07	0.18	2.06
VI	GM8.1p	2009	33.79	1.61	32.73	157.34
IV	N12.4a	2009	0.10	0.07	0.04	-0.15
IV	D14a	2008	0.08	0.09	0.00	2.83
IV	D14b	2008	0.19	0.07	0.13	0.16

THC, CH<sub>4</sub>, NMHC, and CO emissions for the Local port cycle (g/mile)

Category	Vehicle		Emission Factor (g/mi)			
	Engine	MY	THC	CH <sub>4</sub>	NMHC	CO
VIII	C8.3p	2010	0.03	0.04	0.00	-0.03
VIII	C11.9	2011	0.45	0.17	0.30	5.13
VIII	V12.8	2011	0.19	0.04	0.15	1.07
VII	N12.4b	2011	27.88	1.50	26.86	117.82
VII	N12.4c	2011	0.06	0.04	0.03	-0.31
VI	GM8.1p	2009	-0.02	0.07	-0.08	0.45
IV	N12.4a	2009	0.07	0.05	0.03	0.10
IV	D14a	2008	0.00	0.00	0.00	0.00
IV	D14b	2008	-0.01	0.01	-0.02	-0.26

THC, CH<sub>4</sub>, NMHC, and CO emissions for the Regional port cycle

Category	Vehicle		Emission Factor (g/mi)			
	Engine	MY	THC	CH4	NMHC	CO
VIII	C8.3p	2010	-0.01	0.01	-0.02	-0.26
VIII	C11.9	2011	0.01	0.02	-0.01	-0.18
VIII	V12.8	2011	0.00	0.02	-0.02	-0.15
VII	N12.4b	2011	0.09	0.06	0.04	1.76
VII	N12.4c	2011	0.05	0.02	0.04	0.19
VI	GM8.1p	2009	11.91	1.02	11.14	60.08
IV	N12.4a	2009	0.02	0.02	0.00	-0.16
IV	D14a	2008	0.02	0.03	0.00	0.23
IV	D14b	2008	0.01	0.02	-0.01	-0.07

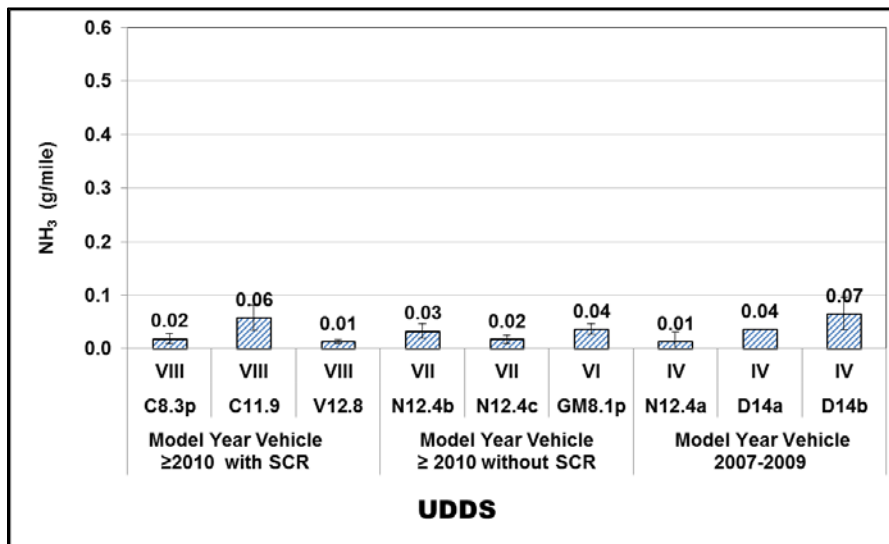


**Figure NH<sub>3</sub> Emission Factors for UDDS cycle (g/mile)<sup>1</sup>**

<sup>1</sup> NH<sub>3</sub> scale is based on 10 ppm raw exhaust concentration

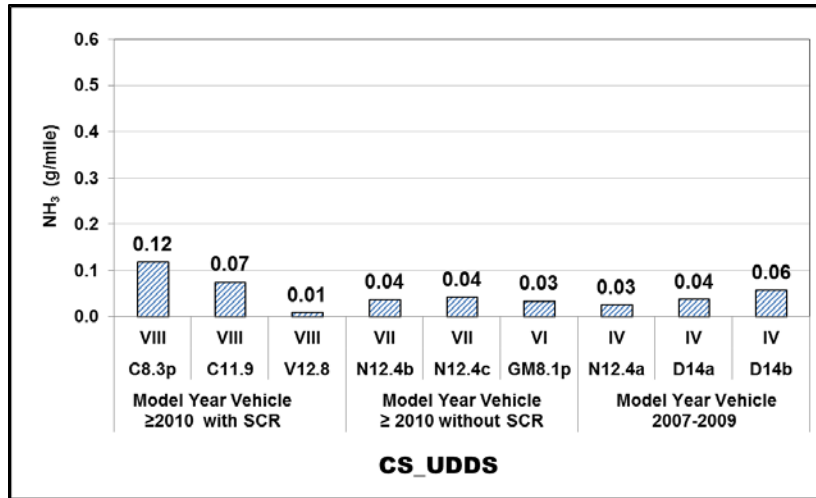
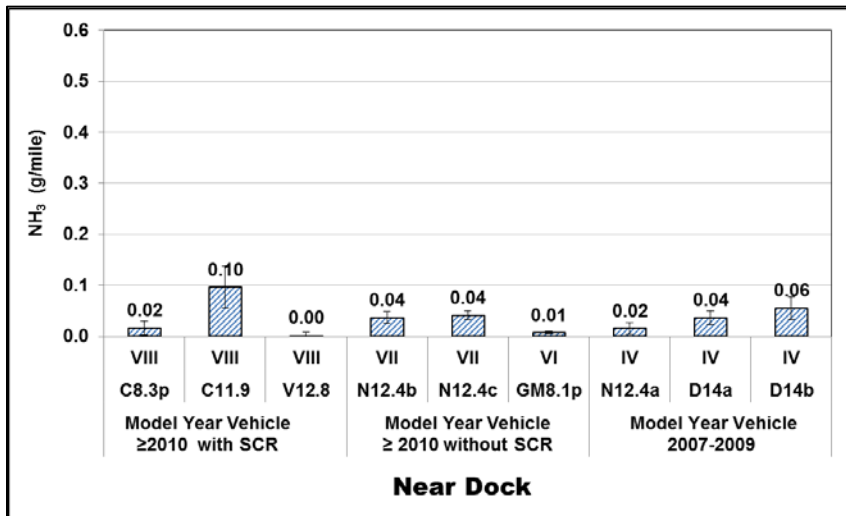


**Figure NH<sub>3</sub> Emission Factors for Cold Start UDDS cycle (g/mile)<sup>1</sup>**

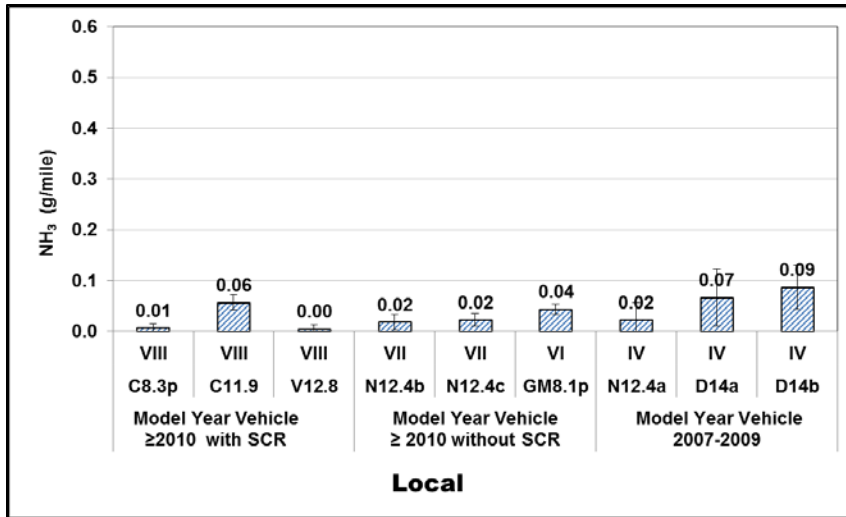
<sup>1</sup> NH<sub>3</sub> scale is based on 10 ppm raw exhaust concentration, thus 10 ppm NH<sub>3</sub> in the raw exhaust will be approximately 0.6 g/mi (full scale) for perspective.

<sup>2</sup> No error bars for the cold start tests because on only one test was performed



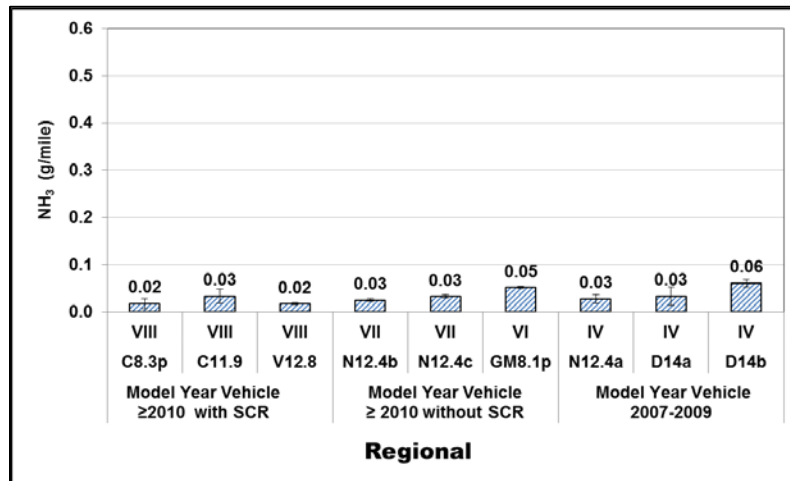
**NH<sub>3</sub> Emission factors for Near Dock Cycle (g/mile)**

<sup>1</sup> NH<sub>3</sub> scale is based on 10 ppm raw exhaust concentration



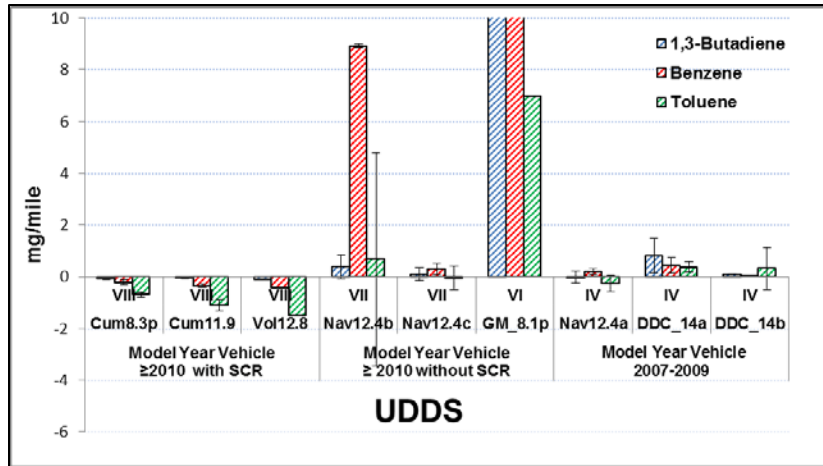
**NH<sub>3</sub> Emission factors for Local Cycle (g/mile)**

<sup>1</sup> NH<sub>3</sub> scale is based on 10 ppm raw exhaust concentration

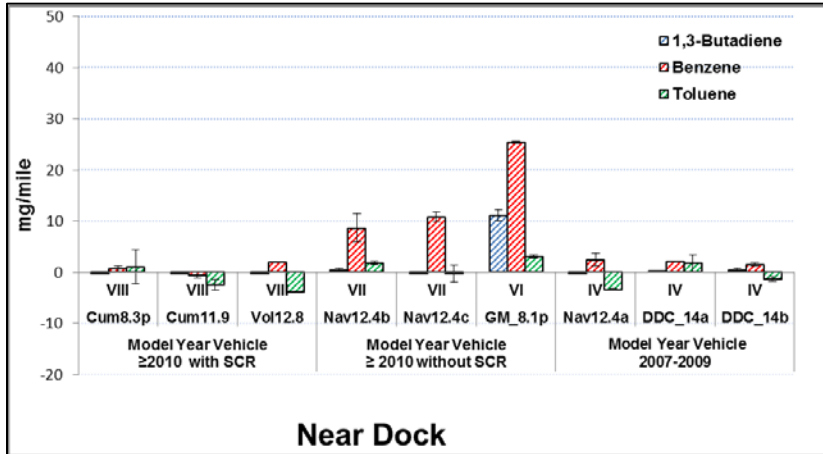


**NH<sub>3</sub> Emission factors for Regional Cycle (g/mile)<sup>1</sup>**

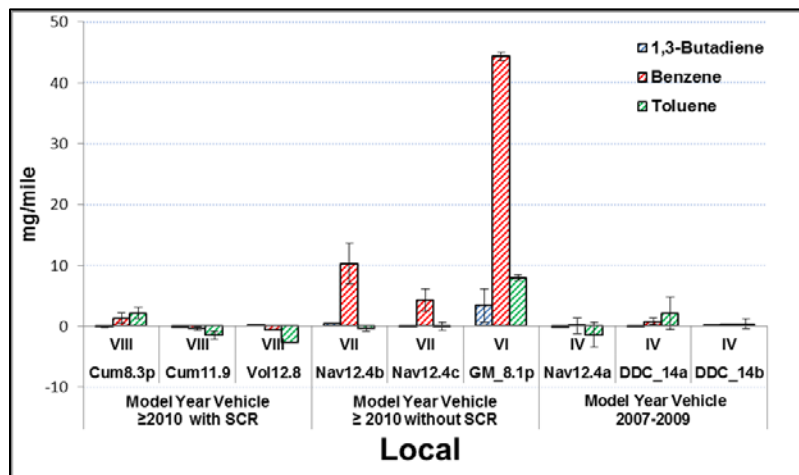
<sup>1</sup> NH<sub>3</sub> scale is based on 10 ppm raw exhaust concentration



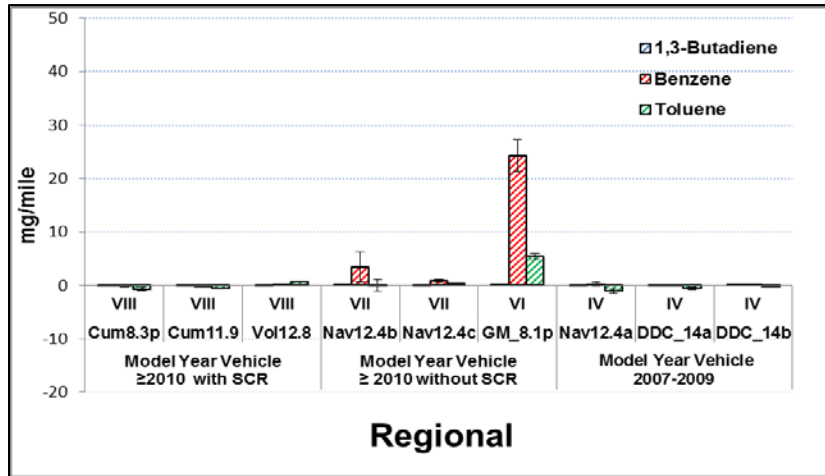
Emissions in mg/mile for Butadiene & BTEX for the UDDS Cycle



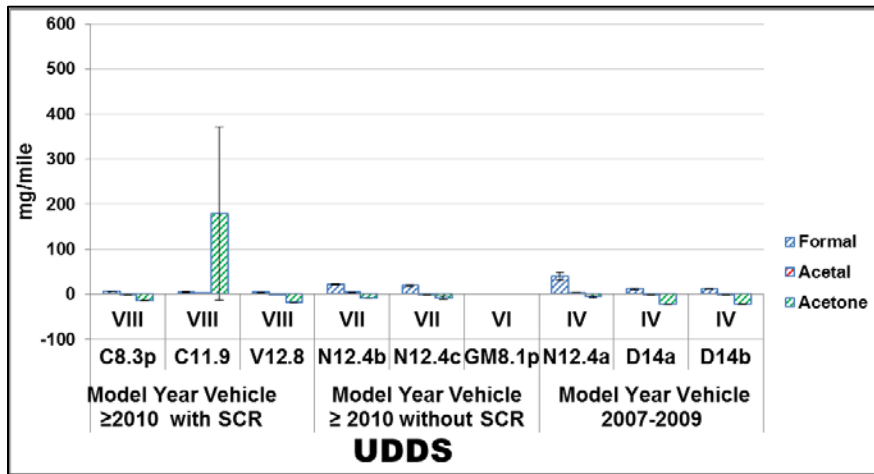
Emissions in mg/mile for Butadiene & BTEX for the Near Port Cycle



Emissions in mg/mile for Butadiene & BTEX for the Local Port Cycle

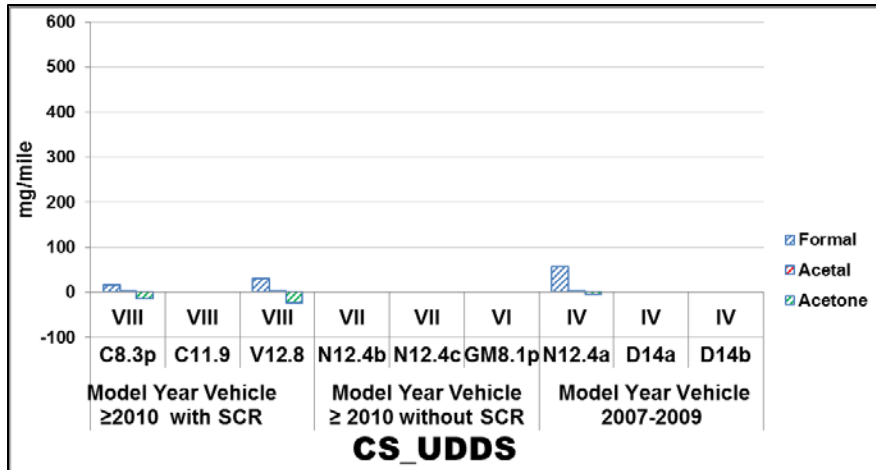


Emissions in mg/mile for Butadiene & BTEX for the Regional Port Cycle



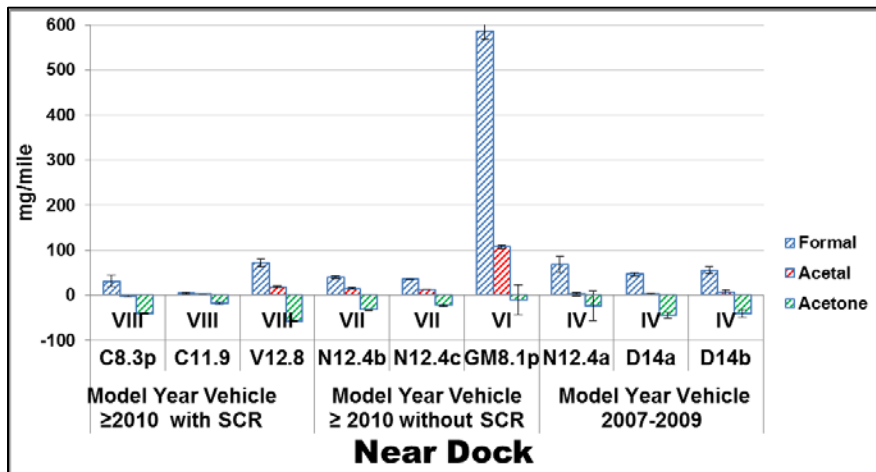
Emissions in mg/mile for Carbonyls & Ketones for the UDDS Cycle



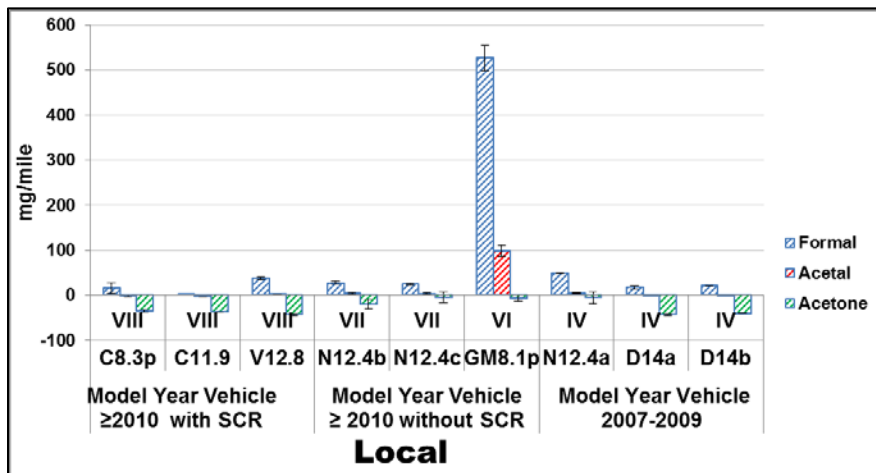


Emissions in mg/mile for Carbonyls & Ketones for cold- UDDS Cycle

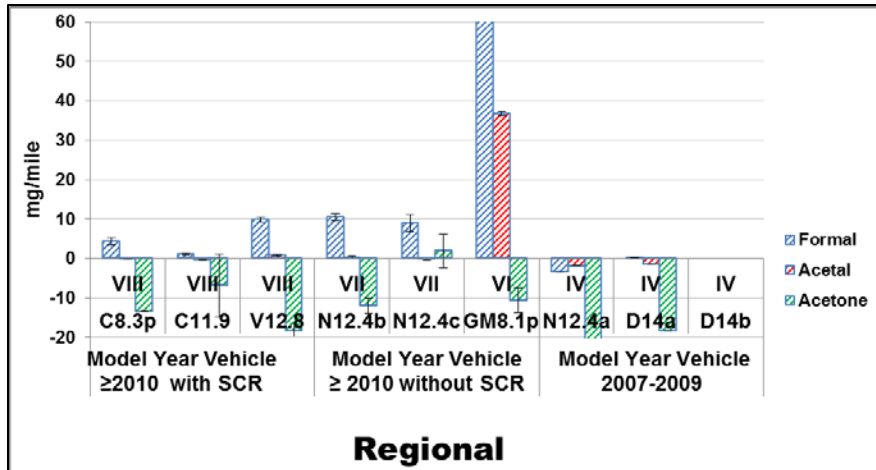
<sup>1</sup> No error bars for the cold start tests because on only one test was performed



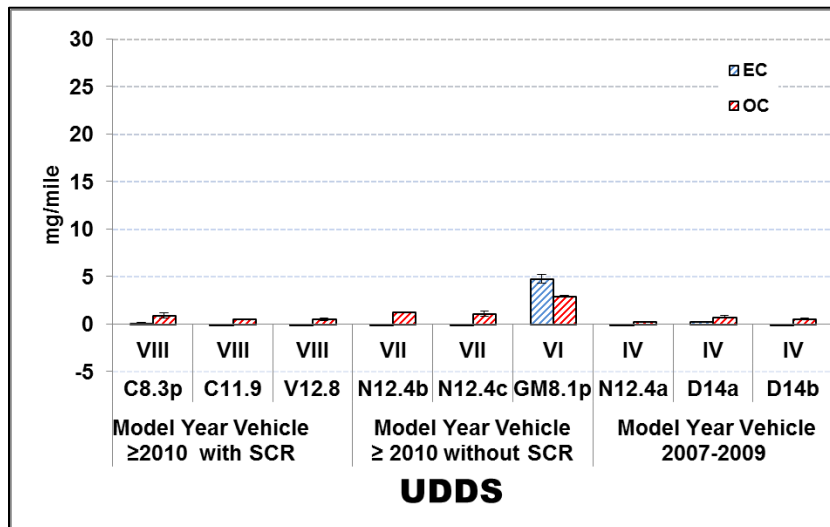
Emissions in mg/mile for Carbonyls & Ketones for the Near Port Cycle



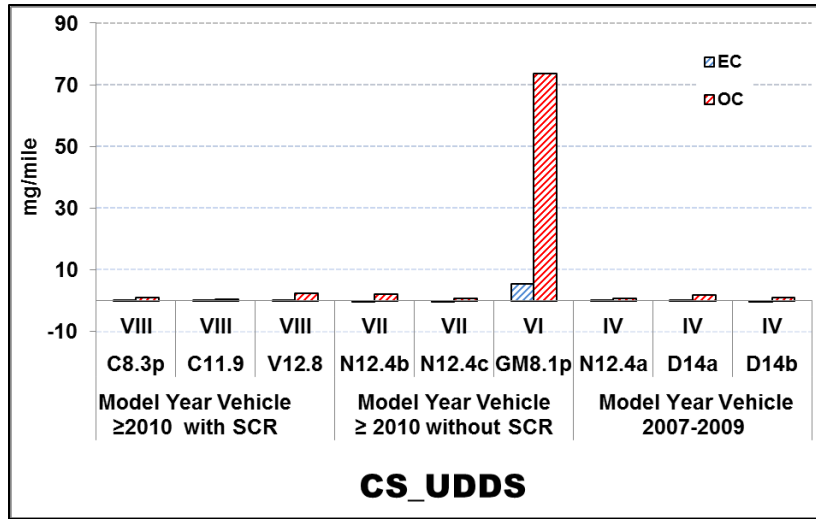
Emissions in mg/mile for Carbonyls & Ketones for the Local Port Cycle



Emissions in mg/mile for Carbonyls & Ketones for the Regional Port Cycle

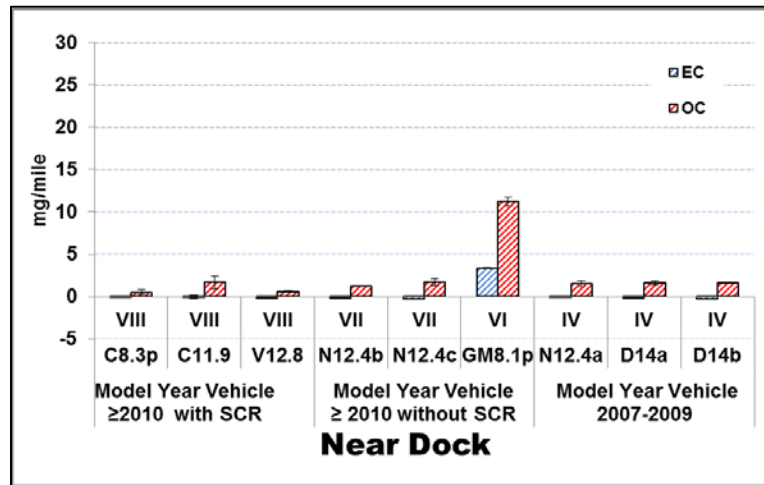


Emissions in grams/mile for the PM as OC & EC for the UDDS Cycle

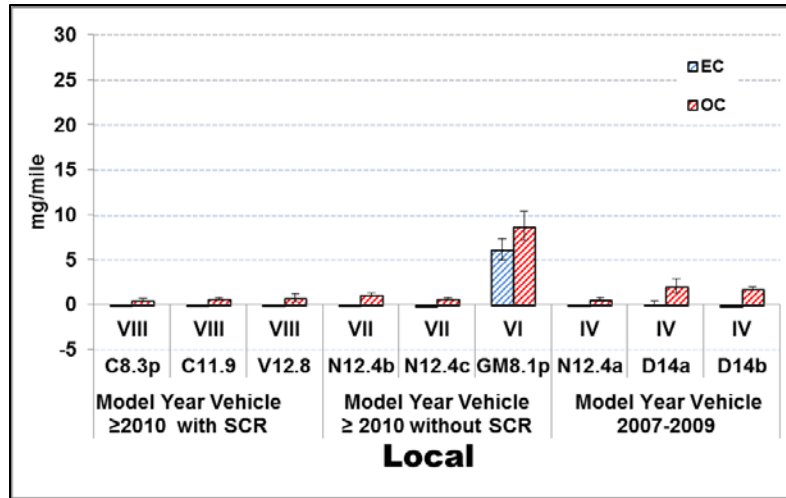


Emissions in grams/mile for the PM as OC & EC for cold- UDDS Cycle

<sup>1</sup> No error bars for the cold start tests because on only one test was performed



Emissions in grams/mile for the PM as OC & EC for the Near Port Cycle



Emissions in grams/mile for the PM as OC & EC for the Local Port Cycle

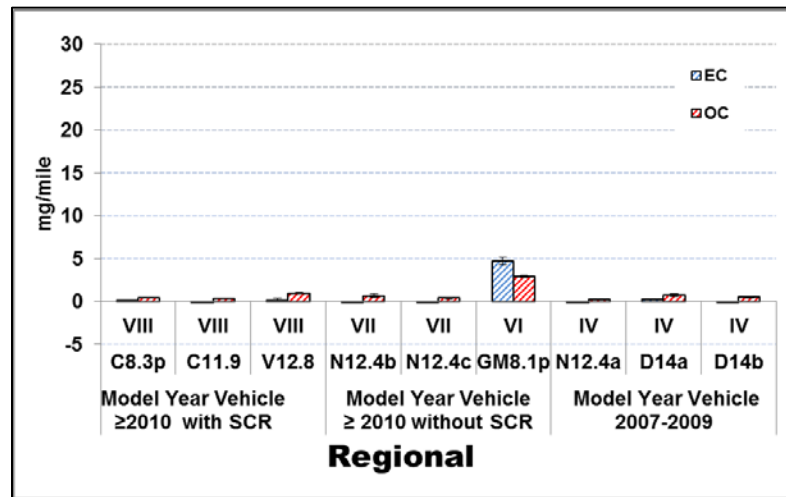


Figure Emissions in grams/mile for the PM as OC & EC for the Regional Port Cycle